Spring 5-15-2016

The Molecular and Cellular Basis for Cold Sensation

Daniel Brenner
Washington University in St. Louis

WASHINGTON UNIVERSITY IN ST. LOUIS

Division of Biology and Biomedical Sciences
Neurosciences

Dissertation Examination Committee:
Robert Gereau IV, Chair
Michael Bruchas
Yu-Qing Cao
Simon Haroutounian
Timothy Holy
Sanjay Jain

The Molecular and Cellular Basis for Cold Sensation

by
Daniel Saul Brenner

A dissertation presented to the
Graduate School of Arts & Sciences
Of Washington University
in partial fulfillment of the
requirements for the degree
of Doctor of Philosophy

May 2016
St. Louis, Missouri

TABLE OF CONTENTS

List of Figures

Chapter 1

Chapter 2

Chapter 3

Chapter 4

Chapter 5

ACKNOWLEDGEMENTS

A huge amount of work goes into something like this, and I did surprisingly little of it. I'd like to start by thanking every member of the Gereau Lab, past and present, for creating an incredibly collaborative and supportive environment. A little more specifically, I'd like to thank Ben Kolber for being my first Gereau Lab mentor, and showing me how to design experiments and organize my records. I also owe Ben Alter a great deal, as one of my projects started when he told me to "just come up with a better assay." I have also benefitted from Steve Davidson's wry wit as well as his insightful approach to experimental design and his master's touch with Photoshop; he has shared all them liberally. Judy Golden has an incredible, encyclopedic knowledge of the pain field and she never turns down an opportunity to help a labmate. Laura Cavallone has been an invaluable resource for surgical implantation strategies, as well as a clinical mentor helping me keep in touch with medicine during my academic diaspora. Last but not least, I probably owe the most thanks to Mike Montana for his friendship, his mentorship, his idea to try optogenetics in the peripheral nervous system, his desk, bench, and his officiating at my wedding. He has been a model of what a physician-scientist and a friend should be, and I hope to continue to follow in his footsteps.

The old guard is, however, only half the story. There are a host of people that joined with me or after me to whom I owe thanks. Clint Morgan both predates me and will be there after I leave, and he's a smart, hard-working individual who will do great things as a clinician and a scientist. Bryan Copits and Vijay Samineni are two of the most creative and driven scientists that I have met. They have been innovating and pushing the limits of our work since the moment they joined the lab, and the opportunity to pilot out new techniques with them was a true honor. Unfortunately for Vijay and Bryan, the Bears are terrible and the Bulls don't seem to want to improve all that much, so there will always be a limit to how happy they can be, regardless of

their inevitable scientific success. It has also been a pleasure watching Mani Valtcheva grow from a tentative first year medical student to the accomplished scientist she is now. I've always appreciated her help, and I'm certain that her reign as senior graduate student will be marked by peace and stability. Tayler Sheahan has also been an excellent addition to the lab, as her unique combination of extreme endurance and scientific curiosity about how that endurance works have made me think about pain and exercise in new light. Megan Bower has been a whirlwind of organization and good cheer since she joined the lab, and I've been lucky to have her help with the immunohistochemical studies described below. Finally, I owe a great deal to my doppelganger, Dan O'Brien. Dan is a man of tremendous integrity and warmth, which he pairs with a keen scientific mind. He's been a support in bad times, a partner in mischief during lab meetings, and an excellent roommate at conferences. I showed up a few months after him, and I'll be following him out the door too; I couldn't have asked for a better person to show me the way through.

From the Gereau side, there are two more incredibly important people I need to acknowledge. Sherri Vogt is our lab manager, and she is also the heart and soul of the lab. She makes the trains run on time, manages the mouse colony, and I'll miss her stabilizing influence in my life. Of course I also need to thank Rob for making all of this possible. Rob is caring, supportive mentor who also happens to be one of the brightest scientists in the pain field. He is a master of everything from the psychology of paper review responses to networking at conferences to balancing personality issue in a large lab, and watching him balance it all has been a privilege. He's also been supportive of my crazy ideas but has shown me when to focus and accomplish before branching out too much. As I prepare to leave the scientific nest, I'm grateful for the

personal and professional training that I've received from Rob, and I will do my best to live up to his example.

I have also been the beneficiary of a terrific administrative structure that has allowed me to focus almost entirely on the scientific work instead of the paperwork. First and foremost, I appreciate the help of the MSTP team including Brian Sullivan, Liz Bayer-Johnson, Christy Durbin, Linda Perniciaro, Wayne Yokoyama, and Robin Klein without whom none of this would have happened. I also appreciate the efforts of the Anesthesia administrative team members past and present including Anne DeSchryver, Christina Saldivar, Kathy Reeves, Lisa Hayes, Amanda Heflin, Katherine Mitchell, and the incomparable Jeff King. I also owe thanks to the DBBS office, particularly Sally Vogt and Shirley McTigue, as well as the entire Room 100 staff for making my return to medical school possible. Finally, the DCM people who have kept my mice alive and well, and in particular our mouse technician Lawrence Fields, have been crucial to completing this work.

I would also like to thank my thesis committee, Michael Bruchas, Yu-Qing Cao, Sanjay Jain, Tim Holy, and Simon Haroutounian for their help and advice. I also appreciate the advice that I have received from Evan Kharasch, Gina Story, and Erik Herzog. I was lucky to rotate in the lab of Bob Heuckeroth when I arrived at Washington University, and while I didn't join his lab he has still been a valuable advisor and mentor throughout this adventure. I have also received help from an incredible number of students and post docs in other labs at Washington University, including Matthew Crisp, Lulu Sun, Jane Symington, Nicole Kretzer, Jordan McCall, Ream al-Hasani, Brandon Holmes, Matt Glasser, and countless others.

Outside of the Washington University bubble, I owe a huge debt to John Rogers at the University of Illinois Urbana-Champaign as well as Tae-Il Kim, Gunchul Shin, and Sung Il Park for all of

their efforts designing and building LED devices for us to use. I've been lucky to work with such brilliant and dedicated engineers, and I hope to continue to work with them in the future. I would also like to thank Mark Hoon at the NIH for providing the TRPV1-cre mice and valuable discussions of the nature of cold sensation. I am also grateful for the financial support that I have received for this work, most of which was funded by grants from the National Institutes of Health National Institute of Neurological Disorders and Stroke, specifically to myself as an NRSA (1F31NS078852) and to Rob as an RO1 (R01NS48602) and a Transformative RO1 (R01NS081707).

There is no way I would have survived this crazy phase of life without the help of my friends. I would like to thank Sara Friedman, Mike Montana, Eric Nolley, Joe Zenga, Janey Symington, Jessen Wabeke, Vitas Wagner, Josh Kittrell, Matt Crisp, Hunter Lanier, Joe Planer, Mia Henderson, Carlin Box, Lydia Luangrangrong, Kyle Mitchell, Alex Dietz, Alicia Oberle, and Michael Galante for all the times that they listened to me whine, patted me on the back, and told me to suck it up and do better the next time. Your support and friendship has made all the difference

I wouldn't be the person that I am without my family. My parents have always supported me and encouraged my ambitions, even if it meant they have to visit St. Louis every once in a while. My sister Naomi has always been a loving and moderating influence on me, and has encouraged me to seek happiness wherever I can find it. Her support, along with that of her husband Ari has been invaluable, and as a bonus they also have two of the cutest little girls around. My older brother Yoni has taken a radically different path in life from me, but he's one of the most successful people I know. We may not always see eye to eye, but I know that he's always been looking out for my best interests, and I'm grateful for his help. My younger brother Bean has

grown up to be an important man over in DC and I'm lucky to have him watching over scientific and medical research funding for me. I also appreciate his willingness to put me up at late notice when I show up nearly unannounced on his doorstep.

Finally, I need to thank my wife, Sara Manning for tolerating years of unpredictable schedules, odd mouse smells, and erratic PhD behavior. I'm thankful that this intelligent, beautiful, and unnaturally patient woman has stuck with me this far. She supports me, but also pushes me past my self-imposed limits and I always end up better as a result. Thank you for everything, Sara.

Dani Brenner

Washington University in St. Louis

May 2016

ABSTRACT OF THE DISSERTATION

The Molecular and Cellular Basis for Cold Sensation

By

Daniel Saul Brenner

Doctor of Philosophy in Biology and Biomedical Sciences

Neurosciences

Washington University in St. Louis, 2016

Professor Robert Gereau, Chairperson

The ability to sense changes in temperature is crucial to surviving harsh environments. Over the last decade several ion channels that have been proposed to be cold sensitive have been identified, most notably TRPM8 and TRPA1. Although these molecules have been extensively studied *in vitro*, their exact roles in cold sensation *in vivo* are still debated. This uncertainty is in large part due to problems with the standard methods of testing cold sensitivity *in vivo*, which often rely on subjective measures of cold responsiveness. Experiments using these subjective measures have been repeated by different groups and have yielded conflicting results, leading to this confusion. To address this issue, I developed a novel method, the cold plantar assay (CPA) to objectively assess the cold sensitivity of mice. Once I characterized the assay, I then used it to test the roles of TRPM8 and TRPA1 using genetically modified knockout mice.

Another aspect of temperature sensation is the ability to adjust to changes in ambient temperature. For organisms that live in areas that have seasonal temperature shifts, it is essential to maintain sensitivity to small temperature changes even when the environment as a whole has been heated or cooled by as much as 40°C. To detect a 2°C change whether the temperature

starts at 45°C or 15°C requires an enormous dynamic range, and sophisticated molecular machinery behind it. The molecular mechanisms that may underlie adaptation have been studied *in* vitro, but has not been quantified or tested *in vivo*. In order to study how live mice adapt their thermal response thresholds to changes in the ambient temperature, I modified the CPA and the classical Hargreaves assay to test the temperature sensitivity of mice at different ambient temperatures. Using these assays, I demonstrated that the most important factor for withdrawal from thermal stimuli is the temperature change from baseline, and that this baseline can be rapidly adjusted. Furthermore, I utilized our transgenic knockout mice and pharmacological agents to demonstrate that phospholipid modulation of TRPM8 is essential for the rapid adaptation of cold sensitivity to changing ambient temperatures.

Finally, the last part of this thesis focuses on the different neuronal populations that express those molecules. While many different populations of nociceptive neurons have been identified using immunohistochemical labels, it has been difficult to directly correlate these populations with specific functions. I used a recently developed tool, optogenetics, to activate or silence selected neuronal populations while applying nocifensive stimuli. To deliver the light necessary for optogenetic modulation, I chronically implanted wireless LED devices to deliver the light directly to the axons of the nociceptive neurons. By silencing specific nocifensive populations while delivering to cold stimuli, I assessed which subsets of nociceptive neurons are necessary for full responses to cold stimuli.

Chapter 1

Introduction to pain and temperature sensation

Why study pain?

Pain is one of the strongest driving forces of human and animal behavior. Clay tablets recording pain treatment with opium date back as far as 3400 B.C.E [94], emphasizing the importance of pain relief even in the earliest moments of recorded human history. Even the word pain is ancient and ominous, originating from the Latin *poena*, which refers to the Greek goddess of retribution, vengeance, and punisher of murderers. Surprising, having too little pain is also notorious in history as the plague of leprosy, which causes loss of pain sensation leading to injury and disfigurement leads to effective banishment from society in the Bible. The historical terror of having too much pain and the stigma and consequences of having too little pain makes clear the importance of finding the middle ground where there is just enough pain sensitivity to encourage recovery from injuries but not so much as to interfere with life. This goal of this work is to understand the mechanisms that underlie pain in an effort to help more people find this all-important middle ground.

One of the results of missing this middle ground is chronic pain, which is relatively common in the modern world. An estimated 100 million adults were affected by chronic pain in 2010 and the prevalence is only expected to increase [131]. Part of this prevalence is that chronic pain is associated with common situations such as post-deployment syndrome [113], diabetes mellitus [174], traumatic spinal cord injury [65], cancer [54], chemotherapy [27,55,67,68,75,164], multiple sclerosis [177], and strokes [74]. Cold pain and hypersensitivity are present in a substantial number of these patients, and this manuscript will focus on the mechanisms underlying cold pain and cold hypersensitivity, and will also introduce novel methods of modulating pain-sensitive neurons that may be applied to treat chronic pain.

What is pain?

The consensus understanding of what pain is and why it happens has evolved along with the ability to assess, understand, and ultimately treat pain [142]. This understanding has evolved from Sophocles' characterization of pain in the 5th century BCE as a possession of the body which 'consumed' or 'devoured' the sufferer/victim [167], to the 18th century when pain was characterized as a sign of the patient's vitality or as a trial sent from God in order to strengthen faith and teach self-sacrifice, to the innovation of anesthesia and the view that pain in general was to be avoided when possible [132,142]**.** As set forth by the International Association of Pain, the current definition of pain is "an unpleasant sensory and emotional experience associated with actual or potential tissue damaged, or described in terms of such damage" [26]. While this term describes the patient experience of pain, the broadness of including an emotional component makes it difficult to study pain in animals, since the emotional experience of animals is difficult to quantify. As such, the majority of animal studies focus instead on nociception, which is defined as the "neural process of encoding noxious stimuli," and lacks the difficult-to-quantify emotional element [26]. In the mouse studies, the "nocifensive" behaviors can include measuring flicking or licking of an injured limb in reflexive assays, quantifying the writhing or evoked muscle contractions in visceral pain models, or measuring the avoidance of an area that has been paired with a noxious stimulus in operant conditioning paradigms. For the purposes of this manuscript, I will be using nocifensive behaviors in mice as a proxy for the sensory transduction and signaling component of pain in humans.

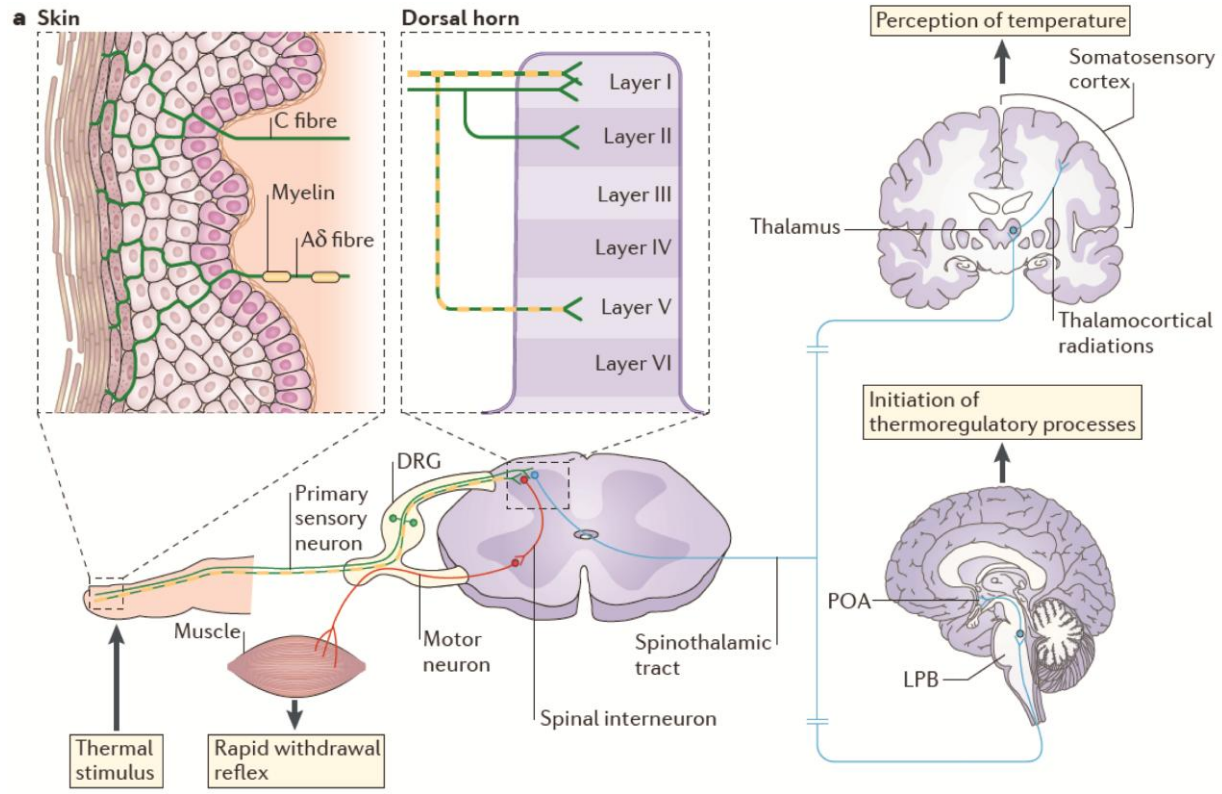

Figure 1 Pathways involved in thermal avoidance responses
A. Cutaneous primary sensory neurons involved in thermosensation (green) include both non-myelinated C fibers and thinly myelinated Aδ fibers. The cell bodies of these neurons are located in the dorsal root ganglia (DRGs) and have axons with two branches. One branch extends towards the periphery with free endings in the skin, where thermal information is coded in the form of electrical action potentials. These action potentials propagate to the end of the other axonal branch, which forms synapses in layers I and II (for C fibers) or layers I and V (for Aδ fibers) of the dorsal horn. Activity of both Aδ and C primary sensory fibers drives three distinct neuronal pathways and ensuing responses: first, motor neurons can be activated via spinal interneurons, leading to a rapid withdrawal reflex in response to noxious temperatures (red neurons); second, thermosensory information is transmitted via second-order sensory neurons of the ascending spinothalamic tract to the thalamus and further relayed to the somatosensory cortex, where the perception of temperature is formed (blue neurons on the coronal section of the human brain); and third, thermosensory information is transmitted via lateral parabrachial neurons, which may also receive input from the spinothalamic neurons, to the pre-optic area of the hypothalamus (blue neurons on the central sagittal section of the human brain), where thermoregulatory processes are initiated. Figure adapted with permission from Vriens et. al 2014.

How do pain and nociception happen?

Centuries of anatomical and physiological studies have shows that the cell bodies of nocifensive neurons are located in the dorsal root ganglia (DRG) that flank the spinal cord. These neurons, which have long axons that stretch from the outer layers of the skin all the way to the spinal cord, transduce sensory stimuli of all types into the electrical signals that travel from the periphery to the central nervous system. When a painful stimulus is applied to the skin, the transduction process begins at the most superficial levels in the fine nerve endings where the DRG (**Figure 1**) [3,190]. Under baseline conditions, the neurons have a negative membrane potential that is

generated by an imbalance of sodium and potassium ions across the membrane, generating a both an electrical and chemical driving force for their movement through the membrane [86]. When a noxious stimulus is applied to the skin, specialized molecules in the skin terminals respond by perturbing cell homeostasis. Many of these responsive molecules are specialized ion channels that respond to different stimuli including cold [129,153,176], heat [28,29,111,139], and mechanical [45,62] stimuli that will described in more detail below. Once enough sodium and calcium ions pass into the cell through these activated channels that the cell membrane potential is no longer deeply negative, ion channels in the membrane that respond to changes in voltage are activated and allow a substantial influx of positive sodium and eventually calcium ions into the cell (**Figure 2**)[10]. This influx results in a dramatic depolarization of the cell membrane called an action potential, which is the signal of neuronal activation [10]. The action potential is terminated when the sodium and calcium channels inactivate, and the calcium influx into the cell activates voltage- and calcium-sensitive potassium channels that allow potassium influx to return the cell to negative membrane potentials [10].

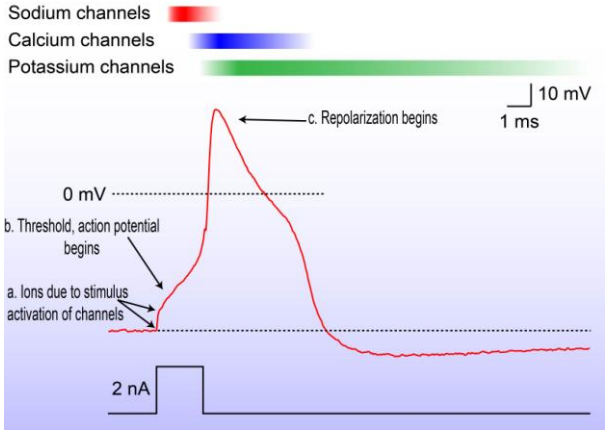

Figure 2: The action potential in human DRG
Ions enter the cell (a) through ion channels activated by a stimulus on the cell (e.g. skin cooling). Once the membrane voltage reaches a threshold (b), voltage-gated sodium channels open to allow sodium influx. As the membrane voltage continues to rise, voltage-gated calcium channels open and contribute to increasing depolarization. Eventually voltage- and calcium-activated potassium channels activate and lead to a repolarization of membrane to negative membrane potentials (c). Figure adapted with permission from Bryan Copits.

These action potentials are conducted from these fine endings into axons which run from the peripheral targets to their cell bodies in the dorsal root ganglia and then onward to the spinal cord (**Figure 1**)[3,190,196]. As the action potentials are conducted along the axons, they periodically

need to be regenerated through the activation of voltage-gated ion channels in the axonal membrane, which allow the influx of sodium ions that reinforce the action potential. The speed of this transit is determined mainly by the diameter of the axons and how thickly the axon is layered with myelin, a lipid-rich coating that insulates the axon from current leakage [80]. The fast conducting, large diameter, heavily myelinated Aβ- fiber axons tend to carry proprioceptive and fine touch signaling, while the slower, smaller, lightly or unmyelinated Aδ- and C- fiber axons tend to carry nociceptive information such as heating, cooling, mechanosensation, and chemical irritation [3]**.**

In the spinal cord, the central terminals of the dorsal root ganglia neurons form synapses on neurons in the dorsal horn of the spinal cord**.** Aδ fibers tend to synapse in spinal cord lamina I with lesser projections to laminae II_0 and V, while C-fibers tend to synapse in spinal cord lamina II_o with lesser projections to laminae I (**Figure 1**) [133,190]**.** Once the DRG neuron action potentials reach the central terminals, they trigger the release of chemical neurotransmitters such as glutamate that diffuse across the synapse to neurons in the spinal cord and may cause to action potentials. The spinal dorsal horn neurons that receive input from Aδ- and C-fibers are also modulated by input from other neurons in the spinal cord and then send axons which project to different parts of the brain via the spinothalamic, spinomesencephalic, spinoreticular, and spinoparabrachial tracts of the spinal cord [3,196]. Some of the input from DRG neurons in the spinal cord also goes to spinal interneurons which directly synapse on motor neurons in the ventral horn of the spinal cord to generate rapid withdrawal reflex arcs (**Figure 1**) [190].

In the brain, neurons from the spinal cord project to a variety of brain regions known to be important for nociceptive processing. Many neurons that travel in the spinothalamic tract synapse in the thalamus, a midline structure that can be divided into several components including the ventroposterolateral (VPL), ventroposteromedial (VPM) and vertroposterioinferior (VPI) nuclei [3]. These thalamic areas receive synaptic input from different types of spinal cord neurons, and then relay the information onwards to the primary and secondary somatosensory cortices as well as the anterior cingulate cortex [133]. The primary and somatosensory cortices process the nocifensive information forwarded by the thalamus into different intensities, codes them temporally, and associates them with learning and memory processes [3]. On the other hand, the projections from the thalamus that terminate in the anterior cingulate cortex are thought to contribute to the motivational-affective processing of nocifensive stimuli [3]**.** Another branch of the spinothalamic tract is the spinomesencephalic tract, which synapses in the periaqueductal grey (PAG), an area around the cerebral aqueduct in the midbrain that is essential for descending modulation of pain sensation [133]. The spinomesencephalic tract also synapses in the parabrachial area, which is important for the cardiovascular, autonomic, and motivational responses to pain and also can relay signals to the amygdala, which is important for the affective component of nociception [105,133]. The spinoreticular tract from the spinal cord contains axons that project to an area involved in motor control called the precerebellar nucleus, as well as the medial pontobulbar reticular formation which is also involved in nociception [3]. The combined efforts of these regions of the brain process the nocifensive signals to generate the sensation known as pain, and plasticity or modulation of any part of these systems from peripheral terminals to somatosensory cortex can lead to hypersensitivity or insensitivity to pain.

Why study mice to learn about human pain?

Most of the data discussed below and the studies discussed in this introduction are based on experiments performed using mice to draw conclusions about the function of the nociceptive system on a wider basis. The use of mice as models of experimental pain also has some significant advantages over human and primate testing models. Mice can be bred quickly and inexpensively, allowing testing of complicated hypotheses that require large cohorts at relatively reasonable costs. One of the biggest advantages of using mice as experimental models, however, is the ability to generate transgenic mouse models that have individual genes removed or overexpressed. Zimmermann et al. demonstrate how the utility of this technique can be when they show that mice lacking the sodium channel Nav1.8 have impaired responses to noxious cold sensation [215]. The opposite experiment where genes are altered to express at higher-than-normal levels is also extremely useful, such as when Kolber et al. engineered mice to overexpress Corticotropin-releasing hormone (CRH) in the forebrain in order to demonstrate the role of juvenile CRH concentrations on anxiety and despair [104]. Without transgenic mouse models, researchers would have to rely on identifying sporadic mutations in order to study the roles of removing or enhancing individual genes in living animals. Indeed, sporadic individual mutations in humans such as congenital insensitivity to pain [46] and in animals such as the spontaneous canine model of amyotrophic lateral sclerosis (ALS) [48] or a spontaneous feline model of Neimann Pick C disease [172] can cause disease and be valuable for understanding the mechanisms of those disease. However, cases where a single mutation causes an obvious phenotype are very rare events, and relying on those rare events to drive the progress of science and medicine is impractical. It is much more efficient and effective to drive scientific progress using transgenic models such as mice and then use the naturally occurring sporadic mutations to

validate and improve the transgenic work when they are available, as has happened with the canine ALS model [48].

There are also other concerns about using mouse models that are most specific to the pain field. Recently there has been significant debate over the whether pain studies done in mice can be applied to human studies, and whether the types of behavioral studies that have been favored can be applied to the study and treatment of human pain [126,135]. One of the most strident objections to the use of mice for pain models is that animal behavioral testing does not include the subjective pain experience that shapes the patient experience. Additionally, the point has been made that "rats and mice simply do not have the neuroanatomical pathway to the forebrain that is crucial tor pain sensation in humans" [47]. While it is true that some specific pathways are not the same, there are a number of similarities between mice and humans that make it worthwhile to use them as a model for human nociception. Structural studies assigning functions to different brain areas and spinal cord tracts in animals seem to correlate relatively well with human injury case studies, suggesting significant overlap in structure despite obvious differences in size and complexity [197]. Like humans, mice have varied responses to nocifensive stimuli based on factors including genotype [136], wakefulness [23], social interaction [110], and gender interaction [61,173].

Another common criticism of pain research conducted with mice is that in many clinical studies, pain measurements are made using the numerical rating systems (NRS) for pain, as well as a variety of other validated pain questionnaires such as the McGill checklist [165]. In response to these criticisms, researchers have developed tools that attempt to parallel these human

questionnaires in mice by assessing pain levels through rodent facial expressions [127], voluntary wheel running [42,73], and voluntary movements [36,185]. Despite the prevalence of NRS use in clinical pain studies, many studies also utilize quantitative sensory testing designed to allow comparison between patients without the confounding element of subjectivity that is inherent to patient-reported pain reports [32,50,74,107,177]. While it is difficult to apply NRS-like protocols to mice, it is relatively simple to devise techniques that parallel the human quantitative sensory testing methods, and thereby mimic the human clinical data. Researchers have developed a wide range of these mouse quantitative sensory testing methods to quantify thermal and cold sensation, some of which are described below.

Behavioral assays for thermal and cold sensation in rodents

In order to understand how thermal sensation works in live animals, it is necessary to assess how those animals respond to noxious and innocuous thermal stimuli. Since mice cannot fill out a questionnaire to report the extent of their discomfort, behavioral assays try to assess how a mouse responds to a consistent warm or cold stimulus, and use that as a correlate for how sensitive the mouse is to that stimulus.

One of the oldest and most commonly used assays to measure both heat and cold sensitivity is the hot/cold plate test [2,38,59,60,204]. In this assay, mice are placed on a metal plate that is heated to 45-55°C or cooled to 0-15°C. After the mice are place on the plate behaviors that are deemed "nocifensive" are measured, including number of jumps, number of paw flinches, number of wet-dog shakes, and the latency to first flinch or jump. Mice that have more vigorous or faster responses after being placed to the cold/hot plate are judged as having increased

sensitivity, while mice that respond more slowly or less vigorously are judged to have decreased sensitivity. While this method has been a mainstay of studies into the nature and mechanisms of thermal sensitivity there are a number of significant limitations. One major limitation is that the cold plate represents a novel environment, and exposure to a novel environment during testing can cause stress [170], which has been shown to alter nocifensive responsiveness [146,157]. Another limitation is that this technique can only test the responsiveness of mice to a single temperature at a time, with no ability to ramp the stimulus in real time. The most important limitation of this technique, however, is the subjective nature of the data interpretation. When 2 different groups both use the cold/hot plate assay on the same mice but one group measures the number of flinches [102] while the other measures the latency to first flinch [96] the groups can yield completely opposing interpretations of the data. Disagreements of this type have retarded progress in understanding the mechanisms of both heat and cold sensation.

Another venerable used behavioral assay for thermal sensitivity is the tail flick test [50,158]. This method involves heating or cooling the tail of a mouse either by illuminating it with high intensity light or dipping it into hot or cold water, and measuring the latency before the mouse flicks the tail away from the heat/cold. The withdrawal latency is correlated to the thermal sensitivity, so mice that have longer withdrawal latencies are presumed to be less sensitive. As with the cold/hot plate this method has been a crucial part of the studies of temperature sensation over the last 70 years, but has some significant limitations. The biggest limitation to this technique is the mice must be handled firmly in order to hold the tails into the water. This handling causes stress, which can profoundly impact how the mice respond to the stimulus [157].

The acetone evaporation test is another classical method for measuring the cold sensitivity of mice [25,38]. This assay involves acclimating the mice on a wire mesh before a droplet of acetone is dabbed onto the underside of the hindpaw. The acetone evaporates almost immediately, which cools the paw. The amount of time that the mouse spends flicking the cooled paw is used as a measure of cold sensitivity. While this assay does remove one of the confounding issues of the hot/cold plate test by allowing acclimation of the mice, there are several significant problems with the acetone evaporation test. The responses to acetone evaporation are confounded by the wet sensation and the smell of the acetone. Also, the cold stimulus applied can vary based on the amount of acetone applied, which can increase inter-trial variability and confound results. Most importantly, wild-type mice without injury have minimal responses to acetone at baseline, making it impossible to measure analgesia in the absence of hypersensitivity with this tool.

Several variants of hot and cold plate tests have been developed more recently to address some of the issues mentioned above. The thermal gradient assay uses a large peltier plate which is divided into 16 zones that vary in temperature from 16°-55°C [139]. The amount of time the mouse spends in any given temperature zone is used as a proxy for their temperature sensitivity, so a mouse that is hypersensitive to cold will spend less time in the zones under 30°C. The 2-plate preference assay uses two connected plates that are heated or cooled to different temperatures. The mouse is allowed move back and forth between the plates, and the amount of time that the mouse spends on one plate compared to the other is used as a proxy for temperature sensitivity [9]. For example, if one plate is at 30°C and the other is at 15°C a mouse that is hypersensitive to cold will spend less time on the 15°C plate than a normal mouse. While both

of these techniques allow the mice to acclimate for significant periods of time on the apparatus, they also both represent temperature preference rather than aversion. This makes it difficult to assess whether, for example, mice are truly evading a colder temperature due to hypersensitivity or if they simply prefer a warmer temperature after the injury.

Another commonly used technique to measure heat sensitivity is the Hargreaves assay. During this test, mice are acclimated on a glass plate which is heated to 30°C until they reach a resting state. At that point, a beam of light is focused on the underside of the hindpaw through the glass, heating the paw until the mouse moves away from the light source [79]. The light beam generates a very consistent warming stimulus that can be intensified if the intensity of the light is increased. The biggest criticisms of this assay are that it measures a spinal reflex and therefore does not test nociception that involves supraspinal processing, and that there was no way to use this technique to measure cold sensitivity in addition to heat.

Molecular mechanisms of temperature responsiveness

The field of temperature sensation had made steady progress since early studies assessing the analgesic potency of novel compounds, but molecular techniques allowing the identification of transient receptor potential or "TRP" channel as transducers of noxious stimuli opened the floodgates for novel work identifying and characterizing these channels. TRP channels had been studied since 1969, when they were isolated in a *Drosophila* strain that was functionally blind under high light conditions despite being able to navigate a maze under low ambient light [44]. Furthermore, using electroretinogram recordings follow up studies showed that the mutant flies had an transient initial light response which decayed during sustained illumination, which led

them to name the mutant for the *transient receptor potential* (TRP) [134]. It would be ten years before the *Drosophila* gene would be cloned in part,[137] and 4 more years after that before it became the first TRP channel cloned and sequenced in its entirety [138,201].

8 years later, the capsaicin receptor TRPV1 was cloned from a dorsal root ganglion cDNA library and identified as a heat-activated, pH-sensitive vanilloid receptor member of the TRP superfamily [30]. Heat-sensitive currents had already been identified in dorsal root ganglia cultures [34,166], as had capsaicin-induced currents [149,203], but cloning of a single receptor that was likely responsible for both currents was a transformative moment in the field. *In vitro*, the cloned TRPV1 receptor begins activating roughly at 40°C (**Figure 3**), and several other members of the TRPV family that were potentially heat sensitive were identified soon afterwards, including TRPV2 [29], TRPV3 [154], and TRPV4 [76], although the heat responsiveness of TRPV2 is now somewhat controversial [155].

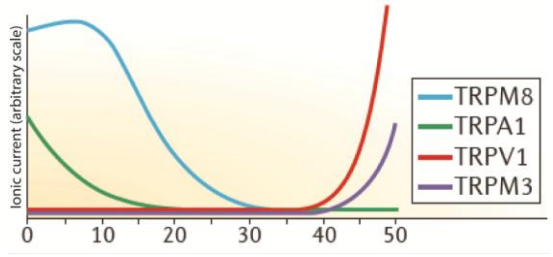

Figure 3: Temperature dependence of ion channels involved in thermosensation
a. Members of the transient receptor potential (TRP) channel family function as excitatory cation channels and respond to cooling or heating. Figure adapted with permission from Vriens et. al 2014

Since its initial discovery, a great deal of work has been done to understand how TRPV1 responds to heat. The mechanisms of the temperature-sensitivity of TRPV1 were described with a 2-state electrophysiological model, which shows that heating shifts the voltage-dependent activation curve of the channel towards more negative potentials, resulting in the channel opening at more negative potentials. Furthermore, they deduce that this shift is due to a decrease in the energy of activation of channel opening at higher temperatures, which increases the open state probability of the channel when it is heated [147,189].

The modulation of TRPV1 has also been a heavily researched subject, in part because TRPV1 is responsive to a wide variety of stimuli, ligands, and messengers in addition to heat and capsaicin. Although it is unclear whether TRPV1 is positively, negatively, or unregulated by phosphoinositol 4,5-bisphosphate ($PIP_{2)}$ and other phosphoinositide lipids in the membrane [24,120], TRPV1 has been shown to associate with, and be modulated by, the phosphoinositide-binding protein Pirt [97]. TRPV1 is also activated and sensitized by a wide variety of other factors including acidic or basic pH [57,183], the vasodilator anandamide [216], lipoxygenase products [89], and oxidized linoleic acid metabolites that are byproducts of tissue heating [151,152].

The role of TRPV1 in thermal and inflammatory responsiveness has also been studied using transgenic knockout mouse models. Under baseline conditions, mice that lack TRPV1 are less sensitive to noxious thermal [111]. Work using these transgenic mice also suggests that inflammatory heat hypersensitivity is dependent on TRPV1 activity, as TRPV1-KO mice are less sensitive after injection of CFA [28,53]. Additionally, Nerve Growth Factor (NGF) and bradykinin, both molecules released during inflammation, have been shown to cause increased TRPV1 activation through activation of PLC to hydrolyze PIP_2[40]

Due to this important role in nociception and hypersensitivity, pharmaceutical companies have attempted to develop analgesic TRPV1 antagonists, but have been stymied in part by the fact that these antagonists can also cause significant hyperthermia in humans [202]. Researchers have attempted to sidestep this problem by inhibiting the neurons expressing TRPV1 rather than

inhibiting the TRPV1 channel itself using a novel lidocaine derivative. Lidocaine is a neutral charged analgesic that diffuses through the cell membrane to bind an intracellular site on voltage-gated sodium channels and thereby inhibit them. The quaternary lidocaine derivative QX-314 is positively charged, which prevents it from diffusing through the cell membrane and causing analgesia under normal circumstances. In the presence of a TRPV1 agonist however, QX-314 can enter cells that express TRPV1 through the opened pore of the channel, where it binds to the voltage-gated sodium channels and inhibits signaling in those cells[17]. This has allowed researchers to definitively confirm that TRPV1-expressing neurons are required for heat, mechanical and cold hypersensitivity [20].

While the vanilloid family of TRP receptors is heavily involved in thermal sensation, the menthol receptor TRPM8 from the melastatin family was identified as one of the primary transducers of cold by two separate group using two different screens [129,153]. *In vitro*, TRPM8 has been shown to activate starting at temperatures below 24°C [153]. As with TRPV1, the likely mechanisms that confer cold sensitivity were deduced using a 2-state electrophysiological model. With TRPM8, cooling shifts the voltage-dependent activation curve towards more negative potentials, resulting in a channel that is more active under hyperpolarized conditions. In contrast with TRPV1, however, the energy of activation of channel opening is unchanged [189]. Instead, with TRPM8 the energy of activation of the channel closing is increased by cooling, which increases the open-state probability of the channel when it is cooled [189].

Although TRPM8 has less promiscuous ligand-binding characteristics than TRPV1, there are still a wide range of factors that modulate TRPM8 activity. In cultured dorsal root ganglion neurons, it has been shown that Protein Kinase C-induced dephosphorylation of decreases TRPM8 activation [162] and that TRPM8 activation is decreased when it is localized to lipid raft microdomains in the cell membrane [141]. It has also been shown that chronic neurturin overexpression in the skin leads to increased expression of TRPM8 and increased cold sensitivity, suggesting that the GDNF-family of ligands such as neurturin may play a role in regulating temperature sensitivity [191]. Another study showed that TRPM8 is necessary for the induction of cold hypersensitivity by Artemin, another member of the GDNF family [117]. The regulation of TRPM8 by Phospholipase-C (PLC) and PIP_2 is much more straightforward than that of TRPV1. Early studies showed in HEK cells that PIP_2 depletion by Ca^{2+}-activated PLC caused desensitization of the TRPM8 [51,169], while follow up studies showed in both HEK cells and dorsal root ganglia cultures that cooling of the ambient temperature led to PIP_2 degradation and TRPM8 desensitization, which allowed the neurons to adjust their response threshold to the cooler environment. Additionally, TRPM8 has also been shown to interact with the PIP_2 binding protein Pirt, and Pirt knockout mice have decreased cold sensitivity, further strengthening the link between PIP_2 interaction and TRPM8 sensitivity [179].

The role of TRPM8 in cold sensation has been confirmed using transgenic knockout mice, which have impaired cold responses in all cold behavioral tests [43,56]. Additionally, tests using the 2-plate temperature preference assay show that TRPM8-KO mice have lower preference for warmer temperatures, suggesting that pleasantly warm thermal sensations may actually be a result of decreased noxious signaling from TRPM8 [159]. Behavioral experiments with these

knockout mice have also suggested that TRPM8 is involved in the cold hypersensitivity induced by treatment with the chemotherapeutic agent oxaliplatin [69] and in the hypersensitivity that develops after the neuropathic Chronic Constriction Injury (CCI) surgery [205]. Finally, studies have shown that TRPM8-expressing neurons have a crucial role in cooling-induced analgesia after nerve injury [103].

Although TRPM8 has been widely accepted as a cold-sensitive ion channel, the role of TRPA1 in cold sensation has been significantly more controversial. TRPA1 was first cloned after a bioinformatics screen suggested that it shared structural and expression pattern characteristics with the previously described thermo sensitive TRP channels [176]. *In vitro* experiments suggested that TRPA1 was responsive to more noxious cold temperatures, starting around 17°C [176].This initial characterization also suggested that in culture TRPA1 activated in response to temperatures below 17°C as well as the cold mimetic icilin [176]. 2-state electrophysiological modeling suggests that as with TRPV1 and TRPM8, the voltage dependence of TRPA1 activation is shifted to more negative voltages upon cooling [96]. As with TRPA1, further experiments showed that cooling was associated with an increased energy of activation of channel closing, which increased the open probability of the channel [96]. Still, the cold sensitivity of TRPA1 has remained controversial, as calcium imaging by other groups have shown that the channel is not cold-responsive *in vitro* [102].

Beyond its responsiveness to cold stimuli, TRPA1 has astonishingly promiscuous ligand-binding characteristics. TRPA1 can be activated by most electrophilic substances through a reversible covalent modification involving cysteine residues in the N-terminus of the channel [85]. This

yields an impressive list of ligands which have been shown to activate TRPA1, including mustard oil and cannabinoids [92], nicotine [178], the oxidative metabolite 15-delta Prostaglandin J2 [49], farnesyl thiosalicylic acid [124], hydrogen sulfide [4], acetaldehyde [7], formalin [130], and zinc [88]. As if this list of ligands was not sufficient, TRPA1 activity is also modulated by intracellular messengers including membrane PIP_2 [95] and local concentrations of Ca^{2+} ions [192]. TRPA1 has also been shown to be required for dry skin-induced itch [200], oxidative stress-induced itch [118], and for the full expression of chloroquine-induced itch [180].

Unfortunately, behavioral experiments in TRPA1-KO mice have not yielded conclusive results about the role of TRPA1 in cold sensation. Although these mice have been tested using the behavioral assays described above, some groups have found that TRPA1-KO mice are less sensitive to noxious cold stimuli [96,108], while others have found that TRPA1-KO mice have normal cold responses [9,102]. Additionally, some studies with the TRPA1-TRPM8-double knockout (DKO) mice show that there is no difference from the single TRPM8-KO mice, which would support the theory that TRPA1 is not involved in cold sensation [102]. Still, there are tantalizing hints that TRPA1 may indeed be involved with cold sensation. Treatment of mice with ciguatoxins isolated from tropical fish leads to cold hypersensitivity and pain that is ultimately caused by TRPA1 hyperactivity [188], and TRPA1 has been implicated in oxaliplatin-induced cold hypersensitivity [145]. There are even hints that TRPA1 is important for cold sensation in humans; single nucleotide polymorphisms in TRPA1 have been identified that are associated with cold hypoalgesia [15,98], and a TRPA1 gain-of-function mutations causes a familial episodic pain syndrome that is triggered by cold, stress, fasting [107].

Adaptation to changes in environmental temperature The ability to survive in areas with seasonal temperature shifts is a significant advantage for survival. In order to tolerate those seasons, it important to adjust the ranges of temperature sensitivity to match the ambient environmental temperature. For example, mice living in seasonal areas must detect cold stimuli during both summer and winter, when ambient temperatures can vary by over 100°F and approach or evade the cold stimulus when appropriate. Humans take this ability for granted, such as when the water in a swimming pool feels intensely cold immediately after entering, but is comfortable after several minutes. Scientifically, this principle was recognized early on by Ernst Heinrich Weber in the early 19th century when he assessed how the cold sensitivity of people changed after he had submerged their hands in cold water for a significant period of time [193,194]. Based on those experiments he concluded that only changes of temperature can lead to the sensation of cold or heat, which became referred to as the "theory of Weber" [83]. However, there was also skepticism in this theory based on "the experiences of everyday life" which suggested that even after long periods of temperature stimulation people still reported "lasting sensations of

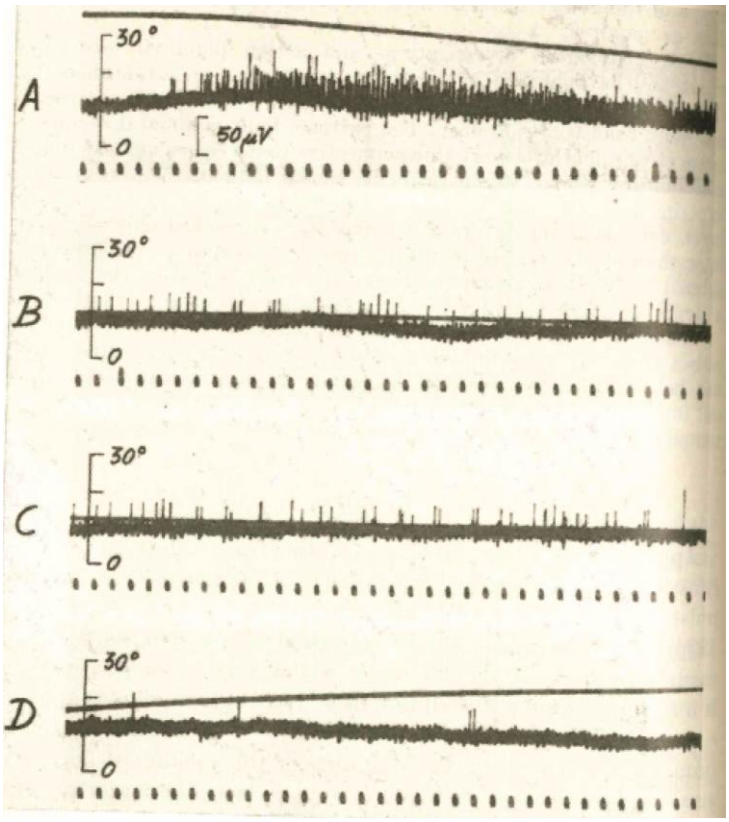

Figure 4: Cold adaptation in the lingual nerve
Action potentials were recorded from a fine branch of the lingual nerve when applying a constant temperature of 13°C to the surface of the tongue. A) Start of cooling, B) After 30 seconds, C) After 100 seconds, D) During rewarming of the tongue. After sustained administration of the cold stimulus, action potentials decrease in frequency and amplitude, representing cold adaptation. Adapted with permission from Hensel & Zotterman et al. 1950.

temperature." [83]. In an effort to test whether cold sensation was based solely on changes of temperature, Hensel & Zotterman anesthetized cats and dogs, and recorded action potentials from the lingual nerve while applying sustained cold temperatures to tongue [82]. The data from these experiments represent one of the first quantified example of cold adaptation, as there was a burst of action potentials when the cold probe was applied (**Figure 4A**) that gradually decreased as the stimulus was maintained on the tongue (**Figure 4B-D**) [83]. Additional studies of adaptation in cold sensation have been recorded using microneurography over the years. For example in monkeys where during constant cold stimulation "all of the [cutaneous cold receptors] soon stopped responding to base temperatures applied" even though they had initially responded to the base temperature cooling [109].

While the microneurographical studies suggested that cold adaptation was happening, it was not until after the characterization of the TRP channels that transduce the cold sensation into electrical potentials that there were hints of what the molecular mechanisms of cold adaptation might be. The first hints came when Rohacs et al. demonstrated using inside-out patches that in the absence of PIP_2, TRPM8 is less sensitive to cold stimulation [169]. Follow up studies demonstrated in heterologous cells that perturbing the PIP_2 levels by activating or inhibiting endogenous Phospholipase C (PLC) could control the sensitivity of the cells to cold [51]. Cold adaptation mediated by TRPM8 *in vitro* was only recently demonstrated in native dorsal root ganglion cells, and this adaptation was dependent on the arginine residue at position 1008 in the channel [66].

The functions of individual dorsal root ganglia neurons have been studied with ablation studies

While it is essential to understand the molecular transducers of nocifensive stimuli, the populations of neurons in which they are expressed is also crucial. This is demonstrated clearly when Han et al. used a transgenic strategy to remove the endogenous TRPV1, and then expressed the TRPV1 receptor in neurons that are thought to carry itch signaling. When those mice are treated with capsaicin, instead of nocifensive flinching the mice respond with itching behavior [78], showing that the identity of the neurons that are being activated is as crucial as the molecular mediators that are transducing the stimulus.

Many different populations of nociceptive neurons have been identified, which are differentiated by their expression of molecular markers including the heat sensor TRPV1 [33], the voltage-gated sodium channel Nav1.8 [215], the calcium regulated actin-binding protein Advillin [81], the Calcitonin gene-related peptide (CGRP) [163], and the ability to bind to the plant lectin IB4 [163]. These neuronal populations have been studied for decades, yet work investigating their individual functions has been mostly limited to ablation studies where those neurons are killed through transgenic expression of the diphtheria toxin receptor to selectively kill those neurons. Ablating the TRPV1-expressing neurons nearly eliminated temperature sensation between 40-50°C [159], ablating the Nav1.8-expressing neurons decreased responsiveness to noxious mechanical pressure and cold and decreased inflammatory pain responses [1], while ablating the CGRP-expressing neurons reduced sensitivity to noxious heat, capsaicin, and itch, and enhanced cold responsiveness [128]. While these studies have advanced the understanding of the role of these cells, they still involve killing those entire populations, which may prompt significant compensatory changes in neuronal architecture and function. These subtle alterations in coding or structure may minimize the effects of the ablation, thus resulting in animals with minimal deficits despite the loss of a neuronal population that is crucial under normal circumstances.

Novel methods for studying the roles of individual neuronal populations

In order to prevent these adaptations, it would be preferable to use an approach that transiently inactivates the neurons of interest without killing them and changing the neuronal architecture. Several approaches capable of inactivating neurons without killing them have been recently developed to fill this need.

One strategy to transiently inactivate neurons utilizes the quaternary lidocaine derivative QX-314. The commonly used lidocaine is uncharged and can diffuse across the cell membrane to inhibit voltage-gated sodium channels, resulting in analgesia [31]. In contrast, QX-314 is charged and therefore unable to diffuse across the cell membrane and has weak analgesic action under normal circumstances. Although it cannot diffuse through the membrane, QX-314 has a molecular mass of 263 Da and can pass through larger ion channel pores such as that of TRPV1, which has been shown to pass molecules as large as 452 Da [17]. When QX-314 is coadministered with capsaicin, the compound selectively enters neurons through activated TRPV1 channels and inhibits those neurons for roughly 3 hours, far longer than the typical duration of lidocaine inhibition [17,20]. This technique has clinical implications for long lasting selective regional anesthetic blocks [214], but can also be used to transiently inhibit selected neuronal populations without killing the cells and changing the neuronal architecture. Studies utilizing this technique have already demonstrated that TRPV1-expressing neurons are required for heat, mechanical and cold hyperalgesia but not cold allodynia [20], and have investigated the complicated networks of neuronal populations that underlie sensations of itch [168]. While this technique is an excellent way to study the roles of individual neuronal populations without ablating cells, there are a few limitations. Although it has the advantage of not requiring any

type of transgenic manipulation, using QX-314 requires that the neurons of interest express an ion channel that has a large enough pore to allow entrance of the compound. This narrows the subsets of which neuronal populations can be studied using this technique to those neurons that express channels with large pores that can be easily activated. Additionally the onset of inhibition can vary as the QX-314 enters into the cell, and the duration of the inhibition is gradual as the QX-314 leaves the cell, which limits its use in experiments with strict timescales. Finally, studies using QX-314 can inhibit specific neuronal populations, but using this technique there is currently perform the inverse experiment and specifically activate neuronal populations.

Chemogenetics is another recently developed technique to modulate specific neuronal subsets. This technique utilizes designer receptor exclusively activated by a designer drugs (DREADDs), which are muscarinic G protein-coupled receptors that have been modified to respond solely to a synthetic ligand, clozapine-n-oxide (CNO), and not to any endogenous ligands [5]. The DREADD receptors are expressed in the neurons of interest, and when CNO is present the cells expressing the DREADD receptors are depolarized, hyperpolarized, or otherwise modulated through G proteins which are coupled to the recombinant receptors [5]. While this technique is powerful, the utility of DREADDs is somewhat limited by the delivery and clearance of the CNO ligand to the receptors. While CNO is highly bioavailable and can cross the blood-brain barrier [11], it still needs to be distributed through blood flow and therefore activation of the receptors in different areas may not be simultaneous. Additionally, the clearance of CNO will likewise be variable, and could affect results. In terms of doing temporally precise behavioral experiments, chemogenetics has serious handicaps.

Optogenetics is another recently developed technique to directly modulate subsets of neuronal populations. Instead of re-engineering chemoreceptors, optogenetics utilizes light-sensitive ion channels to modulate neuronal activity [209]. These light-sensitive channels were originally isolated from light-responsive algae [106,143,144], and then modified to generate an arsenal of channels with varied spectral, kinetic, and conductive properties (**Figure 5**) [101,114,115,208]. These light-sensitive channels can be largely divided into excitatory cation channels and inhibitory channels and pumps that move either chloride or protons. Excitatory channels are generally blue-light sensitive, although variants have been engineered to produce channels with different properties including higher conductance [116]**,** faster kinetic properties [77], improved light sensitivity [14], and red-light sensitivity channels [115]. Inhibitory channels are generally orange/green-light sensitive chloride pumps and proton pumps [39,210], although variants have been developed that improve the red-light sensitivity of the chloride pumps [41], and blue-light sensitive chloride channels have been developed recently as well [13,195].

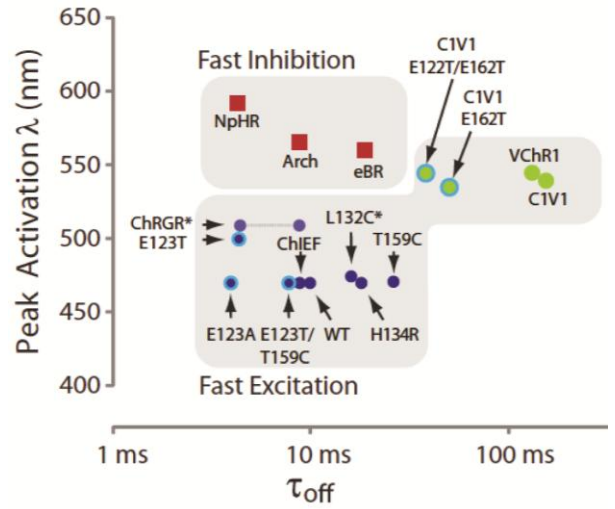

Figure 5: Basic properties of some single-component optogenetic tools Kinetic and spectral attributes of a selection of optotgenetic tool variants. Figure reproduced with permission from Yizhar et al. 2011

As these light-sensitive channels have been developed and refined, they have been applied to a variety of fields, including the pain field. Optogenetic activation of different parts of the locus ceruleus in rats was shown to cause analgesia or hypersensitivity, depending on the region stimulated [84]. Optogenetic modulation has also been demonstrated on the peripheral side of the pain neuraxis, as stimulation of mice expressing channelrhodopsin in Nav1.8-expressing

neurons with a laser on the paw evoked robust nocifensive responses as well as post-stimulation hypersensitivity [52], and optogenetic stimulation of mice expressing the inhibitory eNpHR 3.0 channel in sensory neurons decreases mechanical and heat sensitivity [90]. Optogenetic manipulations of the peripheral nervous system has also been demonstrated by optically stimulating the axons in the sciatic nerve, although in this case activation of motor neuron axons in an *ex vivo* preparation of the sciatic led to an orderly recruitment of motor units that is superior for muscular rehabilitation to electrical stimulation [119]. Subsequent studies using this model allowed the activation of motor neurons through axonal stimulation using a fiber optic cable headmount that then tunneled subcutaneously to the lateral caudal area and terminated in a cuff around the nerve [184]. These studies demonstrate that optogenetic manipulation of the peripheral nervous system is capable of modulating mouse behavior with excellent temporal control, and without physically destroying the neuronal populations being studied.

Conclusion

Maintaining cold sensitivity and adaptation is crucial to survival, but cold hypersensitivity is also a serious clinical issue. The balance between these two extremes is delicate and essential to survival, yet the mechanisms that underlie it are relatively poorly understood. In order to explore these mechanisms that underlie the maintenance of appropriate cold sensitivity, I have developed and validated a novel behavioral assay for cold sensation. In this manuscript, I use this tool, along with a variety of transgenic models and some novel surgical techniques, to investigate the molecular mechanisms and cellular pathways that are essential for normal cold sensation and adaptation.

Chapter 2

The cold plantar assay

Introduction

Cold hypersensitivity is a significant clinical problem which affects a broad subset of patients including multiple sclerosis [177], stroke [74], diabetes mellitus [8], post-herpetic neuralgia [8], and chemotherapy [67,75,93,198] patients. This hypersensitivity significantly affects patient quality of life, and includes both alterations of cold response threshold (cold allodynia) and of the severity of the evoked sensations (cold hyperalgesia) [55,70,74,186]. Treatment of these patients is relatively ineffective in part because the molecular mechanisms that lead to the changes in cold sensitivity are poorly understood. Despite the effort to understand these mechanisms, limitations in the behavioral assays used in these studies have hampered the rate of progress.

As discussed above, while there are a wide variety of techniques to measure cold sensitivity in mice, these techniques also have a number of serious limitations. The cold plate assay measure the behavioral responses once mice are placed on a precooled surface, but is dependent on subjective and unstandardized assessments of response [2] and has extremely high variability. The thermal gradient assay and 2-plate temperature preference test both allow testing for a wide range of temperatures at once, but it is unclear if the data obtained represent temperature aversion or temperature preference [9,139]. The tail flick test measures the latency to withdrawal of the tail from cold water, but requires stressful animal handling during the testing process which can affect the results [157,158]. The acetone test measures sensitivity of acclimated mice to the evaporation of acetone off the hindpaw, but is difficult to standardize and can only measure hypersensitivity from baseline [25,38].

This chapter introduces the cold plantar assay, a novel method for assessing cold sensitivity in mice. The animals are acclimated on a glass plate, and once a rest a pellet made of compressed

dry ice powder is applied the underside of the glass underneath the hindpaw. The amount of time it takes for the mouse to withdraw its paw from the cooling glass can be used as a measure of cold sensitivity. Here I demonstrate that this method delivers a reproducible ramping cold stimulus to fully acclimated mice, and that it can assess hypersensitivity and analgesia with excellent sensitivity and temporal resolution.

Methods

Animal protocols

All mouse protocols were in accordance with National Institutes of Health guidelines and were approved by the Animal Studies Committee of the Washington University School of Medicine (St. Louis, MO). Experiments were carried out with 6-9 week old male Swiss Webster mice purchased from Jackson Labs (Bar Harbor, ME) unless otherwise noted in the text. Mice were housed on a 12/12-hour light/dark cycles with the light cycle beginning at 6 a.m. All mice had *ad libitum* access to rodent chow and water except during the behavioral experiments.

Data analysis

All data were collated in.xlsx files using Microsoft Excel 2011 and analyzed using Graphpad Prism from Graphpad Software (La Jolla, CA). Unless otherwise noted, data graphed represent the mean and the standard error of the mean.

Behavioral analysis

All experiments and analyses were performed by an experimenter blinded to treatment. Behavioral tests were performed between 12 p.m. and 5 pm. Local time unless experimental design required baseline measurements to be assessed in the morning. All experiments in this chapter were performed at room temperature, which was roughly 22°C.

Cold plantar assay

1/8'', 3/16'', and 1/4'' thick pyrex borosilicate float glass was acquired from Stemmerich Inc (St. Louis, MO). Mice were acclimated on the glass plate in transparent plastic enclosures (4'' x 4'' x 11'') and were prevented from seeing each other with opaque black polyvinyl sheets. The lighting was undimmed to maintain the light/dark cycle and a white noise generator was used to isolate the behavioral room from hallway noise.

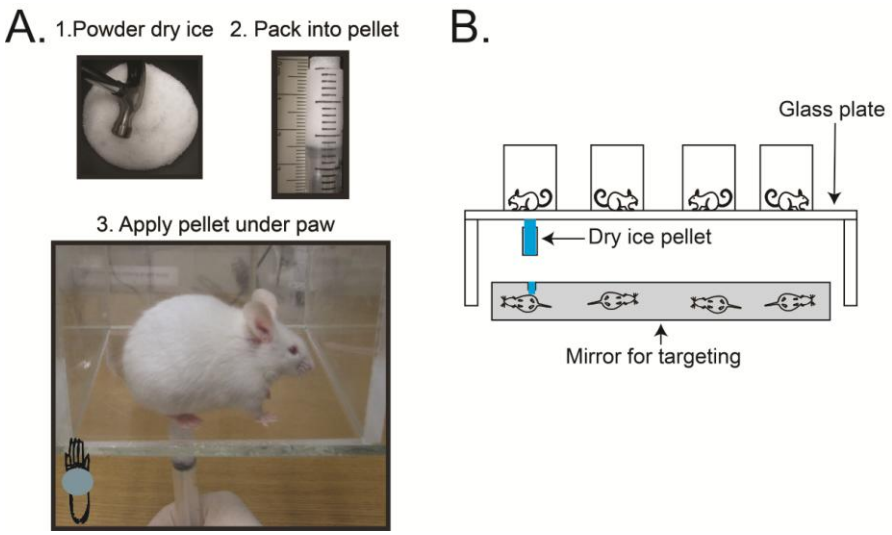

Figure 1. The Cold Plantar Assay
A. Grind dry ice into a fine powder with a hammer (panel 1). Load the dry ice powder into a 3mL syringe and compress against a flat surface until powder cannot be compressed any further (panel 2). Using the syringe plunger, push the dry ice pellet 20-30mm past the tip of the syringe (panel 2). Gently but firmly apply the flat end of the dry ice pellet to the glass surface underneath the paw of the mouse (panel 3) and measure the latency to withdrawal with a stopwatch.
B. Schematic of the cold plantar assay apparatus. Mice are acclimated in plastic enclosures on a glass plate. A mirror is placed underneath the apparatus to facilitate targeting of the dry ice probe. Adapted with permission from Brenner et al. 2012

To generate the cold stimulus, dry ice was crushed into a fine powder using a hammer (**Figure 1A**). The top was cut off a 3mL BD syringe (Franklin Lakes, NJ). In order to prevent gas buildup inside the syringe body, a 21g needle was used to make a total of 6 holes in the body of the syringe, 3 holes on opposing sides. The powdered dry ice was scooped into the modified syringe and the open end of the syringe was held against a flat surface while pressure was applied to the plunger to compress the dry ice into a flattened, dense pellet 1cm in diameter (**Figure 1A**). Mice at rest [23] were tested by applying the tip of the dry ice pellet to the underside of the glass underneath the mouse hindpaw, using mirrors to visualize the target (**Figure 1B**). The pellet was applied with light but consistent pressure applied to the plunger of the syringe, and the center of the hindpaw was targeted, taking care to avoid the distal joints.

The latency to withdrawal from the cooling was measured using a stopwatch. Withdrawal was defined as any motion that moved the paw away from the cooled glass, whether vertically or horizontally. Animals were allowed to recover for at least 7 minutes between cold plantar stimulations on opposite hindpaws, and at least 15 minutes between consecutive stimulations on

any single paw. For baseline experiments, the withdrawal latency was measured at least 3 times per paw per mouse. When the experimental design limited the time window for testing, 1-2 measurements were made per timepoint.

For the experiments in this chapter, a maximum cold stimulus time of 20 seconds was used in order to avoid potential tissue damage. This cutoff time was based on empirical preliminary data. Trials in which the animal did not withdraw from the cold stimulus within 20 seconds were repeated. If the second trial also yielded no withdrawal within the cutoff time, the value was recorded as 20 seconds.

Acetone evaporation test

The acetone evaporation test was performed as previously described [25,71]. Briefly, the mice were acclimated in plastic enclosures separated by opaque black polyvinyl dividers on a wire mesh until they were at rest [23]. After acclimation, acetone was drawn into a 1mL BD syringe (Franklin Lakes, NJ). A droplet maintained by surface tension was pushed through the tip of the syringe and dabbed onto the plantar surface of the hindpaw. The first 10 seconds of activity were disregarded as a response to the tactile stimulus of the application and the wetness of the acetone. The time spent flicking or licking the paw for 60 seconds afterwards was measured with a stopwatch.

Glass temperature measurements

The temperature of the glass surface was measured using an IT-24p filament T-type thermocouple probe from Physitemp Instruments Inc. (Clifton, NJ) and the temperatures were collected once every second using an EA15 Dual-Input data logging thermometer from Extech Instruments (Waltham, MA). The data were output into CSV files that were loaded into Microsoft Excel and analyzed using Graphpad Prism from Graphpad Software (La Jolla, CA).

To measure the temperature generated between the animal hindpaw and the glass surface, mice were lightly anesthetized using a ketamine-xylazine-acepromazine cocktail. The T-type thermocouple filament probe was secured to the glass surface with laboratory tape, with the tip of the filament exposed. The paw of the anesthetized animal was secured on top of the filament, with the center of the paw directly over the tip of the filament (**Figure 2C**). A dry ice pellet was then placed against the underside of the glass underneath the tip of the thermocouple for the proscribed amount of time while the change in temperature was tracked. This analysis was performed on each of the 3 thicknesses of glass (1/8'', 3/16'', and 1/4''). Temperature measurements were also performed using a Hargreaves radiant heat assay apparatus from IITC Life Sciences (Woodland Hills, CA) where active intensity was engaged as soon as the light was focused onto the paw to avoid premature warming from the resting intensity beam. The light stimulus was applied for the average withdrawal latency with the active intensity of 15% (10 seconds).

Morphine injection

Mice were acclimated as described above, and 3 baseline measurements of cold sensitivity were made. Morphine sulfate from Baxter Healthcare (Deerfield, IL) was then diluted in saline and injected subcutaneously in the back at a final dosage of 1.5mg/kg to induce short-term analgesia. Mice were injected with either morphine or saline vehicle, and the experimenter was blind to the contents of each syringe until after data analysis was complete. Measurements of withdrawal latency were taken from the right paw of each animal every 30 minutes until all mice had returned to baseline latency values. No mice were excluded from this analysis.

Complete Freund's Adjuvant

20μL of Complete Freund's Adjuvant (CFA) from Sigma-Aldrich (St. Louis, MO) or .95% Saline from Hospira Inc (Lake Forest, IL) was injected into the right hindpaw of each mouse. Mice were acclimated as described above and at least 3 baseline measurements of withdrawal latency for each paw were taken for each mouse. All mice were then injected in the right hindpaw with either CFA or saline and the withdrawal latencies on both paws were measured at 1 hour, 2 hours, and 3 hours post-injection. 4 hours after intraplantar injection, all mice were given subcutaneous injections of 1.5mg/kg. The withdrawal latencies then were measured 4.5, 5, and 5.5 hours post intraplantar injection. Finally, withdrawal latency measurements were also made at 24 and 48 hours post-intraplantar injection. The experimenter was blinded to the contents of each syringe until after data analysis was completed. No mice were excluded from the analysis.

Spinal Nerve Ligation (SNL)

The spinal nerve ligation procedure was performed as described previously [100,187]. Baseline withdrawal latency and acetone evaporation responses were measured on all mice. The mice were then deeply anesthetized with ketamine/acepromazine/xylazine cocktail and the paraspinal muscles were bluntly dissected to expose the left L5 transverse process. Mice receiving the full ligation procedure had the L5 process removed and the left L4 spinal nerve was tightly ligated with 6-0 silk suture from Ethicon (Cornelia, GA) and transected distal to the ligation. Mice receiving a sham procedure had the L5 transverse process exposed, but not removed and the nerve was untouched. The cold plantar assay withdrawal latency was then measured 3, 6, and 10 days after surgery. The responses to acetone application were measured 2, 5, and 11 days after surgery. After the baseline measurements on days 10/11, on both days the mice were injected subcutaneously with 1.5mg/kg morphine and then tested for their cold responsiveness 30, 60, and

90 minutes after morphine injection. The experimenter was blinded to the surgical procedure received by each mouse until after data analysis was completed. No mice were excluded from analysis.

Results

The cold plantar assay (CPA) elicits consistent responses

To measure the cold response threshold of mice to a cold stimulus, a compressed dry ice pellet is applied to the underside of the glass plate underneath the hindpaw (**Figure 1**). Condensation generally appeared on the glass around the cooled area after the stimulation, but not during. Application of the cold stimulus resulted in nocifensive responses including lifting of the paw followed by a combination of licking, flicking, or biting of the tested paw lasting 1 second to one minute. The latency to withdrawal from the cooling glass can be used as a measure of the cold sensitivity of the animal.

The withdrawal latency of naïve Swiss Webster mice was measured on 1/8'', 3/16'', and 1/4'' thick glass. The latency to hindpaw withdrawal from the glass surface was lowest for the 1/8'' plate (3.79s±0.5s), and increased as the thickness increased to 3/16'' (7.29s±0.9s) and then 1/4'' (11.63s±1.3s) (**Figure 2A** 1-way ANOVA with Bonferroni post-hoc test ***$p<0.0001$ for all comparisons). The average cold plantar withdrawal latency of C57BL/6 mice was also measured on all three thicknesses and found that the latencies were consistent between backgrounds (**Figure 2B** 1/8''=3.83s±0.5s, 3/16''=7.0±1.4s, 1/4''=10.4±0.9s, 1-way ANOVA with Bonferroni post-hoc test ***$p<0.0001$ for all comparisons).

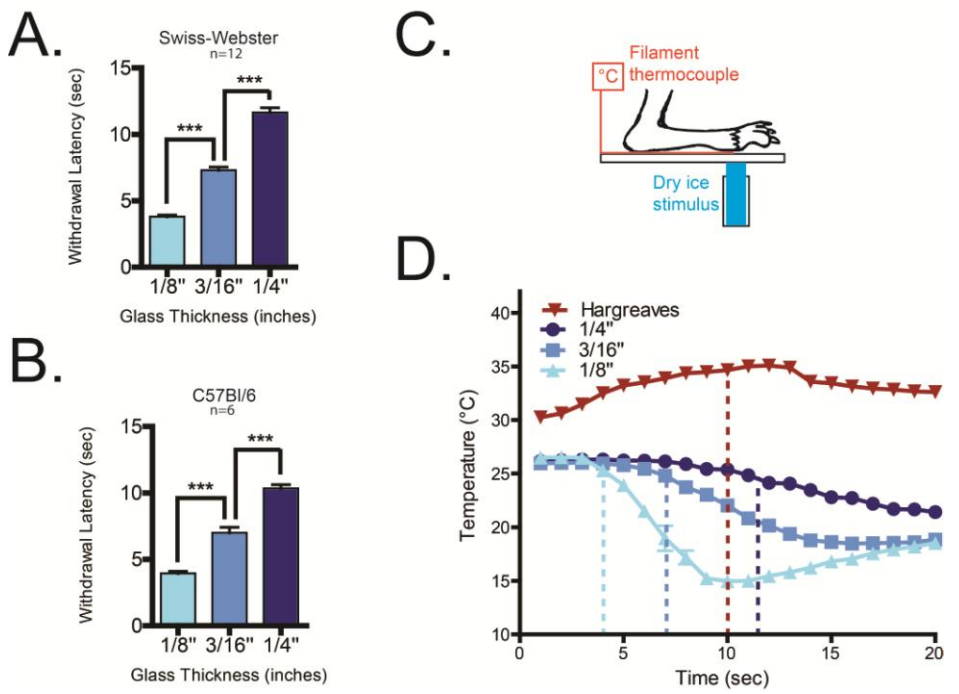

Figure 2. The cold plantar assay applies a consistent ramping cold stimulus
A. The cold plantar withdrawal latency increases as thicker glass plates are used. With Swiss Webster mice, on the 1/8'' glass the average latency is 3.79±0.5 seconds, on the 3/16'' glass the average latency is 7.29±0.9 seconds, and on the 1/4'' glass the average latency is 11.63±1.3 seconds. The average latencies on each glass are significantly different (1-way ANOVA with Bonferroni post-hoc test ***p<.0001 between all thicknesses; n= 12 mice per glass)
B. With C57 mice, on the 1/8'' glass the average latency is 3.83±0.5 seconds, on the 3/16'' glass the average latency is 7.0±1.4 seconds, and on the 1/4'' glass the average latency is 10.4±0.9 seconds. The average latencies on each glass are significantly different (1-way ANOVA with Bonferroni post-hoc test ***p<.0001 between all thicknesses; n= 10 mice per glass)
C. Schematic showing how the temperature between the paw and the glass was measured.
D. Curves representing the change in temperature between the paw and the glass during and shortly after dry ice stimulation. For each curve, the dry ice stimulus begins at x=1, and ends at the colored arrow for that thickness (from 2A, 1/8'': 3.79 seconds, 3/16'': 7.29 seconds, 1/4'': 11.63 seconds). Based on these curves, mice withdraw after a 1.3°C (1/8''), 1.5°C (3/16''), or 2°C (1/4'') change in temperature (n= 6 per glass thickness). Adapted with permission from Brenner et al. 2012

Consistent drops in temperature cause CPA responses

It is important to know the magnitude of the cold stimulus being delivered to the mouse paw. In order to measure this stimulus, mice were anesthetized and their paws were secured over a filament thermocouple probe on the glass (**Figure 2C**). In order to mimic the experimental conditions, the cold stimulus was applied underneath the thermocouple for the amount of time that would cause an awake mouse to withdraw from the cooled glass (**Figure 2D**). On the 1/8'' thick glass the stimulus ends at 4s, and the temperature between paw and glass decreased by 1.3°C (**light blue triangles, dotted light blue line**). On the 3/16'' thick glass the stimulus ends at 7s, and the temperature between paw and glass decreased by 1.5°C (**royal blue squares, dotted royal blue line**). On the ¼'' thick glass the stimulus ends at 10 seconds, and the temperature between paw and glass decreased by 2°C (**dark blue circles, dotted dark blue**

line). This temperature measurement analysis was also performed using the conventional Hargreaves radiant heat apparatus with a pre-heated glass plate, and after 10 seconds of radiant thermal stimulation (the average stimulus capable of causing withdrawal under these conditions) the temperature between the glass and the paw increased by 4.3°C (**Figure 2C** n=6).

The CPA requires direct contact between paw and glass surface

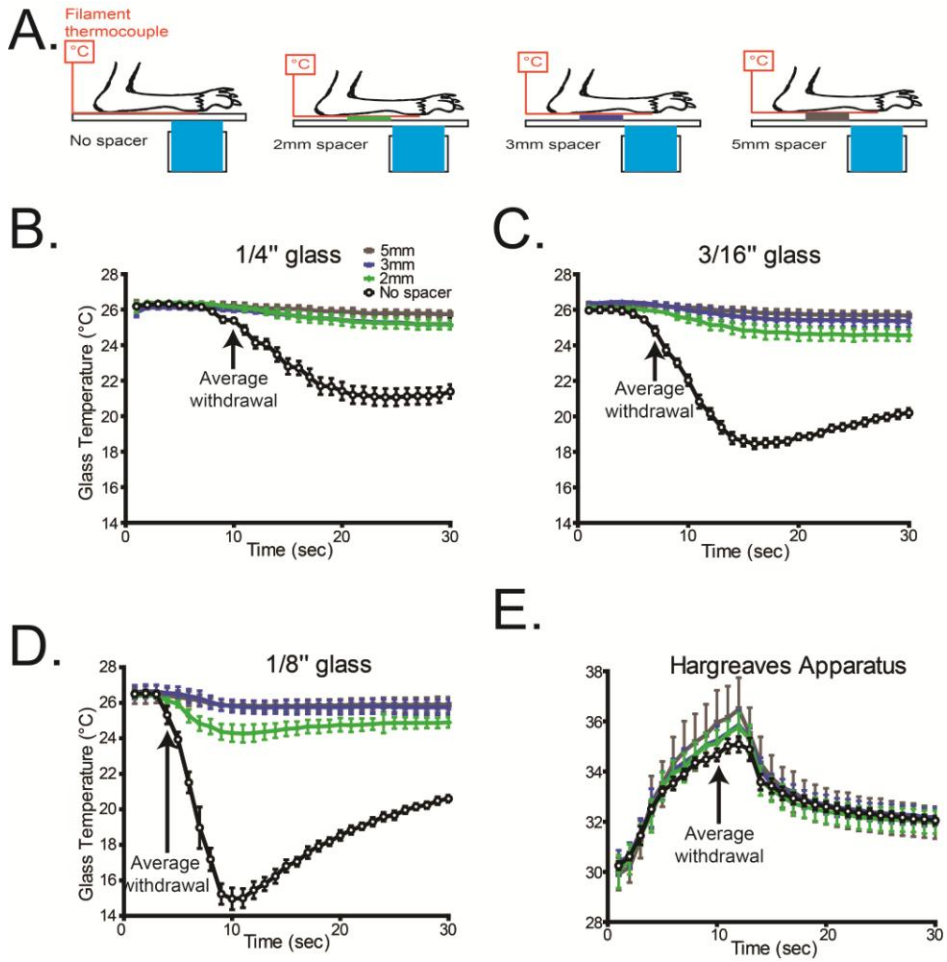

Figure 3. The cold plantar assay requires direct paw-glass contact
A. Schematic diagramming the experimental design
B-D. The temperature during cold plantar stimulus underneath the paw was measured on all three glass thicknesses under normal conditions, and with styrofoam spacers propping the paw away from the glass surface. In all cases, propping the paw away from the glass caused a dramatic decrease in the cold stimulus measured at the paw (n= 6 per glass thickness).
E. The temperature underneath the paw was measured during Hargreaves radiant heat stimulation with the paw propped up with styrofoam. Unlike the cold plantar assay, the thermal stimulus in the Hargreaves assay is largely unaltered when the paw is propped away from the glass (n= 6). Adapted with permission from Brenner et al. 2012

It is important to know how experimental conditions must be standardized. In order to test whether direct contact between the paw and the glass is necessary to generate a consistent cold stimulus, thin styrofoam spacers were used to incrementally separate the paw and thermocouple from the cooling glass surface (**Figure 3A**). When the paw is separated from

the glass surface, the cold stimulus from the dry ice probe is dramatically decreased (**Figure 3B-D**, n=6). This analysis was also performed using the Hargreaves apparatus and found that the radiant heat stimulus was unaffected by the separation of the paw from the glass (**Figure 3E**, n=6).

The CPA can quantify rapid changes in nocifensive responsiveness

An important part of behavioral assays is the ability to detect transient changes in nocifensive sensitivity. In order to show that the CPA can detect rapid changes in nocifensive responsiveness, transient analgesia was induced using subcutaneous injections of 1.5 mg/kg morphine over the coccyx. Baseline CPA withdrawal latencies were measured, and then latencies were measured at 30, 60, and 90 minutes after injection of morphine or a saline control. The latency to withdrawal was significantly increased after 30 minutes for the morphine-injected group compared to the saline-injected group (**Figure 4A** 2-way ANOVA main effect *$p<0.05$ with Bonferroni post-hoc test; 30 minutes Morphine=16.4s±1.5s, Saline=12.4s±0.8s **$p<0.01$; n=12 per group). By 60 minutes post-morphine, the latency to withdrawal returned to baseline levels, consistent with the typical rate of morphine metabolism in mice [212].

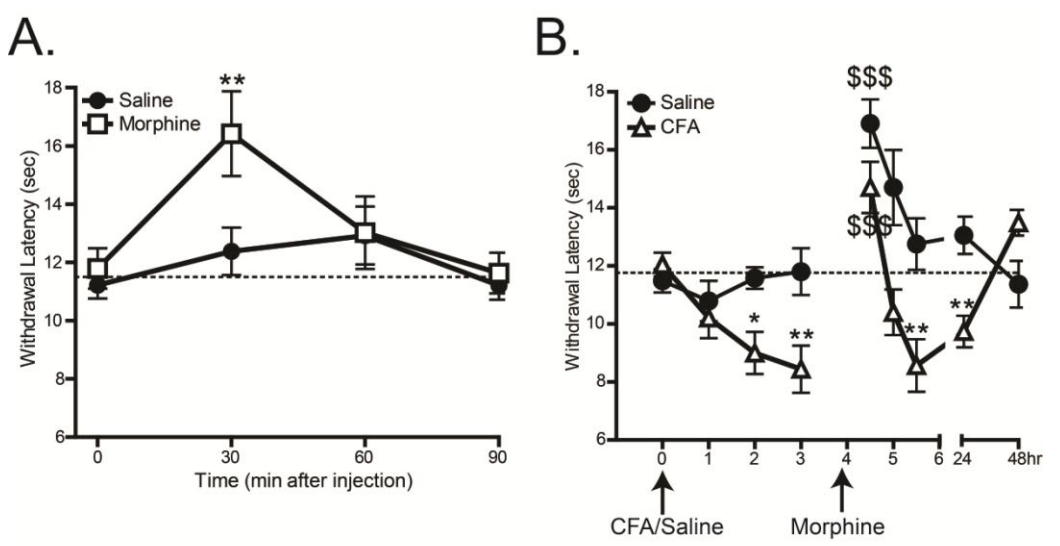

Figure 4. The cold plantar assay can measure analgesia and allodynia
A. Mice were given subcutaneous injections of 1.5mg/kg morphine or saline. Thirty minutes after injection, morphine-injected mice had significantly higher withdrawal latencies on the 1/4" glass, but 60 minutes after injection the morphine injected mice had returned to baseline latency values (2-way ANOVA main effect *p<0.05 with Bonferroni post-hoc test; 30 minutes **p<0.01; n= 12 per group).
B. Mice were given intraplantar injections of Complete Freund's Adjuvant or saline. 2 and 3 hours after injection, CFA-injected mice had significantly lower withdrawal latencies on the 1/4'' glass than the saline-injected controls (2-way ANOVA main effect p<.0001 with Bonferroni post-hoc test; 120 minutes *p<0.05, 180 minutes **p<0.01 n= 12 per group). 4 hours after intraplantar injection, all animals were given subcutaneous injections of 1.5mg/kg morphine. At 4.5 hours both CFA- and Saline-injected animals had significantly increased withdrawal latencies compared to their values at 3 hours (1-way ANOVA with Dunnett's post-hoc test; CFA 3hours vs. CFA 4.5 hours $$$ p<0.0001, Saline 3 hours vs. Saline 4.5 hours $$$ p<0.0001). At 5.5 hours, the CFA-injected mice had significantly lower withdrawal latencies than their saline-injected counterparts (2-way ANOVA with Bonferroni post-hoc test; 5.5 hours **p<0.01). 24 hours after intraplantar injection, the CFA-injected mice still had significantly lower withdrawal latencies than their saline-injected counterparts, but this difference resolved by 48 hours (2-way ANOVA with Bonferroni post-hoc test; 24 hours ** p<0.01, 48 hours p>0.05). Adapted with permission from Brenner et al. 2012

It is also important to show that a behavioral assay can quantify the interaction between hypersensitivity and analgesics. In order to demonstrate that the CPA is capable of measuring this interaction in mice, intraplantar injections of Complete Freund's Adjuvant (CFA) were administered to cause cold hypersensitivity, and then transiently blocked the hypersensitivity with subcutaneous injections of morphine (**Figure 4B**). Baseline measurements of cold sensitivity were made, and then inflammation was induced with 20μL intraplantar injections of CFA or a saline control. The cold plantar withdrawal latency was measured on both hindpaws (injected and contralateral) at 1, 2, and 3 hours after injection. The withdrawal latency of the CFA-injected mice was significantly decreased at 2 and 3 hours post injection, demonstrating that the CPA can measure inflammatory cold hypersensitivity (**Figure 4B**; 2-way ANOVA main effect p<0.001 with Bonferroni post-hoc test; 2 hours Saline=11.6s±0.4s, CFA=8.9s±0.7

*p<0.05; 3 hours Saline=11.8s±0.8s, CFA=8.4s±0.8s**p<0.01 n=12 per group). At 4 hours post intraplantar injection, after the cold hypersensitivity had been established, all mice were given subcutaneous injections of 1.5mg/kg morphine. 30 minutes after morphine injection, both control- and CFA-injected mice had increased withdrawal latencies compared to their pre-morphine injection latencies (**Figure 4B** 4.5 hours; 1 way ANOVA with Dunnett's post-hoc test; Saline 3 hours=11.8s±0.8s, Saline 4.5 hours=16.9s±0.8s $$$p<0.0001; CFA 3 hours=8.4s±0.8s, CFA 4.5 hours=14.7s±0.9s $$$p<0.0001; n=12). Once the morphine had been metabolized (5 hours), neither group was significantly different from the withdrawal latencies at 3 hours (**Figure 4B** 5 hours; 1-way ANOVA with Dunnett's post-hoc test; CFA and Saline p>0.05). By 5.5 hours after intraplantar injection, the inflammatory cold hypersensitivity was again detectable as the mice injected with CFA had significantly lower withdrawal latencies than mice injected with saline (**Figure 4B** 2-way ANOVA with Bonferroni post-hoc test; 5.5 hours Saline=12.8s±0.9s, CFA=8.6s±0.9s; n=12). The cold hypersensitivity that was induced by intraplantar CFA was maintained for 24 hours (**Figure 4B** 2-way ANOVA with Bonferroni post-hoc test; Saline=13.1s±0.6s, CFA=9.7s±0.5s **p<0.01; n=12), but returned to the same values as the saline-injected mice by 48 hours (**Figure 4B** 2-way ANOVA with Bonferroni post-hoc test; p>0.05, n=12). Contralateral paw withdrawal latencies were measured at all time points, and were unchanged by experimental manipulations (data not shown).

The cold plantar assay can also quantify the interaction between neuropathic injury and analgesics. This was demonstrated using the L4 Spinal Nerve Ligation (SNL) procedure. Baseline cold sensitivity was assessed using both the cold plantar assay and the acetone evaporation test, before the mice were treated with either the SNL procedure or a sham procedure. After the surgical procedures, the amount of time that was spent flicking the injured

paw after acetone application was significantly increased in SNL mice compared to the shame mice (**Figure 5B** 2-way ANOVA main effect *p<0.05 with Bonferroni post-hoc test; individual timepoints not significantly different, Sham n=5, SNL n=6). When tested with the CPA, the SNL mice had significantly decreased withdrawal latency at 3, 6, and 10 days after surgery (**Figure 5A** 2-way ANOVA main effect ***p<0.001 with Bonferroni post-hoc test; 3 days Sham=12.6s±0.7s, SNL=7.6s±0.7s ***p<0.001; 6 days Sham=12.5s±1.0s, SNL=8.2s±0.7s **p<0.01; 10 days Sham=12.1s±0.1s, SNL=7.4s±0.6s **p<0.01; Sham n=5, SNL n=6).

Ten days after surgery, cold plantar withdrawal latencies were measured and then 1.5mg/kg morphine was injected subcutaneously. Both sham and SNL groups showed increased withdrawal latencies 30 minutes after morphine injection (**Figure 5A** 1-way ANOVA with Dunnett's post-hoc test; Sham 10d=12.1s±0.1s, 30m=16.2s±0.7s $$p<0.05, CFA 10d=7.4s±0.6s, 30m=13.5s±2.2s $p<0.05). By 60 minutes post-morphine, the SNL mice were hypersensitive to cold plantar stimulus again, while the sham mice had returned to their baseline measurements (**Figure 5A** 2-way ANOVA with Bonferroni post-hoc test; Sham 90m=13.3s±1.3s, SNL 90m=6.7s±1.6s***p<0.001).

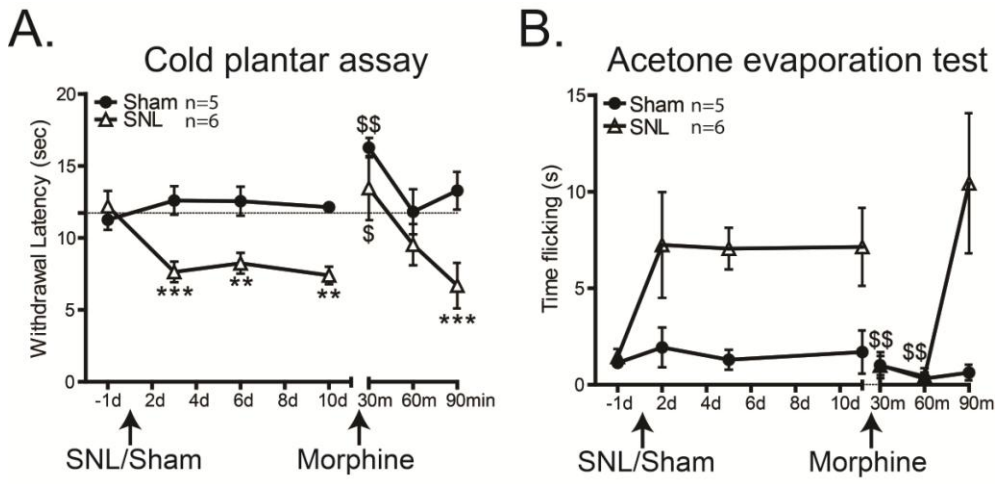

Figure 5: The cold plantar assay can measure L4 spinal nerve ligation induced allodynia
Mice underwent the spinal nerve ligation (SNL) procedure or a sham procedure on day 0.
A. On days 3, 6, and 10 post surgery SNL mice had significantly lower cold plantar withdrawal latencies on the 1/4" glass than sham mice (2-way ANOVA main effect ***p<0.001 with Bonferroni post-hoc test; 3d ***p<0.001, 6d **p<0.01, 10d **p<0.01; Sham n=5, SNL n=6). After baseline measurements on day 10 post surgery, mice were injected with 1.5mg/kg morphine. Thirty minutes after morphine injection, both SNL and sham mice had withdrawal latencies that were significantly elevated from their baseline values that day (1-way ANOVA with Dunnett's post-hoc test; Sham $ p<0.05, SNL $$ p<0.01). By 90 minutes after morphine injection, the SNL mice again had significantly decreased withdrawal latencies than the sham mice (2-way ANOVA with Bonferroni post-hoc test; ***p<0.001).
B. On days 2, 5, and 11 post surgery SNL mice spent more time flicking after acetone application than sham mice (2-way ANOVA main effect *p<0.05 with Bonferroni post-hoc test; 2 days p>0.05, 5 days p>0.05, 11 days p>0.05). After baseline measurements on day 11 post surgery, mice were injected with 1.5mg/kg morphine. There was a significant reduction in the time responding to acetone in the SNL group but not in the Sham group (1-way ANOVA with Dunnett's post-hoc test; Sham p>0.05, SNL $$ p<0.01). Adapted with permission from Brenner et al. 2012.

Eleven days after surgery, acetone evaporation baselines were measured and then 1.5mg/kg morphine was injected subcutaneously. There was a significant reduction in the time responding to acetone in the SNL group but not in the Sham group (**Figure 5B** 1-way ANOVA with Dunnett's post-hoc test; SNL 11d=7.1s±2.0s, 30 min=0.9s±0.5s, 60 min=0.4s±0.4 $$p<0.05, Sham p>0.05).

Discussion

In this chapter, we demonstrate that the cold plantar assay applies a focal ramping cold stimulus to unrestrained, acclimated mice. This stimulus is consistent, and can be used to measure both cold hypersensitivity and cold analgesia with relatively low variability. It can also be used to quantify the interactions between hypersensitivity and analgesia in ways that were not possible using prior techniques such as the acetone evaporation test. This technique provides a method of testing TRPM8-KO and TRPA1-KO knockout mice without relying on subjective interpretations of mouse behavior.

The biggest limitation is that the paw being tested must be fully contacting the glass plate for the cold stimulus to be delivered. Since mice that are at rest after acclimation generally has their paws in contact with the glass plate this limitation does not present an insurmountable obstacle. However, it is important to keep this limitation in mind when testing mice using inflammatory and neuropathic injury models, as paw guarding and changes in weight distribution may occur after injury. Still, despite this we have found that consistent measurements of cold sensitivity can be made using the CPA even in these injury models (**Figures 4, 5**). Interestingly, the parallel studies using the Hargreaves radiant heat assay show that the Hargreaves stimulus delivered to the paw is largely unchanged whether the paw is in contact with the glass or not.

It is surprising that naïve mice withdraw from temperature drops that range from 1.3-2°C. Even the data using the Hargreaves apparatus show that naïve mice withdraw after an increase of just 4-5°C, much smaller than the previously recorded values [79]. That such small changes in temperature are sufficient to generate a nocifensive response may suggest that the highly specialized mechanisms are acting to ensure that sensitivity to small changes in temperature is constantly maintained.

Chapter 3

The extended cold plantar assay

Introduction

Results obtained with the cold plantar assay suggest that mice respond to very small decreases in temperature. If mice are acutely sensitive to small temperature shifts, large shifts in ambient temperature would overload the mechanisms of cold sensitivity, and the effective dynamic range of cold sensitivity would relatively small. Since mice and other animals have survived in seasonal areas for millennia, this suggests that there are mechanisms that allow the shifting of cold sensitivity levels to match the environmental conditions. In order to study these mechanisms *in vivo*, behavioral assays that can measure the effect of altering the environmental temperature on cold sensitivity are necessary.

Previously, the only assay capable of measuring the effect of changing environmental temperatures on was the "dynamic cold plate," [55,206] in which mice are put on a room temperature Peltier device which is then rapidly cooled (1°C/min) until it reaches 1°C. Behavioral responses such as licking, rearing, and jumping are measured at different temperature ranges and used to estimate cold responsiveness. While this assay can dynamically test the responses of animals to cooling it also has some limitations. It measures how a mouse responds to a cooling environment, but does not provide a way to test responsiveness to a discrete cold stimulus in the context of environmental cooling. Like the regular cold plate, the dynamic cold plate is also confounded by environmental novelty since the animals are tested on the cold plate without the chance to acclimate to the environment unless they are acclimated for significant periods before the cooing begins, which increases the amount of time necessary to test each

mouse. It also requires expensive equipment, can only test one mouse at a time, and relies on subjective characterizations of mouse behavior during the cooling.

In order to investigate the factors that lead to withdrawal from cold stimuli, the cold plantar assay was extended to test the responses to cold stimuli with different starting temperatures. This new assay, the extended Cold Plantar Assay (eCPA) can test the cold responsiveness of mice at any ambient temperature range between 5-30°C. The eCPA provides an easily quantified, objective measure of cold responsiveness to a uniform cold stimulus at different environmental temperatures. This modification is a significant improvement for testing cold sensitivity under different environmental changes.

Methods

Animal protocols

All mouse protocols were approved by the Animal Care and Use Committee of the Washington University School of Medicine (St. Louis, MO) and were in accordance with National Institutes of Health Guide for the Care and Use of Laboratory Animals. Experiments were carried out with Swiss Webster mice acquired from Jackson Labs (Bar Harbor, ME) unless otherwise noted. Efforts were made to minimize the number of animals used, to minimize suffering. All mice used were male and 6-9 weeks old unless specifically noted. Mice were housed on a 12/12 hour light/dark cycle with the light cycle beginning at 6am. All mice had ad libitum access to rodent chow and water. Cage bedding was changed once a week, always allowing at least 48 hours after a bedding change before behavioral testing was carried out. Mice were allowed at least 3 days between behavioral testing at any ambient temperature, and were tested first using at room temperature, followed by 17°C, 12°C, 5°C, and 30°C.

Behavioral analysis.

All behavioral tests and analyses were conducted by an experimenter blinded to treatment. Behavioral tests were performed between 12pm and 5pm.

The extended cold plantar assay (eCPA).

.125'', .1875'', and .25'' thick pyrex borosilicate float glass was purchased from Stemmerich Inc. (St. Louis, MO). Transparent plastic enclosures (4'' x 4'' x 11'') separated by opaque black dividers were arranged in one line along the center of the plate (**Figure 1A-B)**.

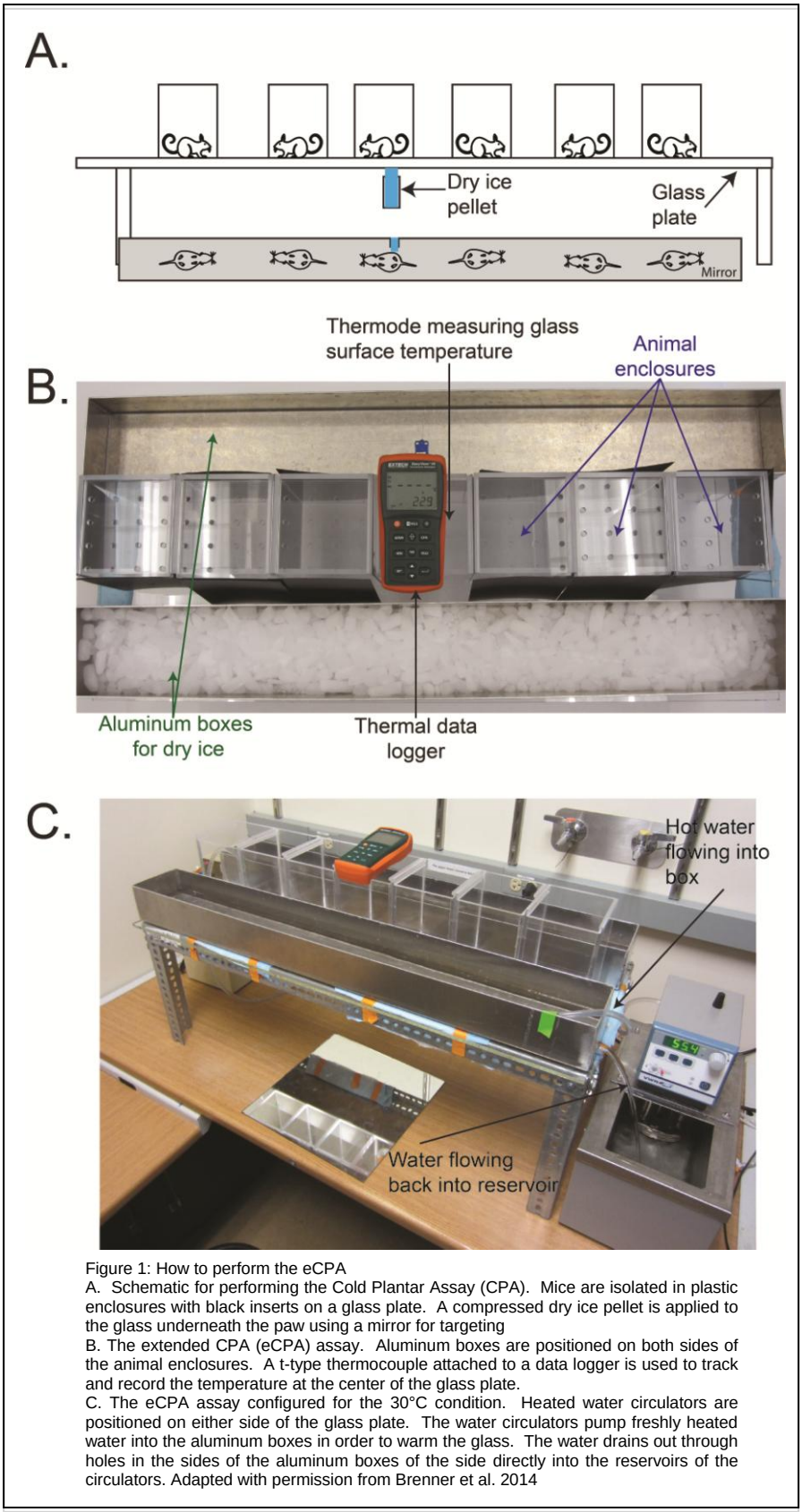

Figure 1: How to perform the eCPA
A. Schematic for performing the Cold Plantar Assay (CPA). Mice are isolated in plastic enclosures with black inserts on a glass plate. A compressed dry ice pellet is applied to the glass underneath the paw using a mirror for targeting
B. The extended CPA (eCPA) assay. Aluminum boxes are positioned on both sides of the animal enclosures. A t-type thermocouple attached to a data logger is used to track and record the temperature at the center of the glass plate.
C. The eCPA assay configured for the 30°C condition. Heated water circulators are positioned on either side of the glass plate. The water circulators pump freshly heated water into the aluminum boxes in order to warm the glass. The water drains out through holes in the sides of the aluminum boxes of the side directly into the reservoirs of the circulators. Adapted with permission from Brenner et al. 2014

The cold probe was generated as previously described [21]. Briefly, powdered dry ice with a surface temperature of -78.5°C was compressed against a flat surface in a 3mL BD syringe (Franklin Lakes, NJ) with the top cut off until it reached a dense, uniform consistency. Awake mice were tested by extending the tip of the dry ice pellet past the end of the syringe and pressing it against the glass underneath the hindpaw with light pressure using the syringe plunger. The center of the hindpaw was targeted, avoiding the distal joints, and ensuring that the paw itself was touching the

glass surface.

The latency to withdrawal of the hindpaw was measured with a stopwatch. Withdrawal was defined as any action to move the paw vertically or horizontally away from the cold glass. Trials on separate paws of the same animal were separated by 7 minutes, and at least 15 minutes separated trials on any single paw. At least 3 trials per paw per mouse were recorded unless otherwise noted.

The glass temperature was monitored with an IT-24P T-type filament thermocouple probe from Physitemp Instruments, Inc. (Clifton, NJ) that was secured in the middle of the plate with laboratory tape. Plate temperature data were collected from the thermocouple using an EA15 Data-Logging Dual Input Thermometer from Extech Instruments (Waltham, MA) (**Figure 1A-B**). Dry ice or wet ice was piled on either side of the enclosures to uniformly cool the glass plate. The ice was contained either in packets made of heavy-gauge aluminum foil, or in custom-built aluminum boxes (**Figure 1A-B).** The boxes were the same length as the glass plate, 4.5 inches wide and 3 inches tall with a lid. A drain with a stopcock was installed at the bottom of one short end of each box to allow easy drainage. The glass temperature was be adjusted by moving the ice containers closer to or further from the plastic enclosures (**Figure 2A-B**), or by filling the container with hot water. After the plate reached the desired temperature, mice were acclimated in the enclosures for 3 hours before testing. White noise was used to decrease noise disturbances. Due to the CO_2 generated when using dry ice, we found that it was essential to have adequate ventilation over the apparatus or the mice may enter torpor. With proper ventilation, there were no signs of CO_2 intoxication in any condition.

Testing mice at 30°C

To warm the glass plate to 30°C, the aluminum boxes were positioned approximately .25'' away from the animal enclosures on either side. A VWR water circulator continually fed water heated to between 50-60°C into the aluminum boxes in order to warm the plate up (**Figure 1C**). The exact temperature of the water circulators was calibrated during each experiment to keep the plate at 30°C. The water exited the aluminum boxes through the drain holes at the bottom of the short ends, and flowed directly back into the reservoir of the circulators for reheating. After approximately 90 minutes the plate warmed to 30°C and remained at that temperature as long as the circulators were active (**Figure 2A-B**).

T*esting mice at 17°C*

To cool the glass plate to 17°C, the aluminum boxes were positioned approximately .25'' away from the animal enclosures on either side, and filled with wet ice (**Figure 2A-B**). After approximately 60 minutes the plate cooled to 17°C and remained at that temperature as long as the boxes were refilled with wet ice roughly every 90 minutes and excess water was drained.

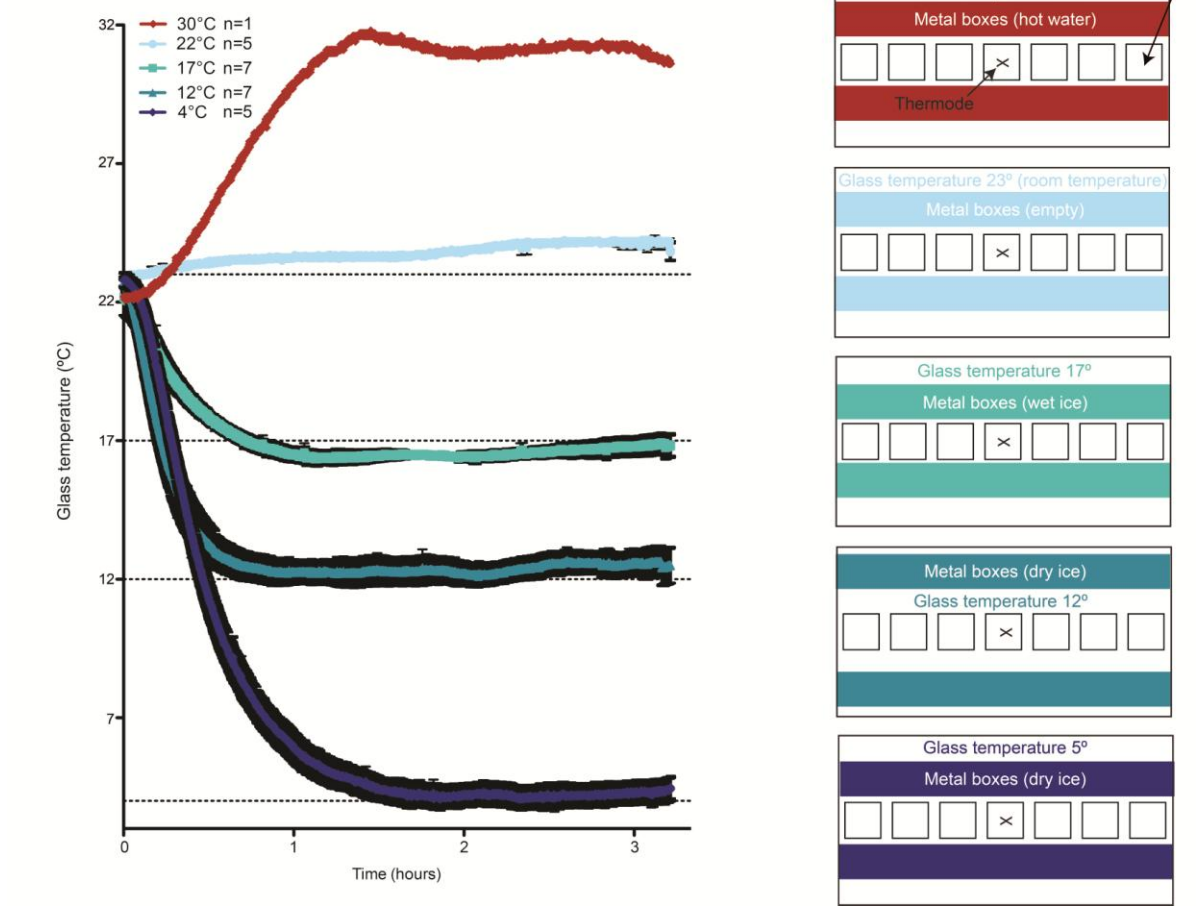

Figure 2: The eCPA can stably generate a wide range of temperatures for cold response testing
A. The surface temperature of the glass plate was measured during behavioral experiments. The targeted temperature ranges were reproducibly generated using the eCPA apparatus. Each curve is generated by averaging the glass plate temperature during behavioral experiments with 6 mice on the plate for the entire course of the measurements. 30°C n=1 experiment, 23°C n=5 experiments averaged, 17°C n=7 experiments averaged, 12°C n=7 experiments averaged, and 5°C n=5 experiments averaged.
B. Schematic illustrating eCPA temperature management. To generate a surface temperature of 30°C the aluminum boxes are filled with hot water as shown in Figure 1C. To generate a surface temperature of 17°C the aluminum boxes are filled with wet ice and placed ~.25'' away from the animal enclosures. To generate a surface temperature of 12°C the boxes are filled with dry ice and placed towards the edge of the plate, ~1.25'' away from the enclosures. To generate a surface temperature of 5°C the boxes are filled with dry ice and placed ~.25'' away from the animal enclosures. Adapted with permission from Brenner et al. 2014

Testing mice at 12°C

To cool the glass plate to 12°C, the aluminum boxes were positioned roughly 1.25'' away from the animal enclosures on either side and filled with dry ice pellets (**Figure 2A-B)**. After approximately 20 minutes, the plate cooled to 12°C and remained at that temperature as long as the boxes were refilled with dry ice roughly every 90 minutes.

Testing mice at 5°C

To cool the glass plate to 5°C, the aluminum boxes were positioned roughly .25'' away from the animal enclosures on either side and filled with dry ice pellets (**Figure 2A-B**). After approximately 60 minutes the plate cooled to 5°C and remained at that temperature as long as the boxes were refilled with dry ice roughly every 90 minutes.

Testing mice during the dynamic cooling phase

To measure the cold sensitivity of the mice during the dynamic cooling phase, the mice were acclimated in enclosures as described above at room temperature. Baseline withdrawal latency was measured at room temperature. The aluminum boxes are pre-filled with dry ice and allowed to cool before being placed on the glass surface roughly 1.25'' from the animal enclosures on either side to cool the plate. Withdrawal latencies are measured immediately as the plate cools, and the temperature of the glass plate was recorded along with every latency.

Results

The cold plantar assay, introduced in Chapter 2, measures the cold sensitivity of mice at room temperature. The testing involves applying a pellet made of compressed dry ice to the underside of a glass plate underneath the hindpaw. Naïve mice generally respond after 11 seconds, which corresponds to a temperature decrease of roughly 1.3°C [21]. While the CPA can only test responsiveness in a small temperature range close to room temperature, it would be better to test cold sensation at a wide range of temperatures.

To extend the utility of the CPA and enable studies of cold sensation at different ambient temperatures, the entire glass testing plate is cooled to a lower starting temperature. From these lower starting temperatures, the withdrawal latencies of the animals were measured. Using 2 custom-built 1/8'' aluminum boxes, the CPA testing glass was warmed to 30°C, left at room temperature (23°C), cooled stably to 17°C using wet ice, or cooled stably to 12°C using dry ice (**Figure 2)**. Although the experiments in this manuscript test responses using plate temperatures of 30°C, 23°C, 17°C, and 12°C, the apparatus has also been used to test cold responses at starting temperatures as low as 5°C (**Figure 2**).

Glass plate temperatures in the eCPA were stable

The temperature of the glass surface was monitored constantly throughout the eCPA testing using an IT-24p t-type thermocouple probe attached to the center of the plate (**Figure 1B**). Temperature recordings of the eCPA glass surface under the 30°C, 23°C, 17°C, 12°C, and 5°C conditions showed that the testing surface rapidly cooled/warmed to the desired temperature, and that this temperature remained stable for the length of the experiment (**Figure 2A**). The conditions used to generate these temperature curves are described in depth in the methods section and pictured in **Figure 2B**. Briefly, the 30°C condition was generated using hot water

circulators, the 17°C condition was generated using wet ice, and the 12°C and 5°C conditions were generated using dry ice and varying the distance from the enclosure to fine-tune the glass surface temperature.

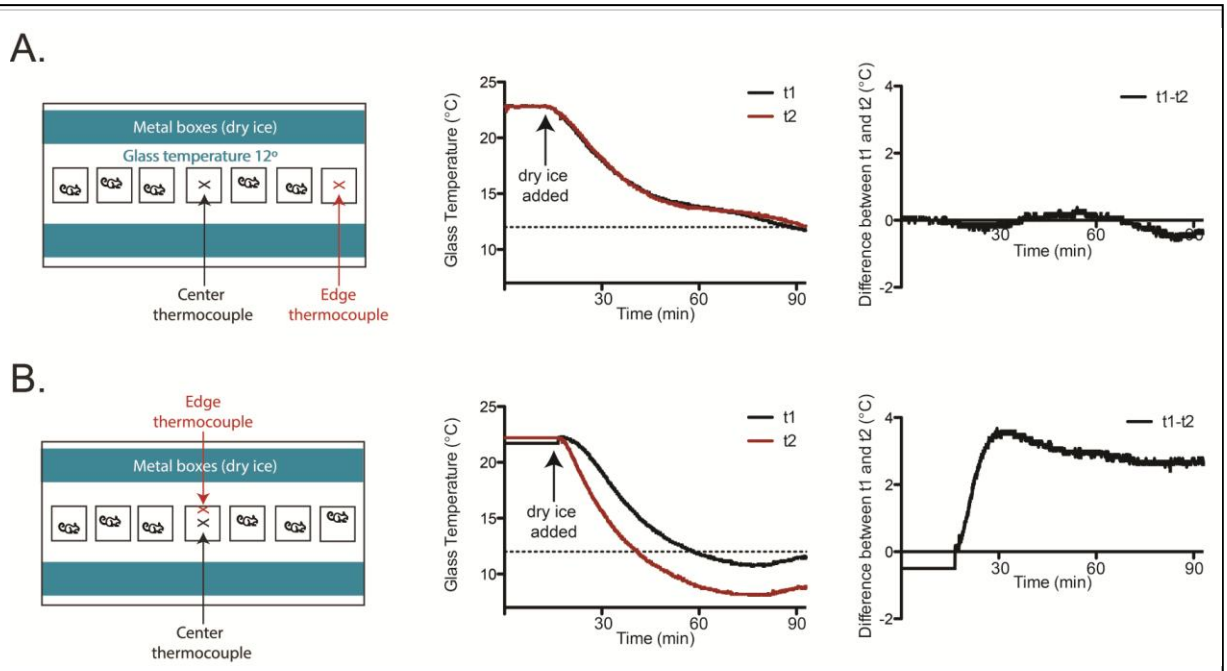

Figure 3: Temperatures generated are consistent across the glass plate
A. Thermocouple t1 (black) was placed at the center of the plate. Thermocouple t2 (red) was placed in the behavioral enclosure closes to the right edge of the plate. The temperature tracings and the graph at the far right (t1-t2) show nearly identical temperatures at t1 and t2 throughout the course of the experiment.
B. Thermocouple t1 (black) was placed at the center of the plate. Thermocouple t2 (red) was placed in the central behavioral enclosure, at the wall closer to the dry ice-filled aluminum boxes. The temperature tracings and the graph at the far right (t1-t2) show that there is a roughly 3°C difference between t1 and t2 once the plate has reached a stable temperature. Adapted from Brenner et al. 2014

Glass plate cooling in the eCPA was uniform across the plate To ensure that the glass was being uniformly cooled, behavioral tests were performed using 2 IT-24p thermocouples to simultaneously monitor the glass temperature at different locations (**Figure 3**). The glass surface was cooled to 12°C while measuring both at the center of the glass plate, and in the middle of the plate along the far edge. The temperatures reported at both thermocouples were identical, suggesting that the middle of the glass plate is uniformly cooled from edge to edge (**Figure 3A**). It was also hypothesized that the edge of the enclosures, which were closer to the dry ice, would be colder than the center of the enclosures. In order to test this hypothesis, the glass plate was cooled to 12°C and the temperature at the center of the testing enclosure was compared to the temperature at the edge of the testing enclosure. As expected, a cold gradient was generated on the glass surface in the eCPA, with the glass at the edge of the testing enclosures roughly 3°C colder than the glass in the middle of the testing enclosures (**Figure 3B**). While this variation in

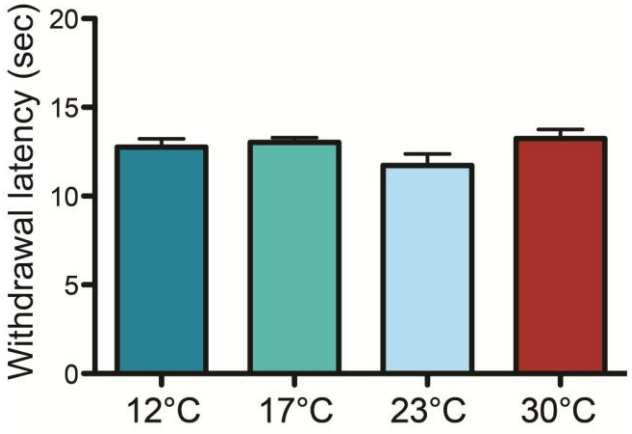

Figure 4: eCPA withdrawal latencies are consistent
6-9 week old male Swiss Webster mice were tested using the eCPA with the glass plate starting at 12°C (latency=12.8s±.5), 17°C (latency=13.0s±.3), 23°C (latency=11.7s±.7), or 30°C (latency=12.38s±.4). n=6 for all groups. 1-way ANOVA with Bonferroni post-hoc test, no significant differences between any groups. Adapted with permission from Brenner et al. 2014

glass temperature is substantial, when the plate is cooled to 12°C mice spent most of their time in the central area of the enclosure where the temperature was more uniform. Additionally, the standard deviation for the withdrawal latencies measured in this condition was quite low, suggesting low variability between the mouse responses despite the temperature gradient of the plate.

eCPA withdrawal latencies are consistent

Despite the variability in temperature across the testing enclosure, the withdrawal latencies measured at these temperatures were very consistent. The withdrawal latencies of adult Swiss Webster mice tested at all three temperature ranges had relatively low variability (**Figure 4** 12°C=12.8s±0.5, 17°C=13.0s±0.3 23°C=11.7s±0.7, 30°C=12.38s±0.4, n=6 mice tested under each temperature condition; 1-way ANOVA with Bonferroni post-hoc test, no significant differences between any groups).

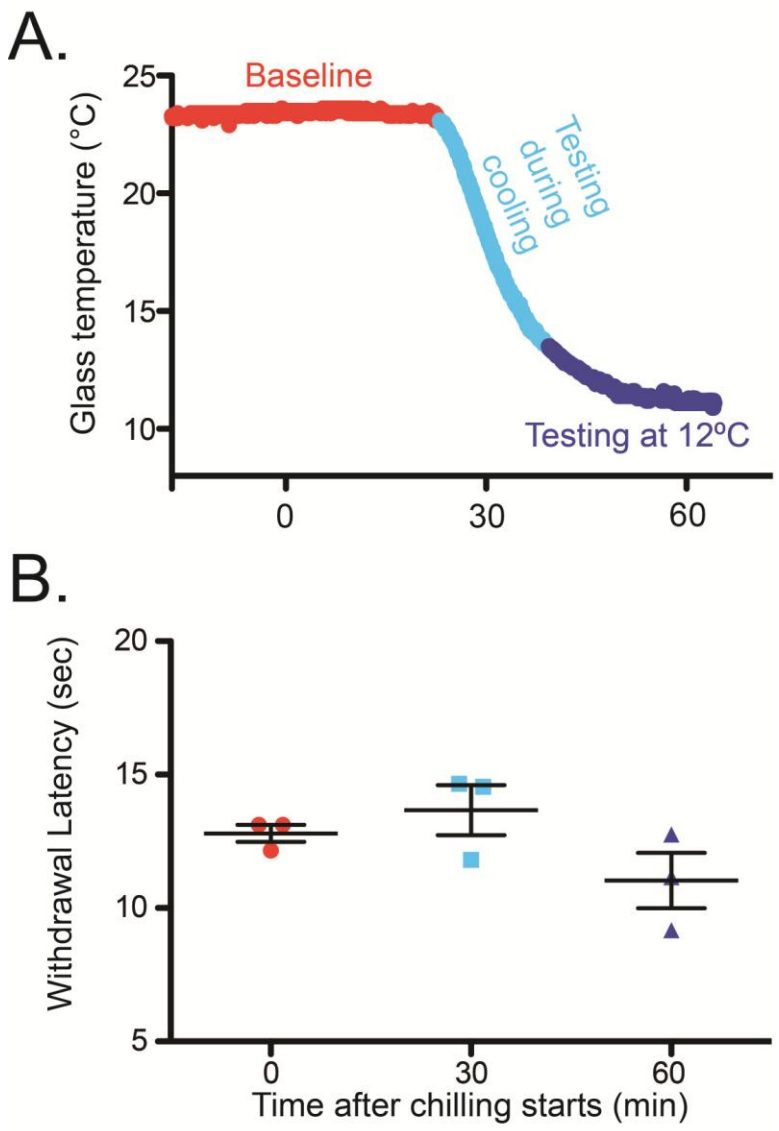

Figure 5: The eCPA can measure withdrawal latency as mice adapt to cold ambient temperatures
A. The surface temperature of the glass plate was measured during a behavioral experiment. Baseline withdrawal latencies (red) were measured at room temperature and then precooled aluminum boxes containing dry ice were placed on the glass surface. As the glass cooled, withdrawal latencies were measured (light blue), and latencies were also measured once the glass had stabilized at 12°C (dark blue).
B. eCPA withdrawal latencies are unchanged as the glass plate cools. Adult male C57 mice were tested as the glass plate cooled, and there was no significant difference between any of the timepoints (Baseline=12.8s±.3, 30 min=13.67s±.9, 60 min=11.03s±1.0, n=3 mice; 1-way ANOVA with Bonferroni post-hoc test, no significant differences between any groups) . Adapted with permission from Brenner et al. 2014

The withdrawal latencies measured as the plate is cooling represent cold adaptation. When measured on wild-type C57/Bl6 males, these latencies were also very consistent (**Figure 5** Baseline=12.8s±0.3, 30 min=13.67s±0.9, 60 min=11.03s±1.0; 1-way ANOVA with Bonferroni post-hoc test, no significant differences between any groups), suggesting that the measurements were consistent and that under baseline conditions, the mice adjust to the cold environment faster than the eCPA could measure.

Discussion

The eCPA is a new tool for assessing cold behavior in mice that has low overhead costs, an objective behavioral endpoint, and can test cold responsiveness at a wide variety of physiologically relevant temperatures. Other behavioral assays for cold such as the cold plate [2,38] and tail flick [96,158]) can test animals at these temperature ranges as well, but they usually involve rapidly moving the animal from room temperature to the testing temperature rather than fully acclimated mice at rest. In contrast, the eCPA allows the experimenter to change the environmental temperature, and then assess how the mice respond to a standardized cold stimulus in the context of this cooler environment. This is a significant methodological improvement for understanding how mice adjust to long periods at colder ambient temperatures.

The eCPA can also test mice during the process of adaptation, as the environment is in the process of cooling. The dynamic cold plate is the only other technique that allows the gradual changing of the environment [55,206], but even the dynamic cold plate only measures the behavioral responses of the mice as the environment cools. The eCPA allows the measurement of cold sensitivity to a standardized cooling stimulus as the environment is in the process of cooling, allowing the experimenters to quantify and study the mechanisms of cold adaptation.

Chapter 4

The mechanisms of cold adaptation

Introduction

The ability to adapt to environmental temperature conditions is crucial for survival. Species that live in areas with significant seasonal temperature shifts need to sense threatening or rewarding temperature changes across many environmental settings. For example, mice living in seasonal areas must detect cold stimuli during both summer and winter, when ambient temperatures can vary by over 100°F, and approach or evade when appropriate. Even humans in the modern era need to sense a wide range of temperatures to avoid dangerously cold or hot situations [19,22].

Recent work has revealed a crucial role of the *Transient Receptor Potential* (TRP) family of ion channels in transduction and amplification of sensory stimuli. TRPV1-4 are essential for heat responses [29,111,125,139,189], TRPA1 is crucial for full responses to some nociceptive[107,108,118,121,130,156,176,180,199,200], pruriceptive [118,180,199,200], and possibly cold stimuli [7,96,107,176,189,213], and TRPM8 is important for normal responses to cold stimuli[9,43,56,63,70,102,103,123,205]. While much effort has been expended studying responses to thermal stimuli at room temperature and in testing precipitous changes in temperature, relatively little work has explored how organisms maintain thermal sensitivity when environmental temperatures change.

Early studies recording from cold-responsive fibers in cats showed that cold stimuli initially increased the number of action potentials fired, but that this response quickly adapted as the stimulus continued [82,83]. These findings were confirmed in primates, and the cold sensitive fibers were also identified as Aδ and C-fibers [109,112,160,161,171]. More recent work has shown *in vitro* that phospholipase C (PLC) modulation of phosphoinositol 4,5-bisphosphate (PIP_2) levels affects TRPM8 activity [51,169], and that dorsal root ganglion neurons isolated from TrpM8-KO mice did not adjust their temperature thresholds in response to varied ambient

temperatures [66]. The same study also showed that changes in PIP_2 concentration affected *in vitro* cold threshold adjustments. Evidence also suggests that the PIP_2-binding protein Pirt modulates TRPM8 activity, further highlighting a key role for PIP_2 in regulating cold sensitivity [179] *in vitro*.

While temperature adaptation has been characterized *in vitro*, this effect has been difficult to study *in vivo*. In this chapter, I use the new eCPA assay to test the cold responses of mice at a variety of baseline temperatures to assess how mice adapt to these temperatures. These studies demonstrate for the first time *in vivo* that TRPM8 is required for adaptation to cold stimuli, likely via a PIP_2-dependent mechanism.

Methods

Animals. All mouse protocols were approved by the Animal Care and Use Committee of the Washington University School of Medicine (St. Louis, MO) and were in accord with National Institutes of Health guidelines. Experiments were carried out with in-house bred C57BL/6 mice originally acquired from Jackson Labs (Bar Harbor, ME), TrpM8-KO mice on a mixed C57/FVB background, TrpA1-KO mice on a pure C57BL/6 background, and TrpA1-TrpM8 dKO mice bred on a mixed C57/FVB background in-house from the single knockout strains. All mice used were male and 6-9 weeks old unless specifically noted. Mice were housed on a 12/12-hour light/dark cycle with the light cycle beginning at 6am. All mice had ad libitum access to rodent chow and water. Cage bedding was changed once a week, always allowing at least 48 hours after a bedding change before behavioral testing was carried out.

Behavioral analysis. All behavioral tests and analyses were conducted by an experimenter blinded to treatment and/or genotype. Behavioral tests were performed between 12pm and 5pm.

extended Cold Plantar Assay (eCPA). The eCPA is described in detail elsewhere (Brenner et al. *in submission*). Briefly, .125'', .1875'', and .25'' thick pyrex borosilicate float glass was purchased from Stemmerich Inc. (St. Louis, MO). Transparent plastic enclosures (4'' x 4'' x 11'') separated by opaque black dividers were arranged in one line along the center of a glass plate. The glass temperature was monitored with an IT-24P T-type filament thermocouple probe from Physitemp Instruments, Inc. (Clifton, NJ) that was secured in the middle of the plate with laboratory tape. Plate temperature data were collected from the thermocouple using an EA15

Data-Logging Dual Input Thermometer from Extech Instruments (Waltham, MA). Dry ice or wet ice was placed in aluminum boxes on either side of the enclosures to uniformly cool the glass plate. The ice was contained either in packets made of heavy-gauge aluminum foil, or in custom-built aluminum boxes**.** The boxes are the same length as the glass plate, 4.5 inches wide and 3 inches tall with a lid. The glass temperature can be adjusted by moving the ice containers closer to or further from the plastic enclosures. After the plate reached the desired temperature, mice were acclimated in the enclosures for 3 hours before testing. White noise was used to decrease noise disturbances.

To cool the glass plate to 17°C, the aluminum boxes were positioned approximately .25'' away from the animal enclosures on either side, and filled with wet ice. After approximately 60 minutes the plate cooled to 17°C and remained at that temperature as long as the boxes were refilled with wet ice roughly every 90 minutes and excess water was drained.

To cool the glass plate to 12°C, the aluminum boxes were positioned roughly 1.25'' away from the animal enclosures on either side and filled with dry ice pellets. After approximately 20 minutes, the plate cooled to 12°C and remained at that temperature as long as the boxes were refilled with dry ice roughly every 90 minutes.

To warm the glass plate up to 30°C, the aluminum boxes were positioned .125'' away from the animal enclosures on either side. Water circulators set to warm the water to 48°C were positioned on either side of the glass plate. Each circulator emptied hot water into one of the aluminum boxes. Water drained directly back into the circulator reservoir via the side drains to

be reheated and pumped back into the boxes. After approximately 80 minutes, the plate warmed to 30°C and remained at that temperature as long as the circulators were active.

The cold probe was generated as we have previously described[21]. Briefly, powdered dry ice was compressed against a flat surface in a 3mL BD syringe (Franklin Lakes, NJ) with the top cut off until it reached a dense, uniform consistency. Awake mice were tested by extending the tip of the dry ice pellet past the end of the syringe and pressing it against the glass underneath the hindpaw with light pressure using the syringe plunger. The center of the hindpaw was targeted, avoiding the distal joints, and ensuring that the paw itself was touching the glass surface.

The latency to withdrawal of the hindpaw was measured with a stopwatch. Withdrawal was defined as any action to move the paw vertically or horizontally away from the cold glass. Trials on separate paws on the same animal were separated by 7 minutes, and at least 15 minutes separated trials on any single paw. At least 3 trials per paw per mouse were recorded unless otherwise noted.

Hargreaves radiant heat assay. Mice were acclimated on a Hargreaves apparatus from IITC Life Sciences (Woodland Hills, CA) in transparent plastic enclosures (4'' x 4'' x 11'') separated by opaque black dividers for 3 hours. White noise was used to decrease noise disturbances. The heated testing plate of the Hargreaves apparatus was replaced with the pyrex eCPA plate, and the cooling protocol was carried out as described above. The Hargreaves apparatus starting temperature and active intensity were varied as described in the text below, and the resting intensity was set to 2%. The resting intensity was used to target the beam to the center of the

hindpaw while avoiding distal joints and ensuring that the mouse paw was fully in contact with the glass surface. Once the beam was targeted, the active intensity (AI) level was applied and the built-in timer was used to measure the withdrawal latency. Low Intensity is defined as AI=12, Moderate Intensity is defined as AI=17, and High Intensity is defined as AI=23. Unless otherwise noted, Moderate Intensity (AI=17) was used for all stimuli.

Glass temperature measurements. Temperature values between the paw and glass were measured using an IT-24P filament T-type thermocouple probe from Physitemp Instruments Inc. (Clifton, NJ). A mouse was anesthetized using a cocktail of Ketamine (Fort Dodge Animal Health, Fort Dodge IA), Xylazine (Lloyd Labs Lloyd Labs Shenandoah, IA), Acepromazine (Butler Schein Animal Health Dublin, OH). The filament thermocouple was secured flush to the glass surface with the tip exposed. The anesthetized animal's paw was taped to the glass surface over the filament thermocouple tip and allowed to reach a stable equilibrium temperature. An eCPA pellet or Hargreaves light stimulus was applied to the secured paw over the thermocouple as described below.

During the stimuli described above, data were collected using an EA15 Data-Logging Dual Input Thermometer from Extech Instruments (Waltham, MA). The data were output into CSV files that were loaded into Microsoft Excel files and analyzed using Graphpad Prism from Graphpad Software (La Jolla, CA).

PLC inhibition experiments

The PLC inhibitor U73122 and its inactive control U73343 (Tocris Bioscience, UK) were diluted in DMSO to a concentration of 320μM. Aliquots of this stock solution were kept frozen at -20°C. On experimental days, baseline eCPA latencies for the right hindpaw were measured starting at 11am. Once baseline measurements were concluded, aliquots of the drugs were defrosted and diluted with saline to a working concentration of 50μM (final solutions were 80% saline, 20%DMSO). 10μL of this solution was injected into the right hindpaw for an effective dose of 0.5 nanomoles, a dose that has been used previously to inhibit PLC activity *in vivo* [211]. Immediately after the injections, aluminum boxes filled with dry ice were place on the glass plate in the configuration shown in Figure 1D labeled "Glass temperature 12°C". eCPA latencies were measured on the right hindpaw between 20-30 minutes after injection, as the glass plate was being cooled.

L4 Spinal nerve ligation (SNL) model The L4 spinal nerve ligation surgery was performed as described previously[100,187]. For all behavior tests, the experimenter was blinded to the surgical procedure that each mouse received. No mice were excluded from analysis. Briefly, baseline measurements of withdrawal latency in the eCPA were made on all mice at 22°C, 17°C, and 12°C. The mice were then deeply anesthetized with vaporized isofluorane. In all mice, the paraspinal muscles were bluntly dissected to expose the L5 transverse process. Mice receiving the full ligation procedure also had the L5 process removed, the L4 spinal nerve tightly ligated with silk suture (6-0, Ethicon; Cornelia, GA) and the nerve was transected distal to the ligation. Mice receiving the sham procedure had the L5 transverse process exposed but not removed, and the nerve was untouched. eCPA latencies at 22°C, 17°C, and 12°C were then measured at 2, 4, and 6 days after surgery, respectively.

Statistical analysis

All data presented are mean±standard error of the error. Analyses were performed using Graphpad Prism (La Jolla, CA) and The R Project for Statistical Computing (http://www.r-project.org/). For tests comparing a single group of animals under several conditions, a 1-way ANOVA with Bonferroni post-hoc test was used to measure overall effect as well as pairwise comparisons. The only exception for this was in **Figure 6**, where a Dunnett's post-hoc test was substituted in order to compare all columns to the baseline condition.

For experiments comparing more than one group of animals under several conditions, a 2-way ANOVA with Bonferroni post-hoc test was used to measure overall effect as well as pairwise comparisons. Statistical significance in each case was denoted as follows * or # $p<0.05$; ** or ## $p<0.01$; *** or ### $p<0.001$.

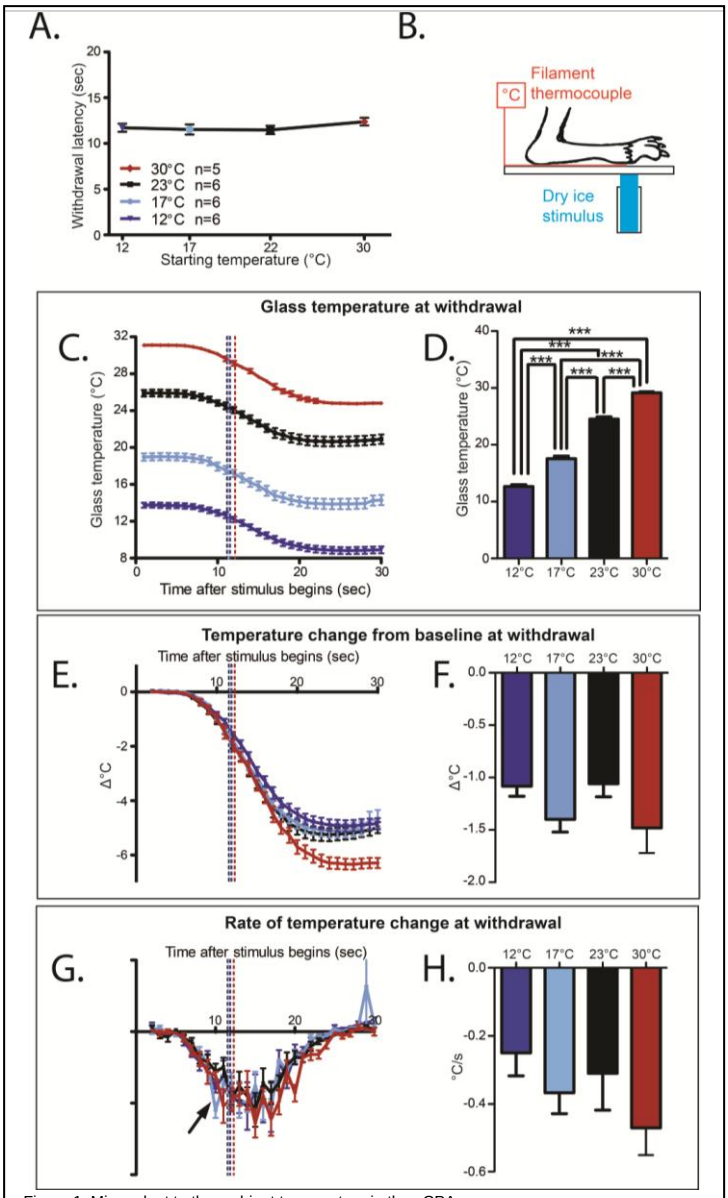

Figure 1: Mice adapt to the ambient temperature in the eCPA
A. The withdrawal latency is unchanged at all 4 starting temperatures (1-way ANOVA with Bonferroni post-hoc test, n=6 for 30°C, n=16 for 23°C , 17°C , and 12°C not significant).
B. Schematic for measuring the cold stimulus on the eCPA. The paw is secured to the glass over a thin filament thermocouple. The dry ice stimulus is placed on the underside of the glass under the paw/thermocouple.
C. Temperatures at the glass/hindpaw interface generated by the eCPA at all starting temperatures. The tracings start slightly higher than the overall plate temperature due to local plate warming by the mouse paw. Dotted lines represent average withdrawal latency of mice under each condition. n=5 for 30°C, n=6 for the other three conditions.
D. Temperature at the glass/hindpaw interface average withdrawal latency for each condition (marked in 1C at the dotted lines). The temperature at withdrawal is significantly different in each condition (1-way ANOVA main effect p=4.84x10-11 with Bonferroni post hoc test 12°C vs 17°C p=1.1x10-5, 12°Cvs 23°C p=6.0x10-10, 12°C vs 30°C p<2x10-16, 17°C vs 23°C p=2.7x10-7, 17°C vs 30°C p=1.1x10-13, 23°C vs 30°C p=6.9x10-7,1df n=5 for 30°C, n=6 for the other groups)
E. Temperature change from baseline (TCFB) temperature through the course of the eCPA stimulus. The dotted line indicates the TCFB at the average withdrawal latency for wild-type mice under that condition. n=5 for 30°C , n=6 for other groups.
F. TCFB at the average withdrawal latency for each condition (marked in 1E at the dotted line). The TCFB at withdrawal is not significantly different between the conditions (1-way ANOVA not significant n=5 for 30°C ,n=6 for other groups)
G. Rate of change (ROTC) of temperature through the course of the eCPA stimulus. The dotted line marks the ROTC at the average withdrawal latency for wild-type mice under that condition. n=5 for 30°C , n=6 for other groups.
H. ROTC at the average withdrawal latency for each condition (marked in 1G at the dotted line). The ROTC at withdrawal is not significantly different between the conditions (1-way ANOVA not significant n=5 for 30°C, n=6 for other groups). All data presented are mean±standard error. Adapted with permission from Brenner et al. 2014

Results

Cold adaptation to environmental temperature changes

The average withdrawal latency of wild-type mice to the cold plantar assay stimulus at room temperature is roughly 11 seconds. Surprisingly, this withdrawal latency was unchanged by major alterations of the starting temperature of the plate (**Figure 1A**, 30°C = 12.3s±0.4, 23°C=11.5s±0.5, 17°C=11.5s±0.6, 12°C=11.7°C±0.4, 1-way ANOVA not significant, n=6 for 30°C, n=16 for 23°C, 17°C, and 12°C). In order to measure the temperatures generated at the glass-skin interface, the mice were anesthetized and the hind paw was secured on top of a filament thermocouple attached to the glass surface using laboratory tape (**Figure 1B**). This arrangement allowed the measurement of the temperature generated at the glass-skin interface

during dry ice. Although ketamine anesthesia is known to depress core body temperature, positioning the anesthetized mice over the thermocouple warmed the baseline glass temperature from 22°C to 25°C (**Figure 1C**), suggesting that it is a reasonable approximation of a mouse at rest on the glass surface. As the starting temperature of the plate decreased, the temperature at which the mice responded also decreased (**Figure 1C,** dotted lines represent average withdrawal latency of mice under each condition). The average withdrawal threshold with the glass starting at 30°C was 29.2°C±0.3°C while the average thresholds with the glass plate starting at 23°C, 17°C, and 12°C were, 24.5°C±0.4°C, 17.6°C±0.5°C and 12.7°C±0.3°C, respectively (in some cases the average withdrawal temperatures are higher than the overall glass temperature due to the body heat of the animals warming the glass underneath the paws, **Figure 1D**, 1-way ANOVA $p=4.84x10^{-11}$ with Bonferroni post hoc test 12°C vs. 17°C $p=1.1x10^{-5}$, 12°Cvs 23°C $p=6.0x10^{-10}$, 12°C vs. 30°C $p<2x10^{-16}$, 17°C vs. 23°C $p=2.7x10^{-7}$, 17°C vs. 30°C $p=1.1x10^{-13}$, 23°C vs. 30°C $p=6.9x10^{-7}$,1df n=5 for 30°C, n=6 for the other groups). This demonstrates that between ambient temperatures of 12 and 30°C, murine temperature sensation is dynamic. Although the temperature of the dry ice stimulation is constant, the withdrawal threshold is dynamic when the ambient temperature is changed.

I hypothesized that withdrawal may be initiated by one of two other parameters: the relative change of temperature from baseline (**Figure 1E**) or the rate of change of temperature (**Figure 1G**). At all three initial glass temperatures, there was a temperature change from baseline (TCFB) at withdrawal, suggesting that TCFB could be the factor that prompts withdrawal (**Figure 1E-F**, dotted lines represent average withdrawal latency of mice under each condition, 12°=-1.1°C±0.1, 17°=-1.4°C±0.1, 23°=-1.0°C±0.1, 30°C=-1.4°C±0.2, 1-way ANOVA not significant). Likewise the rate of temperature change (ROTC) was similar at withdrawal in all

three conditions, suggesting that ROTC could also be the factor that prompts withdrawal from cold stimuli (**Figure 1G-H**, dotted lines represent average withdrawal latency of mice under each condition, 12°=-.3°C/s±0.1, 17°=-.4°C/s±0.1, 23°=-.3°C/s±0.1, 30°C=-.5°C/s±0.1, 1-way ANOVA not significant).

To assess whether temperature change from baseline (TCFB) or rate of temperature change (ROTC) prompts withdrawal from cold stimuli, the cold ramp delivered by a dry ice pellet was measured using 3 thicknesses of glass (**Figure 2B**: .125'', .1875'', and .25''). Work described in Chapter 2 has demonstrated that the rate of cooling has an inverse relationship with the glass thickness [21]. Under these conditions the withdrawal latency (**Figure 2A**), the raw temperature (**Figure 2C-D**), the TCFB (**Figure 2E-F**) and the ROTC (**Figure**

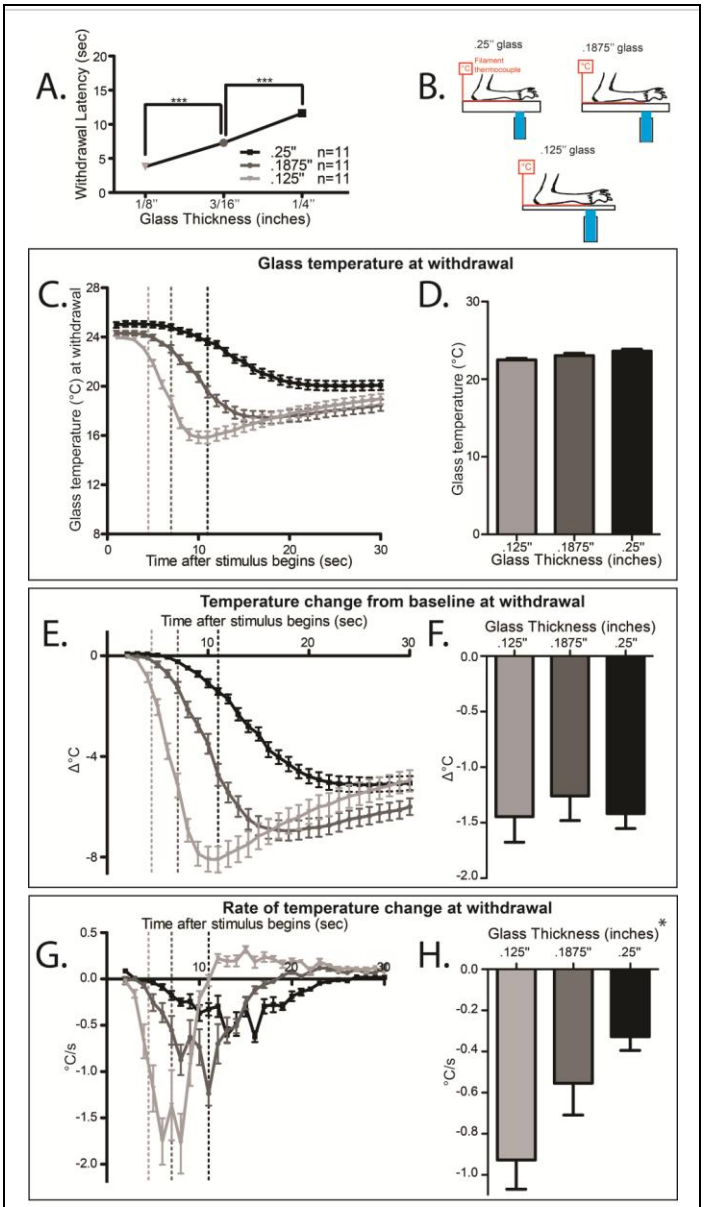

Figure 2: Withdrawal from cold is dependent on the temperature change from baseline

A. Withdrawal latency in the CPA using different thicknesses of glass. Mice on the thicker plates have significantly longer withdrawal latencies (1-way ANOVA with Bonferroni post hoc test; main effect p<2.8x10-16, .125'' vs. .1875'' p=5.3x10-10, .125'' vs. .25'' p<2.10-16, .1875'' vs. .25'' p=2.4x10-12; df=2, n=12 per group)

B. Schematic for measuring the cold stimulus on the CPA. The anesthetized mouse paw is held to the glass on top of a thin filament thermocouple using laboratory tape. The dry ice stimulus is placed on the underside of the glass under the paw/thermocouple.

C. Temperatures generated by the CPA using .125'', .1875'', and .25'' glass plates. Dotted lines mark the temperature at the average withdrawal latency for wild-type mice under that condition. n=11 per group.

D. Glass temperature at the average latency for each glass thickness (marked in 2C at the dotted lines). The temperature at withdrawal is not different in each condition (1-way ANOVA with Bonferroni post hoc test not significant n=11 per condition)

E. Temperature change from baseline (TCFB) temperature through the course of the CPA stimulus. The dotted line indicates the TCFB at the average withdrawal latency for wild-type mice under that condition. n=11 per group.

F. TCFB at the average withdrawal latency for each condition (marked in 2E at the dotted line). The TCFB at withdrawal is not significantly different between the conditions (1-way ANOVA not significant n=11 per condition)

G. Rate of change (ROTC) of temperature through the course of the CPA stimulus. The dotted lines mark the ROTC at the average withdrawal latency for wild-type mice under that condition. n=11 per group.

H. ROTC at the average withdrawal latency for each condition (marked in 2G at the dotted line). The ROTC at withdrawal is significantly different between the conditions (1-way ANOVA main effect *p=0.01 n=1 per condition). All data presented are mean±standard error. Adapted with permission from Brenner et al. 2014

2G-H) were all measured. As the glass thickness decreased, the withdrawal latency significantly decreased (**Figure 2A** 1-way ANOVA with Bonferroni post hoc test; main effect $p<2.8x10^{-16}$, .125'' vs. .1875'' $p=5.3x10^{-10}$, .125'' vs. .25'' $p<2.10^{-16}$, .1875'' vs. .25'' $p=2.4x10^{-12}$; df=2, n=12 per group). The TCFB at withdrawal on the different glass thicknesses is roughly the same, suggesting that the mice could be responding to a consistent TCFB (**Figure 2E-F** dotted lines represent average withdrawal latency of mice under each condition, .125''=-1.5°C±0.2, .1875''=-1.3°C±0.3, .25''=-1.4°C±0.2, 1-way ANOVA not significant n=11 per condition). In contrast, the ROTC at withdrawal on the different glass thicknesses is significantly different (**Figure 2G-H** dotted lines represent average withdrawal latency of mice under each condition, .125''=-.9°C/s±0.2, .1875''=-.6°C±0.3, .25''=-.3°C±0.1, 1-way ANOVA main effect *p=0.01 n=11 per condition). These results suggest that the temperature change from baseline (TCFB) is the determining factor for withdrawal responses to cold stimuli.

<u>Heat adaptation to environmental temperature changes</u>

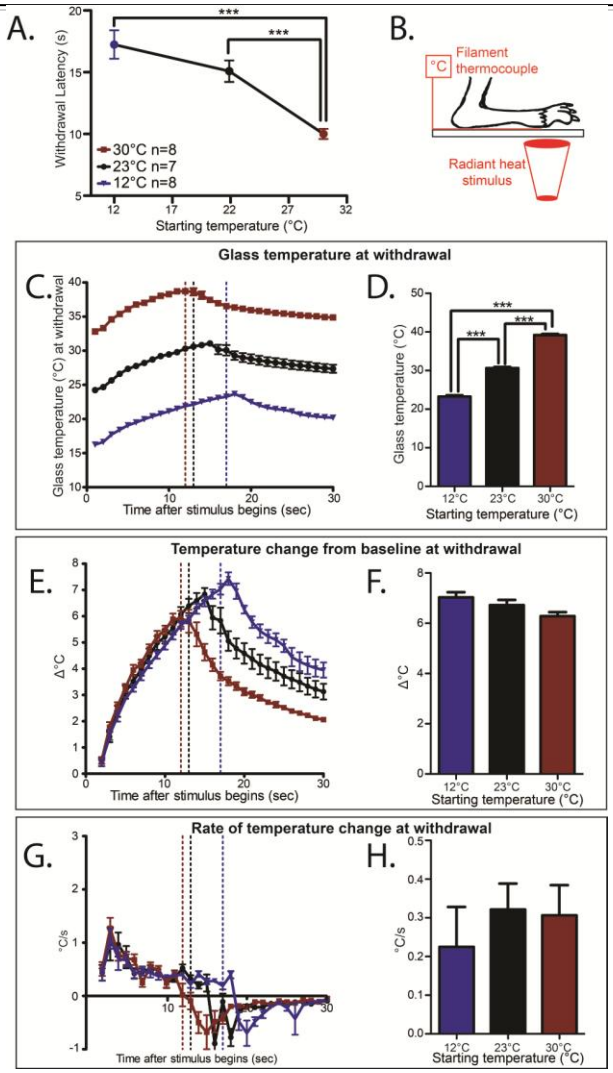

Figure 3: Mice adapt to ambient temperatures with the Hargreaves radiant heat assay

A. Withdrawal latency in the Hargreaves assay with different starting temperatures. Blue (12°C) and Black (23°C) points were performed using the pyrex eCPA glass plate, and Red (30°C) were performed using the Hargreaves heated plate. Mice tested at these different temperatures have different withdrawal latencies (1-way ANOVA with Bonferroni post-hoc test; main effect p=.0007, 12°C vs 30°C p=.0007, RT-pyrex vs. 30°C p=.005; **p<0.01, ***p<0.001, df=3 n=5)

B. Schematic for measuring the heat stimulus temperature on the Hargreaves apparatus. The mouse paw is taped to the glass on top of a thin filament thermocouple. The light stimulus is briefly targeted on the paw/thermocouple with the resting intensity before the active intensity is triggered.

C. Temperatures at the glass/hindpaw interface generated by the Hargreaves with different starting temperatures. Dotted lines mark the temperature at the average withdrawal latency for wild-type mice under that condition. n=8 for 12°C and 30°C n=7 for 23°C.

D. Glass temperature at the average withdrawal latency for thickness (marked in 3C at the dotted lines). The temperature at withdrawal is significantly different in each condition (1-way ANOVA with Bonferroni post-hoc test; main effect p=8.3x10-10, 12°C vs. 23°C p=.002, 12°C vs. 30°C p=1.2x10-9, 23°C vs 30°C p=6.5x10-9; **p<0.01, ***p<0.001, df=2 n=8 for 12°C and 30°C n=7 for 23°C)

E. Temperature change from baseline (TCFB) temperature through the course of the Hargreaves stimulus. The dotted lines indicate the TCFB at the average withdrawal latency for wild-type mice under that condition. n=8 for 12°C and 30°C n=7 for 23°C.

F. TCFB at the average withdrawal latency for each condition (marked in 3E at the dotted lines). The TCFB at withdrawal is not significantly different between the conditions (1-way ANOVA with Bonferroni post-hoc test not significant; n=8 for 12°C and 30°C n=7 for 23°C)

G. Rate of temperature change (ROTC) of temperature through the course of the Hargreaves stimulus. The dotted lines mark the ROTC at the average withdrawal latency for wild-type mice under that condition. n=8 for 12°C and 30°C n=7 for 23°C. There is no significant difference between the ROTC in these conditions, but the peak ROTC is long reached long before the average withdrawal (dotted lines).

H. ROTC at the average withdrawal latency for each condition (marked in 3G at the dotted line). The ROTC at withdrawal is not significantly different between the conditions (1-way ANOVA not significant; n=8 for 12°C and 30°C n=7 for 23°C). All data presented are mean±standard error. Adapted with permission from Brenner et al. 2014.

I hypothesized that adaptation to ambient temperatures would also occur with responses to heat stimuli. In order to test this hypothesis, the Hargreaves radiant-heat assay was used to test mice at different starting temperatures including 12°C, 23°C, and 30°(**Figure 3A**). In contrast to the eCPA, changing the starting temperature did have a significant effect on the withdrawal latency (**Figure 3A**, 12°C=17.2s±1.2 n=6, 23°C=15.1s±0.9 n=6, 30°C=10.0±0.4 n=9, 1-way ANOVA with Bonferroni post-hoc test; main effect p=0.0007, 12°C vs. 30°C p=0.0007, 23°C vs. 30°C p=0.005, df=3 n=5)**.** Compared to Figure 1A, this suggests that heat withdrawal latencies is influenced by ambient temperature.

However, when the heat ramps were being applied to the footpads were measured, the temperature that induced withdrawal still varied significantly

between the three starting temperatures (**Figure 3C-D**, 12°C =23.3°±0.3, 23°C=30.6°±0.3, 30°C=39.2°±0.3, 1-way ANOVA with Bonferroni post-hoc test; main effect $p=8.3x10^{-10}$ 12°C vs. 30°C p=0.002, 12°C vs. 23°C $p=1.2x10^{-9}$, 23°C vs. 30°C $p=6.5x10^{-9}$, df=2 n=8 for 12°C and 30°C n=7 for 23°C). This suggests that adaptation to environmental conditions occurs with heat sensation as well as with cold sensation.

Since there is not a constant temperature withdrawal threshold to thermal stimuli, I hypothesized that either a discrete temperature change from baseline (TCFB) or rate of temperature change (ROTC) causes withdrawal responses in the Hargreaves assay. At all three starting temperatures, the TCFB was the same at the withdrawal point, suggesting that change in temperature from baseline could be the determining response factor (**Figure 3E-F**, 12°C=7.0°±0.2, 23°C=6.7°±0.2, 30°C=6.3°±0.2, 1-way ANOVA with Bonferroni post-hoc test not significant, n=8 for 12°C and 30°C n=7 for 23°C). At all three starting temperatures, there was a similar rate of temperature change (ROTC) at withdrawal (**Figure 3G-H**, 12°C=0.2°/s±0.1, 23°C=0.3°/s±0.1, 30°C=0.3°/s±0.1, 1-way ANOVA not significant n=8 for 12°C and 30°C n=7 for 23°C). However, the peak ROTC occurs after roughly 2 seconds, while average withdrawal latency ranged between 10-17 seconds. Since withdrawal does not occur at the peak ROTC of the stimulus, it is very unlikely that ROTC is the definitive factor that induces withdrawal from heat stimuli.

To confirm this finding, the temperatures generated by a Hargreaves stimulus utilizing 3 different active intensities (Low, Moderate, and High) were also measured, which allows the investigation of the effect of changing the rate of heating. Under these conditions, the withdrawal latency (**Figure 4A**), the temperature of withdrawal (**Figure 4C-D**), the TCFB (**Figure 4E-F**) and the ROTC (**Figure 4G-H**) were calculated. At all three active intensities, the maximal TCFB occurred at the respective withdrawal points, suggesting that change in temperature from baseline could be the determining response factor (**Figure 4E-F**, Low Intensity=6.2°±0.2, Moderate Intensity=6.5°±0.2, High Intensity=6.1°±0.1, 1-way ANOVA with Bonferroni post-hoc test not significant n=5 per condition). The ROTC generated by the different active intensities was very different, and as before, the peak ROTC

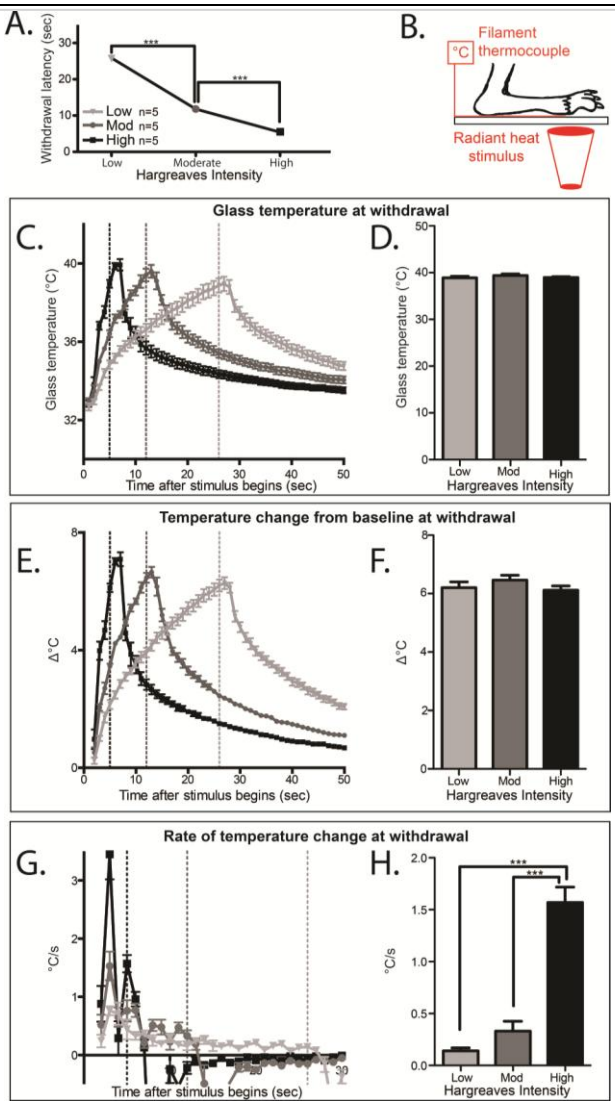

Figure 4: Heat responses in mice are prompted by an increase in temperature from an adjustable baseline

A. Withdrawal latency in the Hargreaves assay with different active intensities. Mice tested using Low, Moderate, or High active intensities have different withdrawal latencies (1-way ANOVA main effect p=9.8x10-15, Low vs. Moderate p=2.1x10-13, Low vs. High p<2x10-16, Moderate vs High p=1.1x10-6; ***p<0.001, df=1, n=9 per group)

B. Schematic for measuring the heat stimulus on the Hargreaves apparatus. The mouse paw is held to the glass on top of a thin filament thermocouple using laboratory tape.

C. Temperatures generated at the glass/hindpaw interface by the Hargreaves with different active intensities. Dotted lines mark the temperature at the average withdrawal latency for wild-type mice under that condition. n=5 per group.

D. Glass temperature at the average withdrawal latency for the active intensities (marked in 4C at the dotted lines). The temperature at withdrawal is not significantly different in each condition (1-way ANOVA with Bonferroni post-hoc test not significant n=5 per group)

E. Temperature change from baseline (TCFB) temperature through the course of the Hargreaves stimulus. The dotted line indicates the TCFB at the average withdrawal latency for wild-type mice under that condition. n=5 per group.

F. TCFB at the average withdrawal latency for each condition (marked in 4E at the dotted lines). The TCFB at withdrawal is not significantly different between the conditions (1-way ANOVA with Bonferroni post-hoc test not significant n=5 per group)

G. Rate of temperature change (ROTC) of temperature through the course of the Hargreaves stimulus. The dotted lines mark the ROTC at the average withdrawal latency for wild-type mice under that condition. n=5 per group. There is no significant difference between the ROTC in these conditions, but the peak ROTC is reached long before the average withdrawal (dotted lines).

H. ROTC at the average withdrawal latency for each condition (marked in 4G at the dotted lines). The ROTC at withdrawal is not significantly different between the conditions (1-way ANOVA with Bonferroni post hoc test; main effect p=7.7x10-7, Low vs. High p=1.3x10-6, Moderate vs. High p=6.0x10-6, df=2, n=5 per condition). All data presented are mean±standard error.

occurs within the first 2-3 seconds in all conditions, which does not correspond to the average withdrawal latencies of the mice under those conditions (**Figure 4G-H**, Low Intensity=0.1°/s±0.03, Moderate Intensity=0.3°/s±0.1, High Intensity=1.6°/s±0.2, 1-way ANOVA with Bonferroni post hoc test; main effect $p=7.7x10^{-7}$, Low vs. High $p=1.3x10^{-6}$, Moderate vs. High $p=6.0x10^{-6}$, df=2, n=5 per condition). This confirms the results from Figure 3, and strongly suggests that responses in the Hargreaves radiant heat assay are provoked by an increase of roughly 6.3°C from a dynamic set point.

Environmental temperature adjustment is dependent on TRP channels

To test the hypothesis that thermo-TRP channels allow mice to adjust the dynamic range of temperature sensation, TrpA1-KO, TrpM8-KO, and TrpA1-TrpM8 double KO (dKO) mice were tested with the eCPA.

Male TrpA1-KO had similar withdrawal latencies to wild-type littermates (**Figure 5A)**, while female TrpA1-KO had a small but statistically significant increase in withdrawal latency compared to their wild-type littermates at all starting temperatures measured (**Figure 5B**, TrpA1-KO 23°C=11.2s±0.4, 17°C= 10.9s±0.4, 12°C=12.8s±0.5, WT 23°C=10.2s±0.7, 17°C=10.2s±-0.4, 12°C=11.7s±0.3; 2-way repeated

measures ANOVA with Bonferroni post-hoc test, main effect p=0.05, no individual points significant; df=1, n=6 WT and 15 KO).

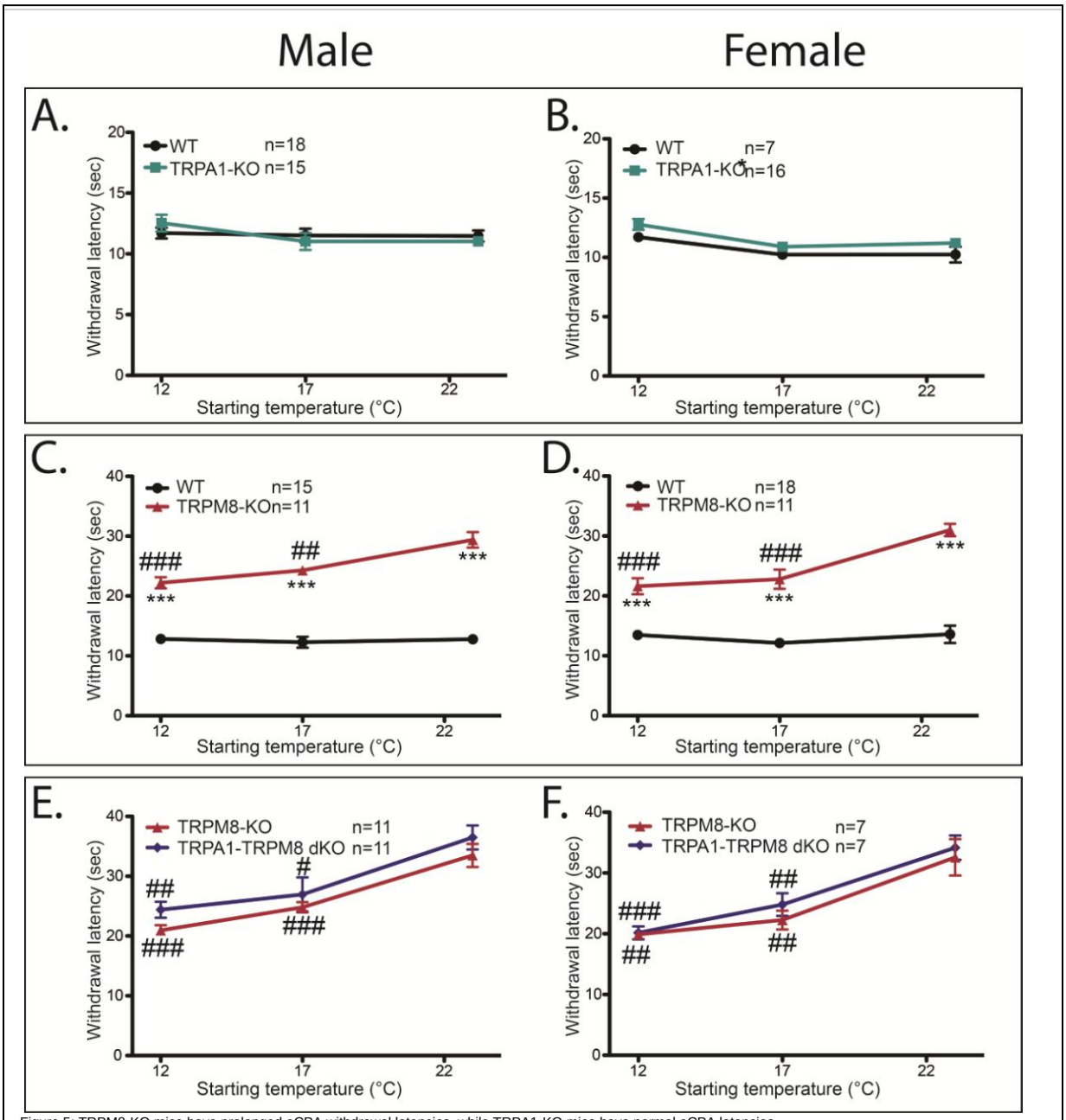

Figure 5: TRPM8-KO mice have prolonged eCPA withdrawal latencies, while TRPA1-KO mice have normal eCPA latencies

A. There is no difference between TrpA1-KO and WT male littermates at any of the temperature ranges tested (2-way ANOVA with Bonferroni post-hoc test, not significant n=18WT and 15KO)

B. TRPA1-KO females have slightly but significantly increased withdrawal latencies compared with their WT littermates(2-way repeated measures ANOVA with Bonferroni post-hoc test, main effect p=.05, no individual points significant; *p<0.01, df=1, n=6WT and 15KO)

C. TRPM8-KO males have significantly increased withdrawal latencies compared with their WT littermates at all starting temperatures (2-way ANOVA with Bonferroni post-hoc test, main effect p<2x10-16, 12°C p=1.1x10-9, 17°C p=6.9x10-10, 23°C p=7.38x10-12; ***p<0.001 df=1, n=15WT and 11KO). TrpM8-KO males exhibit shorter withdrawal latencies as the starting temperature of the glass decreases (1-way ANOVA with Bonferroni post-hoc test, main effect p=1.5x10-5, 12°C vs. 23°C p=6x10-5, 17°C vs. 23°C p=.004; ##p<0.01, ###p<0.001 df=1 n=15WT and 11KO)

D. TRPM8-KO females have significantly increased withdrawal latencies compared with their WT littermates at all starting temperatures (2-way ANOVA with Bonferroni post-hoc test, main effect p<2x10-16, 12°C p=4.2x10-6, 17°C p=4.6x10--8, 23°C p=3.4x10—9; ***p<0.001 df=1, n=18WT and 11KO). TrpM8-KO males exhibit shorter withdrawal latencies as the starting temperature of the glass decreases (1-way ANOVA with Bonferroni post-hoc test, main effect p=3.6x10-5 12°C vs. 23°C p=9.25x10-5, 17°C vs. 23°C p=.0005; ###p<0.001 df=1, n=11 males and 11 females)

E. TRPA1-M8 dKO males have no significant increase in withdrawal latency compared with their WT littermates at all starting temperatures (2-way ANOVA with Bonferroni post-hoc test, not signficant). Both dKO and TRPM8-KO males exhibit shorter withdrawal latencies as the starting temperature the glass decreases (1-way ANOVA with Bonferroni post-hoc test, Male TRPM8-KO main effect=2.9x10-7, 12°C vs. 23°C p=1x10-6 17 vs 23°C p=0.0002 df=1 n=10; Male dKO main effect p=0.0007, 12°C vs 23°C p=0.003, 17°C vs 23°C p=.04; df=1 n=10 ##p<0.01, ###p<0.001)

F. TRPA1-M8 dKO females have no significant increase in withdrawal latency compared to their WT littermates at all starting temperatures (2-way ANOVA with Bonferroni post-hoc test, not signficant). Both dKO and TRPM8-KO females exhibit shorter withdrawal latencies as the starting temperature of the glass decreases (1-way ANOVA with Bonferroni post-hoc test, main effect=.0005, 12°C vs 23°C p=0.002, 17°C vs 23°C p=.01; df=1 n=6; main effect=7.7x10-7, 12°C vs. 17°C p=.03, 12°C vs. 23°C p=4.7x10-6, 17°C vs. 23°C p=0.0008; df=1 n=6 ##p<0.01, ###p<0.001). All data presented are mean±standard error. Adapted with permission from Brenner et al. 2014.

Both male and female TrpM8-KO had significantly increased withdrawal latencies at all

temperature ranges compared to their wild-type littermates (**Figure 5C-D** Males TrpM8-KO 23°C=29.4s±1.3, 17°C=24.3s±0.7, 12°C=22.2s±0.9, WT 23°C=12.8s±0.7, 17°C=12.3s±0.9, 12°C=12.8s±0.5 2-way

repeated measures ANOVA with Bonferroni post-hoc test main effect $p<2x10^{-16}$, 12°C $p=1.1x10^{-9}$, 17°C $p=6.9x10^{-10}$, 23°C $p=7.38x10^{-12}$; df=1, n=15WT and 11KO. Females TrpM8-KO 23°C=30.9s±1.0, 17°C=22.8s±1.6, 12°C=21.6s±1.4, WT 23°C=13.6s±1.5, 17°C=12.2s±0.5, 12°C=13.5s±0.8; 2-way repeated measures ANOVA with Bonferroni post-hoc test main effect $p<2x10^{-16}$, 12°C $p=4.2x10^{-6}$, 17°C $p=4.6x10^{-8}$, 23°C $p=3.4x10^{—9}$; df=1, n=18WT and 11KO). At 12°C or 17°C starting temperatures, TrpM8-KO mice withdrew significantly more quickly compared with the 23°C starting temperature, but still had significantly increased withdrawal latencies compared with their wild-type littermates. (**Figure 5C-D**, 1-way repeated measures ANOVA with Bonferroni post-hoc test; males main effect $p=1.5x10^{-5}$, 12°C vs. 23°C $p=6x10^{-5}$, 17°C vs. 23°C p=0.004; females main effect $p=3.6x10^{-5}$ 12°C vs. 23°C $p=9.25x10^{-5}$, 17°C vs. 23°C p=0.0005; df=1, n=11 males and 11 females).

Since studies suggest that TRPA1 activates at lower temperatures than TRPM8, it is possible that intact TRPM8 signaling could mask a phenotype in the TrpA1-KO mice. To address this issue, TrpA1-TrpM8 double knockout were tested along with their single TrpM8-KO littermates. For both male and female mice, the withdrawal latencies were not significantly different between dKO mice and TrpM8-KO mice (**Figure 5E-F** Males TrpA1-M8 dKO 23°C=36.5s±2.0, 17°C=29.9s±2.9, 12°C=24.4s±1.3, TrpM8-KO 23°C=33.5s±1.9, 17°C=24.8s±0.9, 12°C=20.9s±0.9; 2-way repeated measures ANOVA with Bonferroni post-hoc test; Females TrpA1-M8 dKO 23°C=34.2s±1.9, 17°C=24.8s±1.9, 12°C=20.2s±1.1, TrpM8-KO 23°C=32.6s±2.9, 17°C=22.3s±1.5, 12°C=19.9s±0.8; 2-way repeated measures ANOVA with

Bonferroni post-hoc test). As seen in previous experiments, both the single TrpM8-KO and the TrpA1-TrpM8 dKO mice had lower withdrawal latencies at colder starting temperatures, suggesting impaired environmental adaptation (**Figure 5E-F**, 1-way repeated measures ANOVA with Bonferroni post-hoc test Male TrpM8-KO main effect=$2.9x10^{-7}$, 12°C vs. 23°C p=$1x10^{-6}$, 17 vs. 23°C p=0.0002, df=1 n=10; Male dKO main effect p=0.0007, 12°C vs. 23°C p=0.003, 17°C vs. 23°C p=0.04, df=1 n=10; Female TrpM8-KO main effect=0.0005, 12°C vs. 23°C p=0.002, 17°C vs. 23°C p=0.01, df=1 n=6; Female dKO main effect=$7.7x10^{-7}$, 12°C vs. 17°C p=0.03, 12°C vs. 23°C p=$4.7x10^{-6}$, 17°C vs. 23°C p=0.0008, df=1 n=6). These results suggest that TRPA1 may not play a central role in baseline cold responsiveness or adaptation, and that TRPM8 is crucial to both normal cold responsiveness and cold adaptation.

Environmental temperature adjustment requires PLC activity

Previous work *in vitro* has suggested that depletion of membrane PIP_2 by Ca^{2+}-activated phospholipase C δ (PLCδ) leads to decreased TRPM8 sensitivity, and that this process is critical in adaptation of cold temperature responses [51,66,169]. To test whether this hypothesis is supported *in vivo*, the eCPA procedure was modified to allow testing of cold thresholds during the adaptation process, as the plate was cooling. Briefly, mice were acclimated and withdrawal latencies were tested at room temperature (**Figure 6A**). After the baseline measurements, the dry ice-filled aluminum containers were placed on the glass and withdrawal latencies were measured as the glass cools in order to assess cold responsiveness as cold adaptation is occurring. Under normal conditions, mice adapted to the cooling ambient temperature of the eCPA faster than could be measured with this protocol, showing no change in withdrawal latency as the plate

cooled (**Figure 6B**, 0 min=12.13s±0.8, 30 min=12.1s±1.6, 60 min=13.2s±1.1, 90 min=10.8s±1.2 1-way ANOVA with Bonferroni post hoc test $p>0.05$, $n=6$).

Then, to assess whether PLC activity was required for rapid adaptation to cooling ambient temperature, the PLC inhibitor U73122, or an inactive analog U73343 was injected into the hindpaw while the glass was cooling. This concentration of U73122 has previously been used to locally inhibit intraplantar PLC *in vivo* [211].

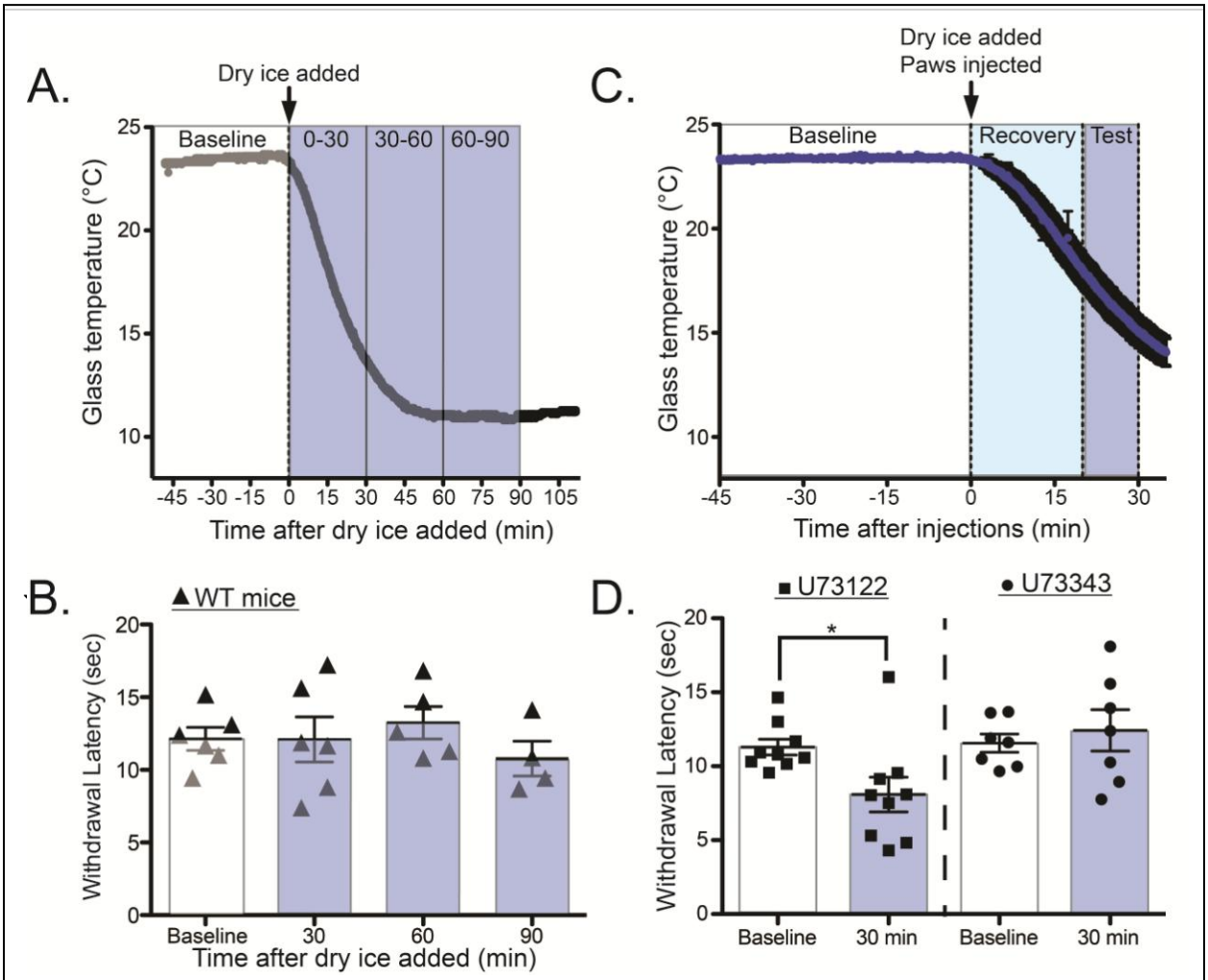

Figure 6: PLC inhibition transiently inhibits cold adaptation
A-B. Mice were acclimated and tested at room temperature, the glass plate was cooled, and withdrawal latencies were assessed as the plate cooled
C. Mice were acclimated at room temperature, and baseline withdrawal latency was measured on the right hindpaw. At t=0 min, either .5nmol U73122 (PLC inhibitor) or .5nmol U73343 (inactive control) was injected into the right hindpaw. Immediately after injections, dry ice was added to the glass plate and eCPA latencies were measured as the glass cooled.
D. Mice injected with U73122 (square markers) have significantly decreased withdrawal latencies at 30min compared to baseline or later timepoint (baseline=11.3s±.5s, 30min =8.1s±.1.2s; 1-way ANOVA with Dunnett's post-hoc test, main effect p=0.02, individual baseline vs. 30min p=.02; df=1 n=9). Mice injected with U73343 (circle markers) had unchanged latencies at 30 minutes compared to baseline or any other timepoint (baseline=11.6s±.6s, 30min=12.2±1.4s; 1-way ANOVA with Dunnett's post-hoc test, no main effect n=7). All data presented are mean±standard error. Adapted with permission from Brenner et al. 2014.

The intraplantar injections of U73122 or U73343 were administered before the ambient temperature was cooled in order to inhibit the local PLC before the cold-induced hydrolysis of PIP_2 began (**Figure 6C)**. Once the glass plate cooling was started, the eCPA withdrawal latency was frequently measured in order to assess whether inhibiting intraplantar PLC would affect cold adaptation as it happened (**Figure 6D**). The mice that were given intraplantar injections of 0.5 nmol U73122 had significantly lower withdrawal latencies at the 30min timepoint compared

with baseline, suggesting impairment of the adaptation process (**Figure 6D**, baseline=11.29s±0.53s, 30min=8.09s±1.17s; 1-way ANOVA with Dunnett's post-hoc test, main effect p=0.02, individual baseline vs. 30min p=0.02; df=1, n=9). In contrast, mice that received intraplantar injections of the control compound U73343 had no change in withdrawal latency at 30min (**Figure 6D**, baseline=11.56s±0.62s, 30min=12.242±1.40s; 1-wav ANOVA with Dunnett's post-hoc test, no main effect n=7). Taken together, these data suggest that TrpM8-dependent cold adaptation *in vivo* is at least partially dependent on PLC activity.

Spinal nerve ligation (SNL)-induced cold hypersensitivity does not affect cold adaptation

The mechanisms of cold hypersensitivity are not fully understood. One possibility is that neuropathic injuries such as the Spinal Nerve Ligation (SNL) procedure compromise the ability to adapt to changes in ambient temperatures, resulting in increased cold sensitivity during cold stimuli. To test this hypothesis, the eCPA withdrawal latencies were measured at three temperatures (12°C, 17°C, 23°C) before and after performing the spinal nerve ligation (SNL) procedure. Animals that underwent the sham procedure had no change in withdrawal latency between the contralateral and ipsilateral paws (**Figure 7A**, 2-way ANOVA with Bonferroni post-hoc test 12°C Ipsi=1.1±0.08 Contra=0.99±0.09, 17°C Ipsi=1.03±0.09 Contra=0.96±0.02, 23°C Ipsi=1.0±0.08 Contra=1.1±0.08). Animals that underwent the SNL procedure had decreased withdrawal latencies on the SNL paw compared to the contralateral paw (**Figure 7B**, 2-way ANOVA with Bonferroni post-hoc test main effect ***p=0.0003, 12°C Ipsi=0.75±0.04 Contra=1.07±0.14 *p<0.05, 17°C Ipsi=0.68±0.06 Contra=1.03±0.04 *p<0.05, 23°C Ipsi=0.66±0.09 Contra=0.86±0.05 p>0.05). Although robust cold hypersensitivity was observed after the SNL procedure, there was no effect of changing the ambient temperature on the cold

hypersensitivity (**Figure 7B**, 2-way ANOVA, p>0.05 for glass plate temperature). This suggests that SNL-induced cold hypersensitivity does not affect the ability to adapt to cold ambient temperatures.

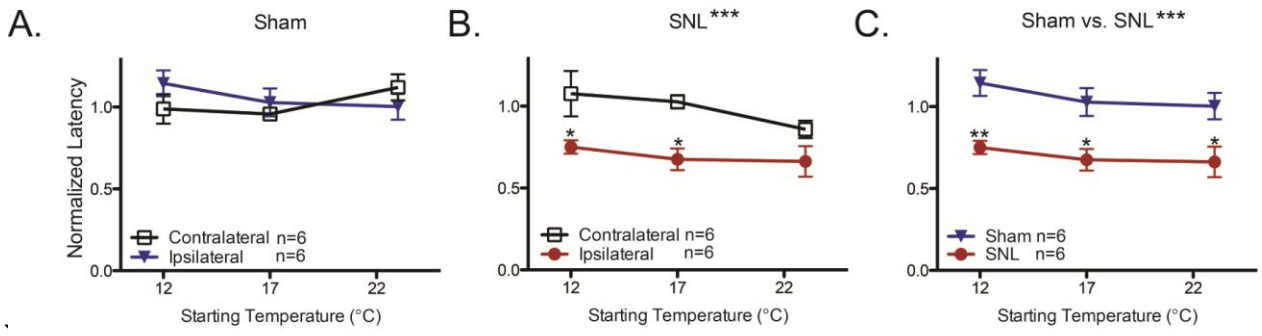

Figure 7: SNL hypersensitivity is unaffected by changes in ambient temperature
A. Mice were tested at 12°C, 17°C, and 23°C before and after the sham procedure. Post-surgical withdrawal latencies were normalized to the baseline values. There was no significant change in withdrawal latency for either ipsilateral or contralateral paws after the sham surgical procedure (2-way ANOVA with Bonferroni post-hoc test, n=6 per group)
B. Mice were tested at 12°C, 17°C, and 23°C before and after the SNL procedure. Post-surgical withdrawal latencies were normalized to the baseline values. The ipsilateral paws had significantly lower withdrawal latencies than the contralateral paws (2-way ANOVA with Bonferroni post-hoc test main effect ***p=0.0003, 12°C Ipsi=.75±.04 Contra=1.07±.14 *p<0.05, 17°C Ipsi=.68±.06 Contra=1.03±.04 *p<0.05, 23°C Ipsi=.66±.09 Contra=.86±.05 p>0.05). Changing the starting temperature of the glass plate had no impact on the withdrawal latency of either the ipsilateral or contralateral paws (2-way ANOVA with Bonferroni post-hoc test, main effect p>0.05).
C. Direct comparison of the ipsilateral paws of mice that received Sham or SNL procedures. Mice were tested at 12°C, 17°C, and 23°C before and after the surgical procedure. Post-surgical withdrawal latencies were normalized to the baseline values. The SNL mice had significantly lower withdrawal latencies than the Sham mice (2-way ANOVA with Bonferroni post-hoc test main effect ***p<0.0001, 12°C Sham=1.1±.08 SNL=.75±.04 **p<0.01, 17°C Sham=1.03±.09 SNL=.68±.06 *p<0.05, 23°C Sham=1.0±.08 SNL=.66±.09 p>0.05). Changing the starting temperature of the glass plate had no impact on the withdrawal latency of either the sham or SNL mice (2-way ANOVA with Bonferroni post-hoc test, main effect p>0.05). All data presented are mean±standard error. Adapted with permission from Brenner et al. 2014.

Discussion

Temperature adaptation is a necessary daily function for mammals. Mice in the wild need to sense cold stimuli in a variety of environmental settings, so as to be able to seek out cooler areas in the hot summer and to avoid dangerously colder areas in the winter. While climate control has made this less of a struggle of life and death for humans, aberrant temperature adaptation could lead to inappropriate thermal pain or an inability to detect dangerous thermal stimuli and death by heat stroke or hypothermia [19,22].

Wild-type mice quickly adapt their response latency to cold stimuli when environmental temperature changes. This finding is consistent with early microneurography studies, which showed that sustained cold stimuli provoked a rapid burst of activity followed by quick adaptation and decreased firing [82,83,109,160,161]. In our efforts to further characterize this phenomenon, I found that mouse responses to both warm and cold stimuli depend on changes from a dynamic temperature 'set-point'. Animals are able to adjust this 'set-point' in response to changes in the ambient temperature, which maintains their ability to detect subtle changes in temperature across a wide range of conditions. This is one of the first demonstrations and quantifications *in vivo* that thermal response thresholds are not based on a specific temperatures, despite early hints that this might be the case [181,182]. Regarding heat sensation, there is strong evidence that mice respond to an increase of roughly 6.3°C from this dynamic 'set-point'. With regard to cold sensation mice respond to a 1.2°C decrease from a dynamic 'set-point' which can be modulated by environmental conditions. These results are also consistent with recent work by Hoon et al. suggesting that temperature responsiveness is reliant on aversive and attractive cues from both warm- and cold-sensitive neurons [159]. Modulating the dynamic 'set-

points' of each population separately or in tandem may be essential to maintaining the balance between the populations and preserving thermal sensitivity and adaptability.

Previous work has demonstrated that TRPM8 is essential for adaptation of cold-induced currents in dissociated dorsal root ganglion cultures [66]. These findings demonstrate for the first time *in* vivo that TRPM8 is essential for full adaptation to colder ambient conditions. Both male and female TrpM8-KO mice showed a significantly impaired ability to adjust their cold response thresholds in response to environmental temperature changes. Despite the obvious deficits in both cold sensation and adaptation to environmental stimuli, TrpM8-KO and TrpA1-TrpM8 dKO mice had consistent and robust responses to the eCPA stimuli in all conditions. This suggests the existence of other, possibly non-TRP channel mediators of cold responsiveness.

There have been conflicting reports on the role of TRPA1 in cold sensation in the literature [9,96,102,176]. Interestingly, male TrpA1-KO mice show no deficit in cold responses at any ambient temperature range, while the female TrpA1-KO mice exhibit a small but significant increase in withdrawal latency at all temperature ranges. This is consistent with some previous findings that female but not male TrpA1-KO mice had more significant deficits in cold responsiveness to the acetone test [108] compared to male TrpA1-KO mice, although other reports have found no sex-dependent difference [9].

Neither the male nor female TrpA1-TrpM8 dKO mice had significantly higher withdrawal latencies than their TrpM8-KO littermates at any ambient temperature condition. Given the small but significant trend in the TrpA1-KO females, it is difficult to make definitive conclusions on the role of TrpA1 in cold sensation based on these data. However, the TrpA1-TrpM8 dKO mice also show impaired cold adaptation as was seen with TrpM8-KO mice, confirming that TRPM8 plays an essential role in this process.

Previous work *in vitro* has suggested that the hydrolysis of PIP_2 during cold adaptation leads to changes in TRPM8 activity [51,66,169]. The findings in this study suggest that PLC activity is important for the modulation of this dynamic set point *in vivo* that governs adaptation to environmental cold responses. Although U73122 has been shown to have non-PLC mediated effects [87], the results of this study are consistent with the *in vitro* model that this set-point is controlled through PIP_2 modulation of TRPM8. Although additional adaptation of cold responsiveness may occur through molecules that control the excitability of cold-sensitive neurons such as TASK-3 [140], or during processing in spinal or supra-spinal processing, these results are the first *in vivo* evidence that as the ambient temperature decreases, PLC-mediated hydrolysis of membrane PIP_2 modulates cold responsiveness in DRG neurons [51,66].

Chapter 5

Optogenetic inhibition of the peripheral nervous system

Introduction

The studies in Chapters 2-4 show a clear role for TRPM8 in the sensitivity and adaptation to cold stimuli, but do not determine which nociceptive neurons are necessary for normal cold sensitivity. As discussed in Chapter 1, many distinct populations of nociceptive neurons have been identified. These populations can be identified by their expression of molecular markers including the heat sensor TRPV1 [33], the voltage-gated sodium channel Nav1.8 [215], and the calcium regulated actin-binding protein Advillin [81]. Ablating these neurons has demonstrated some of their functions, as ablating the TRPV1-expressing neurons nearly eliminated temperature sensation between 40-50°C [159], ablating the Nav1.8-expressing neurons decreased responsiveness to noxious mechanical pressure and cold and decreased inflammatory pain responses [1], while ablating the peptidergic CGRP-expressing neurons reduced sensitivity to noxious heat, capsaicin, and itch, and enhanced cold responsiveness [128]. While these studies demonstrate crucial roles for these neurons they involve killing those entire populations, which may prompt significant compensatory changes in remaining neurons and lead to inaccurate conclusions.

As previously discussed, optogenetics utilizes light-sensitive ion channels to modulate neuronal activity without permanently changing the neuronal architecture [209]. These channels can be used to activate or inhibit specific populations of nociceptive neurons, as was demonstrated when stimulation of mice expressing channelrhodopsin in Nav1.8-expressing neurons with a laser evoked robust nocifensive responses as well as post-stimulation hypersensitivity [52], and optogenetic stimulation of mice expressing the inhibitory eNpHR 3.0 channel in sensory neurons decreased mechanical and heat sensitivity [90]. Optogenetic manipulation of the peripheral nervous system has also been demonstrated by optically stimulating the axons in an *ex vivo* preparation of the sciatic nerve, although in this case activation of motor neuron axons in the

sciatic led to an orderly recruitment of motor units that is superior for muscular rehabilitation to electrical stimulation [119]. Subsequent studies using this model allowed the activation of motor neurons through axonal stimulation using a fiber optic cable headmount that then tunneled subcutaneously to the lateral caudal area and terminated in a cuff around the sciatic nerve [184]. Taken together, these studies show that both control of the peripheral nociceptors and stimulation of the axons in the sciatic nerve is possible. Still, studies utilizing a fully wireless implantable light source to control the axons of peripheral nociceptors have not been demonstrated. In this chapter, I will describe a novel scheme to modulate the activity of peripheral nociceptive neurons using biocompatible light-emitting diode (LED) devices. These devices are implanted without a tether connecting to an external power source, which allows long-term stimulation in a variety of behavioral paradigms. These implantable LED devices are designed and fabricated by the Rogers lab at the University of Illinois Urbana-Champaign based on novel technology to generate interconnected arrays of ultrathin organic light-emitting diodes on flexible water-resistant sheets of plastic [99]. In brief, the semiconductor materials for the LED are printed onto a temporary coated-glass substrate to for the electrical connections between the harvester and the LEDs. The coated-glass substrate is dissolved with acid to release the interconnected semiconductor collection which is then transfer-printed onto a plastic substrate for encapsulation and passivation [99,150]. The inorganic LEDs that are used can vary in size and shape from larger commercial diodes to 100μM x 100μM μLEDs, and can be layered to increase light intensity as necessary [99,150]. The devices are powered utilizing new radiofrequency (RF) harvesting technology that allows long-distance wireless power transmission developed by Sung-Il Park in the Rogers lab. In this chapter I use these wireless LED devices to stimulate and

inhibit peripheral nociception through optogenetic modulation of axons in the sciatic nerve, in order to demonstrate which subsets of nociceptors are necessary for normal cold sensitivity.

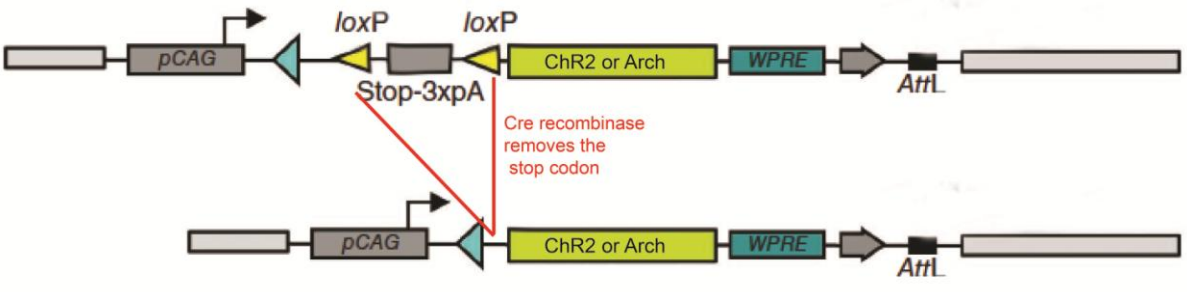

Figure 1: Cre recombinase mediated expression of Channelrhodopsin 2 (ChR2) or Archaerhodopsin (Arch)
Under baseline conditions, a stop codon located between the pCAG promoter and the channel prevents transcription. When cre recombinase is present in the cell, the stop codon is cleaved out of the sequence, and transcription of the channel proceeds. The above mice were bred to mice expressing cre-recombinase in either advillin-, TRPV1-, or Nav1.8-expressing cells. Figure adapted with permission from Madisen et al. 2012

Methods

Animals. All mouse protocols were approved by the Animal Care and Use Committee of the Washington University School of Medicine (St. Louis, MO) and were in accord with National Institutes of Health guidelines. ai32 (flox-stop-flox Rosa26-ChR2-EYFP) or ai35 (flox-stop-flox Rosa26-Arch3.0-GFP) mice described previously (**Figure 1)** [122] were crossbred with mice expressing the Cre recombinase enzyme in cells expressing Advillin [81], TRPV1 [159], or Nav1.8 [175]. These mice were all on a C57BL/6 background and originally acquired from Jackson Labs (Bar Harbor, ME). Mice were housed on a 12/12-hour light/dark cycle with the light cycle beginning at 6am. All mice had ad libitum access to rodent chow and water. Cage bedding was changed once a week, always allowing at least 48 hours after a bedding change before behavioral testing was carried out.

Quadriceps motor response (QMR) testing A mouse expressing ChR2-EYFP in TRPV1-expressing cells was deeply anesthetized using isofluorane and the eyes were covered with Altalube ointment **(**Altaire Pharmaceuticals, Riverhead, NY**)** to prevent corneal drying anesthetized. A small incision was made on the left flank and blunt dissection was used to separate the gluteus maximus and biceps femoris muscles to expose the sciatic nerve. The sciatic

incision was then covered with mineral oil and parafilm to prevent tissue drying. Another small incision was made on the left thigh of the mouse, and two galvanized silver electrodes were inserted into the quadriceps to measure the electromyelographic (EMG) waveform generated during muscle activation. This incision was also covered with parafilm to prevent drying. The isofluorane level was then gradually lowered until the mouse was still unconscious but reliably responded to toe pinches with nocifensive flinches. At this point, the sciatic nerve was re-exposed in the left flank incision, and a laser was applied directly to the nerve at a variety of intensities, or to the overlying muscle. The EMG waveform generated during this stimulation was recorded and analyzed using the Windaq software package.

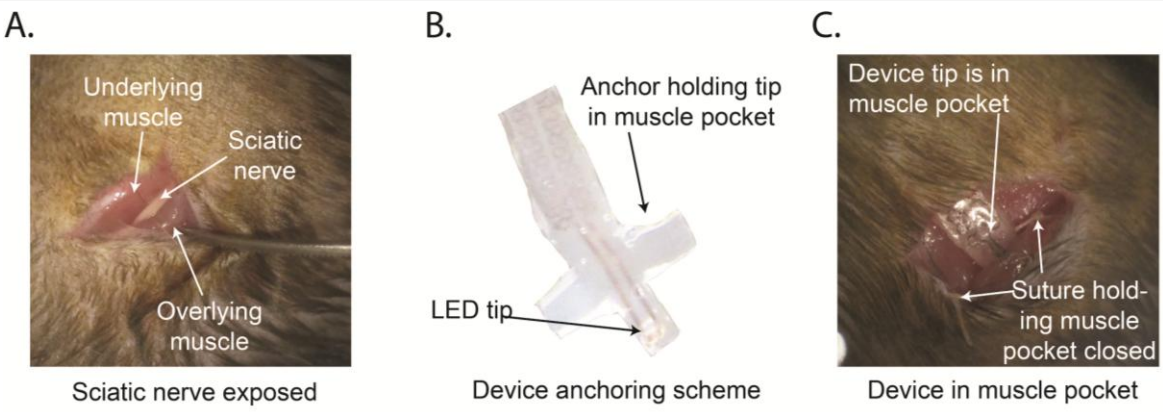

Figure 2: Devices are anchored over the sciatic by closing the muscle pocket around an anchor
A. The sciatic nerve is exposed by making a small incision on the flank. The fascia connecting the overlying gluteus maximus to the underlying biceps femoris is separated, and the overlying muscle is pulled to the side to expose the nerve
B. The LED is at the tip of the device. 3mm from the tip, there is a 3mm plastic "anchor" that extends to either side. This anchor is designed to hold the device inside the narrow muscle pocket.
C. An LED device in the muscle pocket. The LED tip is over the sciatic nerve inside the muscle pocket, and the anchor is inside the pocket, level with the overlying muscle. Sutures were tied on either side of the device on the outside of the pocket, holding the anchor and the tip of the device inside the muscle pocket.

Surgical implantation of stretchable cable μLED devices These devices have an LED at the tip of the device. There is also an anchor t-bar roughly 3mm from the tip of the device (**Figure 2B)** designed to keep the tip of the device inside the muscle pocket near the sciatic nerve. From the t-bar, the stretchable cable measures roughly 6.5cm before the terminal pins that connect to a wireless radiofrequency harvester (**Figure 3A**).

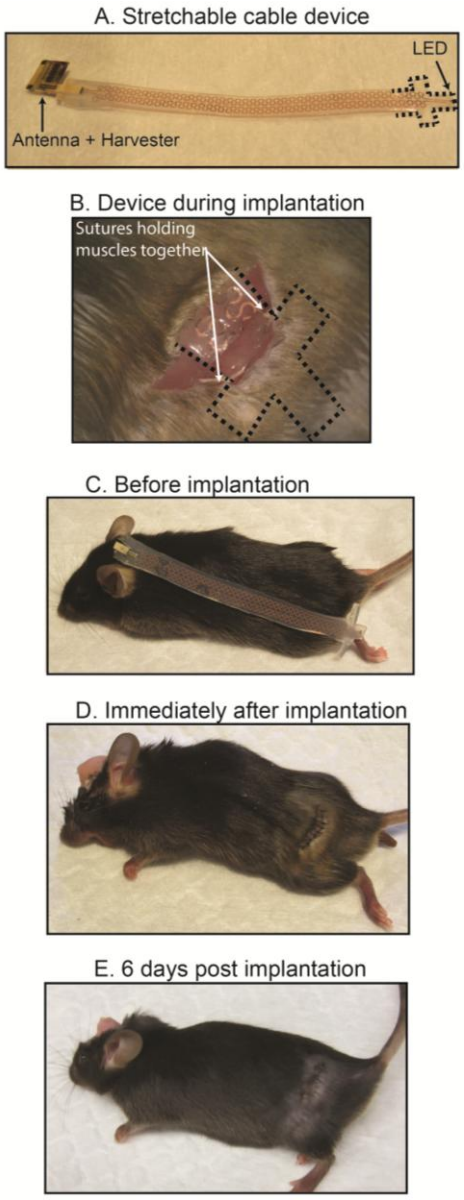

Figure 3: Surgical placement of stretchable cable LED devices
A. The devices include an antenna and RF harvester connected to an LED tip by a highly distensible cable.
B. During implantation, cable portion is tunnel subcutaneously until the LED tip is threaded into the muscle pocket as demonstrated in Figure 4.
C-D. Stretchable cable device before (C), immediately after (D), and 6 days after (E) surgery. D-E demonstrate the dental cement headcap used to anchor the connector for the harvester to the skull.

The surgical procedure to implant these devices was modified from the Chronic Constriction Injury procedure [12]. Briefly, the animal was anesthetized with using isofluorane and the eyes were covered with Altalube ointment **(**Altaire Pharmaceuticals, Riverhead, NY**)** to prevent corneal drying. A small skin incision was made over the greater trochanter of the femur on the left flank of the animals. The fascia connecting the biceps femoris and the gluteus maximus was blunt dissected apart to open a plane between the muscles, in which the sciatic nerve was clearly accessible (**Figure 2A**). Another small skin incision was made vertically over the cranium and the periosteum was removed using #6 sharp curved forceps. A subcutaneous tunnel between the cranial incision and the left flank incision was created using a blunt 1/8'' trochar to separate the skin from underlying muscle moving from cranial to left flank. The cable implant was then attached to the trochar and fed through the subcutaneous tunnel until the LED portion emerged from the flank incision and the harvester pins were at the entrance to the cranial incision, at which point the trochar was detached. The gluteus maximus was pulled caudally to expose the sciatic nerve, and the tip of

the device containing the LED was placed over the nerve. The gluteus maximus fold was then pulled over the tip of the device, and resorbable 6-0 vicryl suture from Ethicon (Cornelia, GA) was used to reconnect the overlying gluteus maximus to the underlying biceps femoris, restoring the original muscle architecture as well as securing the tip of the LED device inside the muscle pocket (**Figures 2C, 3B**). The mouse was then moved to an adjacent Kopf Model 900 stereotaxic instrument (Tujunga, CA), where a hole was drilled with a Kopf Model 1911 stereotaxic drilling unit using a Kemmer Prazision SM 32103303952C drill bit (Dusseldorf, Germany) and an anchor screw (CMA Microdialysis 7431021, Holliston, MA) was threaded into the hole in the cranium. The connector for the RF harvester was then secured to the anchor screw using Jet dental cement (Lang Dental, Wheeling, IL), and any loose skin stretched by the subcutaneous tunneling was sutured tight to the edges of the dental cement headcap using Ethicon 6-0 nylon monofilament suture. The left flank incision was also sutured closed with 6-0 nylon monofilament suture (**Figure 3D**). Both incisions were then coated with antibiotic cream (Actavis Pharmaceuticals, Parsippany, NJ) before the mouse was allowed to recover from anesthesia in a warmed chamber.

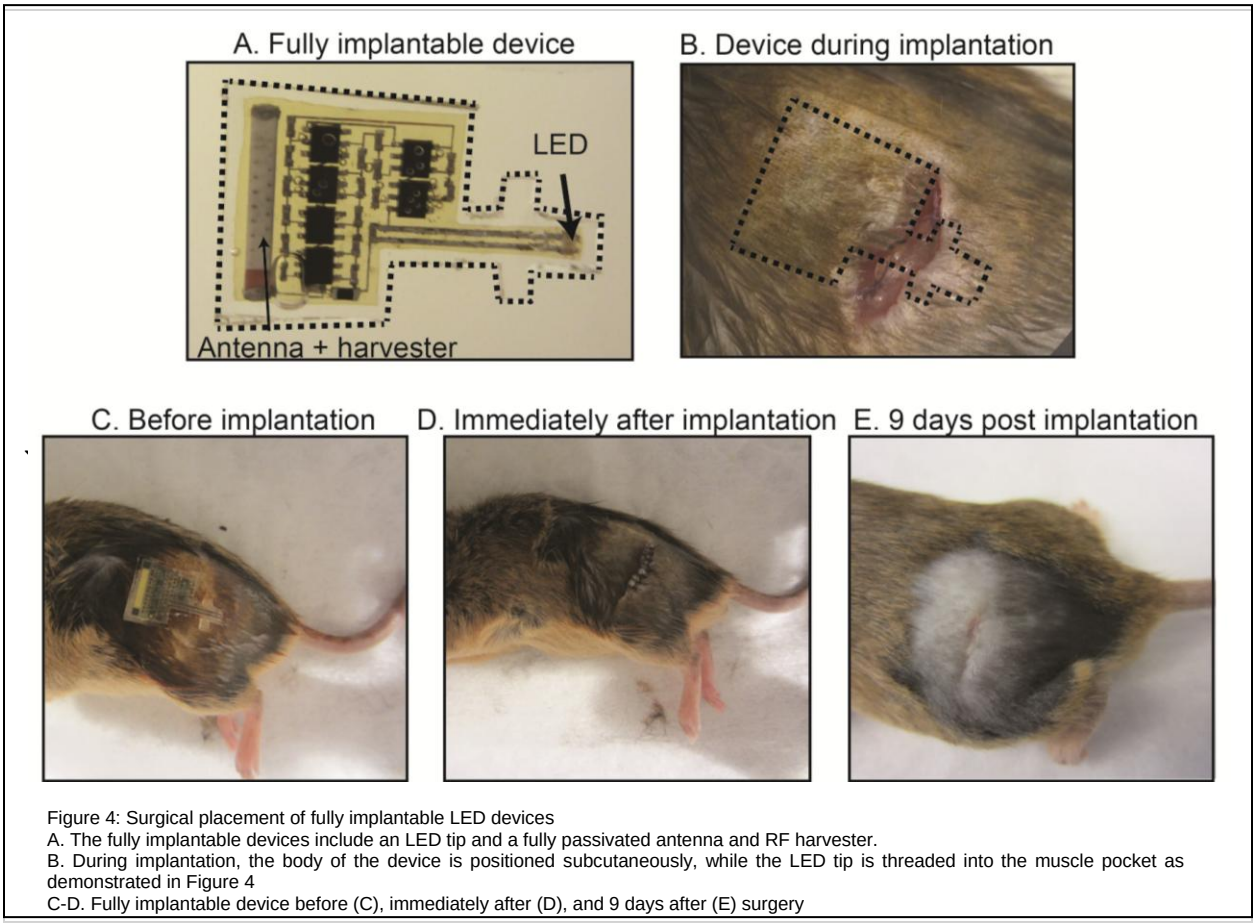

Figure 4: Surgical placement of fully implantable LED devices
A. The fully implantable devices include an LED tip and a fully passivated antenna and RF harvester.
B. During implantation, the body of the device is positioned subcutaneously, while the LED tip is threaded into the muscle pocket as demonstrated in Figure 4
C-D. Fully implantable device before (C), immediately after (D), and 9 days after (E) surgery

Surgical implantation of fully wireless μLED devices These devices have an LED at the tip of the device. There is also an anchor t-bar roughly 3mm from the tip of the device (**Figure 2B)** designed to keep the tip of the device inside the muscle pocket near the sciatic nerve. From the t-bar, there is a 2-3 mm cable leading to the 8mm x 8mm main body of the device that contains a fully passivated antenna and harvester (**Figure 4A**).

The surgical procedure to implant these devices was modified from the Chronic Constriction Injury procedure [12]. Briefly, the animal was anesthetized with isofluorane and the eyes were covered with Altalube ointment to prevent corneal drying. A small skin incision was made over the greater trochanter of the femur on the left flank of the animals. The fascia connecting the biceps femoris and the gluteus maximus was blunt dissected apart to open a plane between the muscles, in which the sciatic nerve was clearly accessible (**Figure 2A**). The fascia connecting the skin to the underlying muscle in the area directly rostral to the incision was blunt dissected apart

using needle driver forceps. The body of the device was inserted under the skin into this subcutaneous pocket. The gluteus maximus was then pulled caudally to expose the sciatic nerve, and the LED tip of the device was folded under the gluteus and placed over the nerve. The gluteus maximus was pulled over the tip of the device, and resorbable Ethicon 6-0 vicryl suture was used to reconnect the overlying gluteus maximus to the underlying biceps femoris around the anchor tip, restoring the original muscle architecture as well as securing the LED tip over the nerve (**Figure 4D**). The incision over the left flank was sutured closed and the mouse was allowed to recover from anesthesia in a warmed chamber (**Figure 4D**).

Immunohistochemistry

Mice were deeply anesthetized with a ketamine/xylazine/acepromazine cocktail. The footpads were removed and preserved in Zamboni's fixative (Picric acid in paraformaldehyde). The heart was exposed and the mice were transcardially perfused with warm phosphate buffered saline (PBS) and then with 4% paraformaldehyde (PFA) in PBS. After fixation, the sciatic nerve, L3-L5 dorsal root ganglia, and spinal cords were dissected and soaked in 30% sucrose for 1 week before being frozen and sectioned in Tissue Tek solution from Sakura Technology (Torrence, CA). Slide were then stained using IB4-555 (Invitrogen, Grand Island, NY) and imaged using an inverted DMI400 CSQ confocal microscope from Leica Microsystems (Buffalo Grove, IL).

Spontaneous blue LED activation

Stretchable cable devices were implanted in mice as described in **Figure 3**. Once they recovered from surgery the next day, mice were briefly restrained to attach the wireless harvester to the headcap connector, and then were acclimated in plastic enclosures on 1/4'' thick pyrex borosilicate float glass acquired from Stemmerich Inc (St. Louis, MO). The lighting was undimmed to maintain the light/dark cycle and a white noise generator was used to isolate the

behavioral room from hallway noise. After the mice reached a resting state, the LED devices were activated using RF power transmission around the 2.4GHz spectrum using an Agilent N5181A analog signal generator (Santa Clara, CA), two Agilent U8031A DC power supplies, and an Empower 1189-BBM3K5KKO amplifier (Inglewood, CA). The antenna was held parallel to the harvester of the device, between 1-4 feet away.

Green LED-induced cold analgesia

Stretchable cable devices were implanted in mice as described in **Figure 3**. Mice were acclimated on the CPA glass plate in transparent plastic enclosures (4'' x 4'' x 11'') and were prevented from seeing each other with opaque black polyvinyl sheets. The lighting was undimmed to maintain the light/dark cycle and a white noise generator was used to isolate the behavioral room from hallway noise.

To generate the cold stimulus, dry ice was crushed into a fine powder using a hammer. The top was cut off a 3mL BD syringe (Franklin Lakes, NJ). In order to prevent gas buildup inside the syringe body, a 21g needle was used to make a total of 6 holes in the body of the syringe, 3 holes on opposing sides. The powdered dry ice was scooped into the modified syringe and the open end of the syringe was held against a flat surface while pressure was applied to the plunger to compress the dry ice into a flattened, dense pellet 1cm in diameter. Mice at rest [23] were tested by applying the tip of the dry ice pellet to the underside of the glass underneath the mouse hindpaw, using mirrors to visualize the target. The pellet was applied with light but consistent pressure applied to the plunger of the syringe, and the center of the hindpaw was targeted, taking care to avoid the distal joints.

The latency to withdrawal from the cooling was measured using a stopwatch. Withdrawal was defined as any motion that moved the paw away from the cooled glass, whether vertically or

horizontally. For baseline experiments, the withdrawal latency was measured at least 3 times per paw per mouse.

After acclimation, the baseline latency was measured. The LED devices were then activated, and the cold plantar withdrawal latency was measured while the LED was active. Afterwards, the cold plantar withdrawal latency without LED activation was measured again to assess for longer-term changes caused by LED activation.

Real time place aversion (RPA) Fully implantable blue LED devices were implanted in mice as described in **Figure 4**. Mice were acclimated to the testing room in their home cages for 2 hours. Each mouse was then placed in the middle of a large plastic box divided into two 10.5'' x 10.5'' x 11'' chambers. Each trial lasted 20 minutes. The LED device was activated using an antenna underneath the testing apparatus when the mice spent time in one of the chambers, but not the other. The mice were recorded from above as they explored both chambers of the box. The amount of time spent in the chamber with the LED on compared to the amount with the LED off was used as a measure of the severity of the aversive stimulus of LED activation.

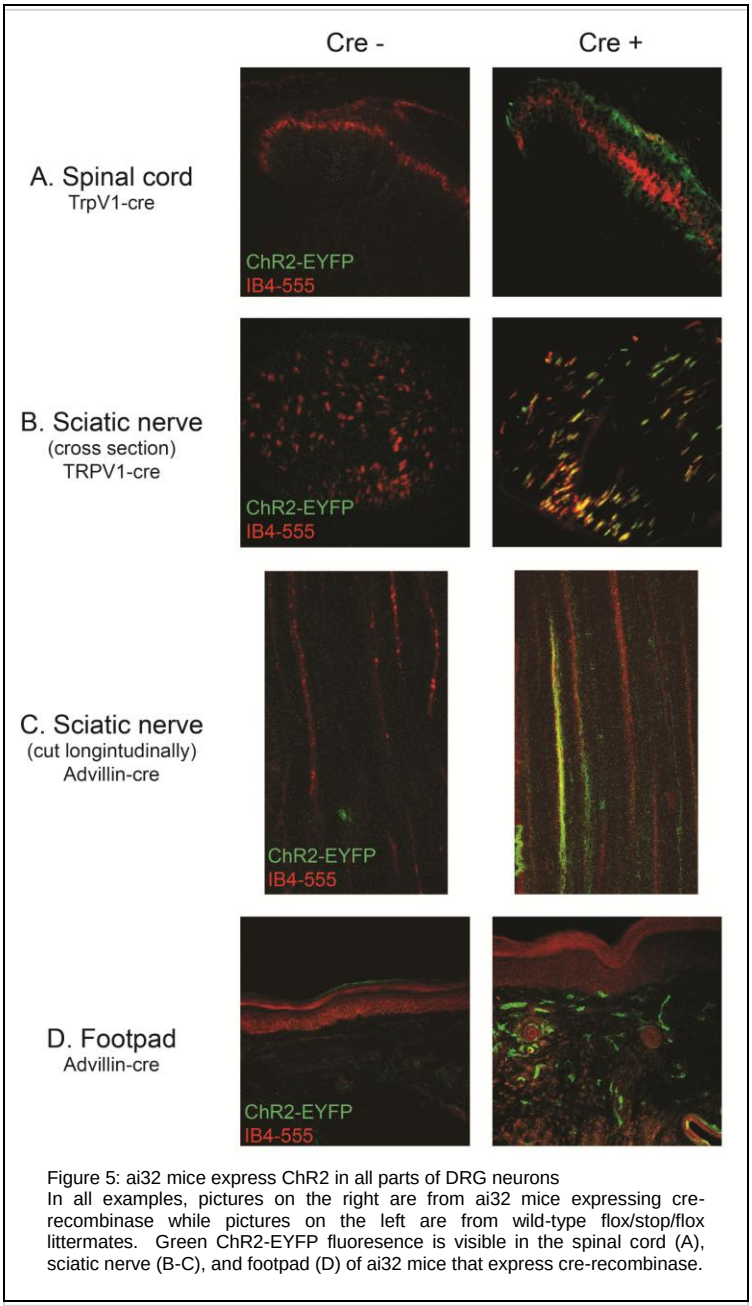

Figure 5: ai32 mice express ChR2 in all parts of DRG neurons
In all examples, pictures on the right are from ai32 mice expressing cre-recombinase while pictures on the left are from wild-type flox/stop/flox littermates. Green ChR2-EYFP fluoresence is visible in the spinal cord (A), sciatic nerve (B-C), and footpad (D) of ai32 mice that express cre-recombinase.

Results

Optogenetic channels are present on all levels of the pain neuraxis

Although the transgenic ai32 (ChR2-EYFP) mice had previously been used to generate nocifensive responses after hindpaw illumination [52], it was essential to ensure that these mice were expressing the optogenetic channels in all relevant tissues. ai32 (ChR2-EYFP) mice crossed with either the advillin-cre or the TRPV1-cre mice were sacrificed, and sections of spinal cord, sciatic nerve (cut across and longitudinally), and footpad were imaged (**Figure 5**). The slides were counterstained with Isolectin B4 (IB4), which binds to the versican present on the membranes of many non-peptidergic nociceptive neurons [18]. In all tissues imaged, mice expressing cre recombinase had robust ChR2-EYFP fluorescence in a subset of neurons while their littermate siblings lacking cre recombinase expression had negligible EYFP fluorescence.

Laser stimulation of the sciatic nerve generates nocifensive responses

Although stimulation of motor axons in the sciatic nerve has been demonstrated in the literature [119,184], optogenetic modulation of the sensory axons has not. In order to demonstrate that optogenetic stimulation of sensory axons could modulate nocifensive responses, a mouse expressing ChR2 in TRPV1-expressing neurons was anesthetized, and the sciatic nerve was exposed (**Figure 6A**). The nerve was directly illuminated with a laser while the electromyelographic (EMG) response of the quadriceps muscle was recorded (**Figure 6**). When

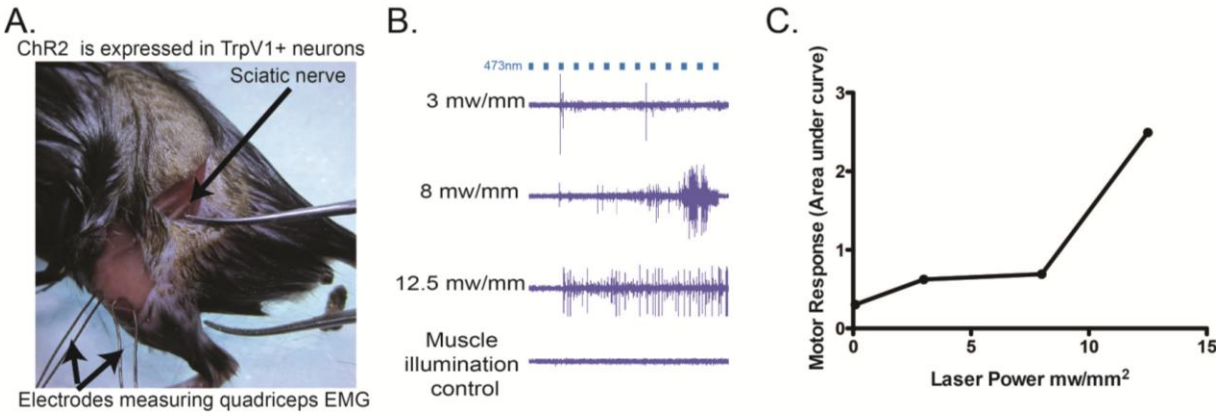

Figure 6: Activating TRPV1-expressing axons in the sciatic nerve evokes nocifensive responses
A. A mouse was anesthetized with isofluorane. Electromyography (EMG) electrodes were inserted in quadreceps and the sciatic nerve was exposed.
B. A 473nm laser was pulsed at 10Hz directly on the exposed sciatic nerve at various intensities (3, 8, or 13mW/mm2) or on the muscle overlying the nerve (muscle illumination control)
C. Summed area under the curve of EMG responses to laser stimulation of the sciatic nerve

the nerve was exposed to laser pulsed at 10Hz, the quadriceps consistently contracted in a way consistent with nociceptive responses (**Figure 6B**). The magnitude of the EMG response was positively correlated with the intensity of the laser illumination, suggesting that more intense optogenetic stimulation led to a more intense nocifensive flinching response. However, when the laser was focused on the overlying gluteus maximus instead of directly on the nerve there was no flinching response in the quadriceps, suggesting that the nocifensive response was dependent on activity evoked in the nerve itself and not the surrounding muscle (**Figure 6B-C**).

Blue LED stimulation of the sciatic nerve induces spontaneous nocifensive responses *in vivo*

In order to test whether optogenetic activation of nociceptive axons in the sciatic nerve could cause nociceptive responses, mice that expressed ChR2-EYFP in the majority of sensory neurons

(Advillin-cre/ai32) were bred. These mice had blue stretchable cable devices implanted running from the sciatic nerve to a dental cement headcap as described above (**Figure 3**). One day after implantation, these devices were extremely bright, easily visible from the exterior under normal ambient light (**Figure 7A**). In order to assess whether blue LED activation could generate nocifensive behaviors, these mice were acclimated in behavioral enclosures with the wireless harvesters already connected. Once the mice were at rest, the LED devices were pulsed between 5Hz and 20Hz using RF power transmission. Pulsing blue light over the sciatic nerve generated significantly more spontaneous nocifensive flinching responses than when the mouse was stimulated with the same RF power without the RF harvester attached (**Figure 7B**; LED on=17.5±1.8 flinches/30 seconds vs. LED off=1.2±0.7 flinches/30 seconds; unpaired t-test ***p<0.0001 n=6 trials).

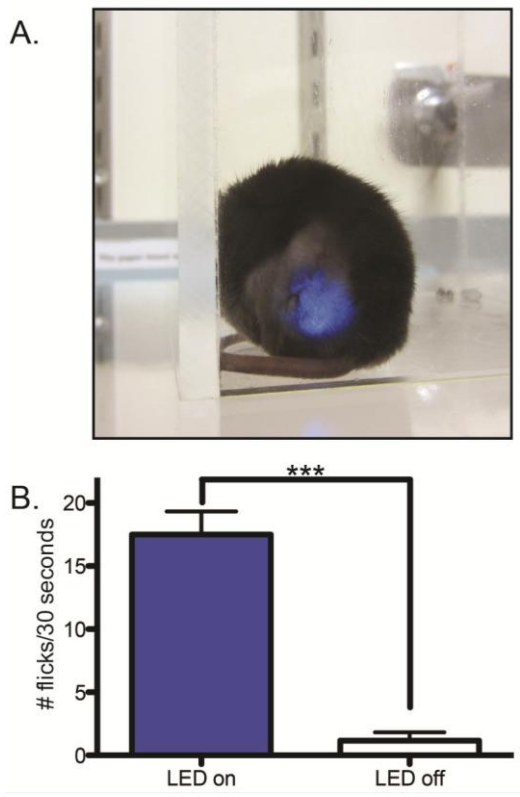

Figure 7: Blue LED activation increases spontaneous nocifensive behavior
A. Activated blue LED device is visible from the exterior
B. Activating blue stretchable cable devices over the sciatic nerve significantly increases the number of nocifensive flicks per 30 second period(t-test, ***p<0.0001; n=6 trials)

Green LED stimulation of the sciatic nerve reduces nocifensive responsiveness *in vivo*

In order to test whether optogenetic hyperpolarization of nociceptive axons in the sciatic nerve could cause nociceptive responses, mice that expressed Arch-GFP in two separate large subsets of sensory neurons (either Advillin-cre/ai35 or TRPV1-cre/ai35) were bred. These mice had green stretchable cable devices implanted running from the sciatic nerve to a dental cement

headcap as described above (**Figure 3**). One day after implantation, these devices were

extremely bright, easily visible from the exterior under normal ambient light (**Figure 8A**). In

order to assess whether green LED activation reduced nocifensive responsiveness, these mice

were acclimated in behavioral enclosures with the wireless harvesters already connected and then baseline measurements of CPA withdrawal were made. Once these baseline measurements were made, the LED devices were pulsed at 20Hz using RF power transmission and the CPA stimulus was applied immediately after the LED illumination started. Pulsing green light over the sciatic nerve during CPA stimulation dramatically increased the withdrawal latency of the mice compared to baseline (**Figure 8B**; 1-way repeated measures ANOVA main effect **p<0.01; with Bonferroni post-hoc test, Baseline=1±0.0 vs. Green LED activation=3.5±0.2, *p<0.05), suggesting that the cold responsiveness was decreased by green light stimulation of the sciatic. When the LED was deactivated, the CPA withdrawal latency returned to roughly baseline levels (**Figure 8B**; 1-way repeated measures ANOVA main effect **p<0.01; with Bonferroni post hoc test, Green LED activation=3.5±0.2 vs. Post LED=1.1±0.2, *p<0.05), suggesting that cessation of the light restored normal cold responsiveness.

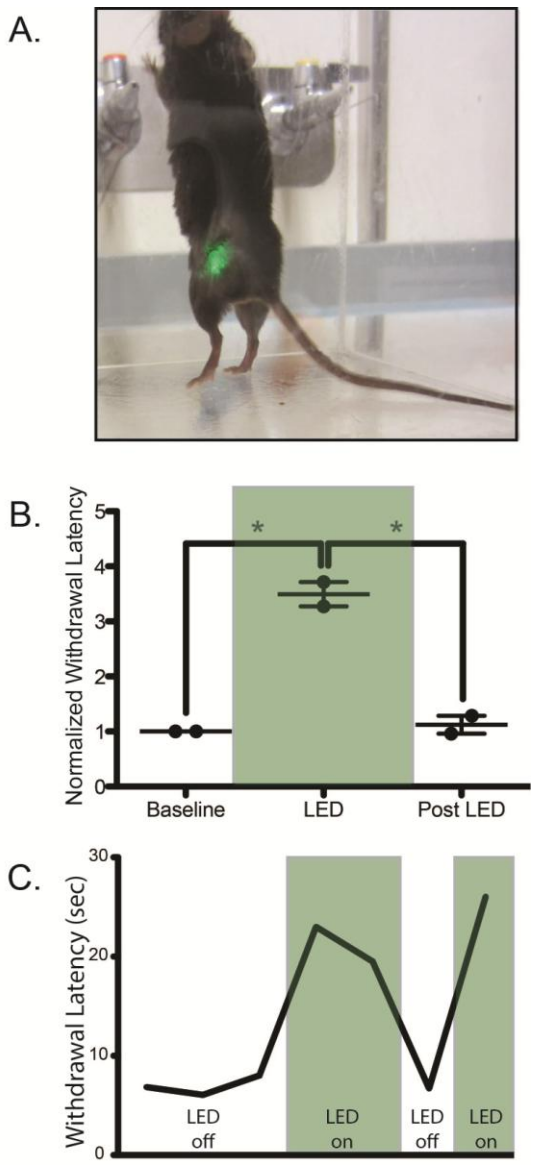

Figure 8: Green LED activation decreases nocifensive responsiveness
Activated green (A) devices are visible from the exterior
B. Activating green stretchable cable devices over the sciatic nerve reversibly increases withdrawal latency in the CPA. 1-way ANOVA with Bonferroni post-hoc test, main effect **p<0.01, Baseline vs. LED and LED vs. Post LED *p<0.05; n=2.
C. A sample trace from a single mouse with a green LED device. When the LED is activated, the withdrawal latency increases dramatically. Once the LED is turned off, the latency decreases back to baseline levels.

Figure 8C details the changes in cold responsiveness caused by LED activation in a single TRPV1-cre/ai35 (Arch-EGFP+) mouse, demonstrating how rapidly changes in nocifensive responsiveness occur upon activation or deactivation of the green LED.

Blue LED stimulation of the sciatic nerve is an aversive stimulus In order to test whether optogenetic activation of axons in the sciatic nerve can generate non-reflexive evasive responses,

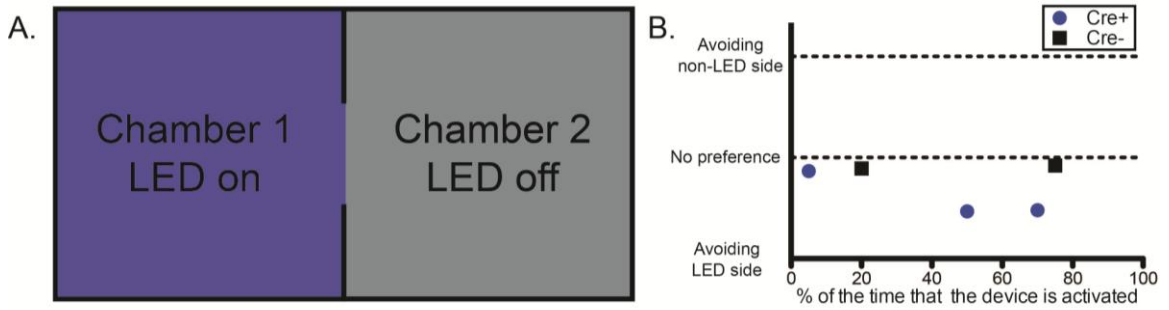

Figure 9: Fully implantable blue LED devices cause evasion behavior in mice expressing ChR2
A. Schematic of the testing apparatus. Mice are placed in a 2-chamber apparatus. The LED devices are activated when the mice are in Chamber 1 but not Chamber 2, and the amount of time spent in each chamber was measured.
B. Scatterplot of chamber evasion. Mice that are expressing ChR2 and have LED devices that activate more than 50% of the time spend significantly less time in the chamber with the LED activated.

fully implantable blue LED devices were implanted in mice expressing ChR2 in either TRPV1- or Nav1.8-positive neurons. 6 weeks after surgery, each mouse was placed in a 2-chamber apparatus and allowed to explore for 20 minutes (**Figure 9A**). During this testing period, the fully implantable devices were activated when the mouse was in one chamber, but not in the other. Mice that were expressing ChR2 and had devices that could be reliably activated spent significantly less time in the "LED-on" chamber than their wild-type littermates (**Figure 9B**; Cre+=34%±0.0 in LED-on vs. Cre-=47%±0.0 in LED-on; Unpaired t-test **p<0.01 n=2 per group). Additionally, a Cre+ mouse with a non-functional device implanted showed negligible aversion to the LED-on box (**Figure 9B**; 46% of time spent in LED-on box), suggesting that the evasion responses require both ChR2 expression and a functional LED device illuminating the sciatic nerve.

Discussion

In this chapter I introduce novel implantable LED devices that can activate or inhibit the axons in the sciatic nerve. These devices can generate robust spontaneous nocifensive responses, non-reflexive evasive responses, and significant analgesia. I utilize them to demonstrate that Advillin-, TRPV1-, and Nav1.8-expressing neurons are all sufficient to generate spontaneous nocifensive responses, and that TRPV1- and Nav1.8-expressing neurons are sufficient to cause significant real time evasive behavior. Additionally, by silencing different subpopulations of nociceptors while applying a cold stimulus, I demonstrate that both Advillin-expressing and TRPV1-lineage neurons are necessary for normal responsiveness to cold stimuli.

These devices, combined with the ever-growing array of optogenetic channels available for use have the potential to be a powerful tool for exploring the mechanisms of nociception. While other studies have demonstrated optogenetic modulation of peripheral nociceptors [52,90] and optogenetic modulation of the sciatic nerve [119,184], the miniaturized and chronic nature of these devices make a whole range of long-term or space-restricted studies possible. Additionally, unlike previous optical sciatic stimulation systems these devices can be activated while the mice are completely untethered. This crucial capability allows their use in situations where having a cable attached to the mouse would interfere such as on exercise wheels or studies of restraint stress.

The untethered, long-term optical stimulation that these devices can generate also opens the door to studies of chronic stimulation which were previously impossible. For example, studies have previously suggested that extended periods of high nociceptor activity, or "afferent barrage," is a crucial element of neuropathic injury that leads to chronic pain [58]. However, whether this

burst of activity alone is sufficient to generate hypersensitivity in absence of actual injury has never been tested. With these devices, it would be relatively simple to implant a blue device in a mouse expressing ChR2 and use it to drive an "afferent barrage" in the absence of tissue damage and assess whether the mouse develops the symptoms of neuropathic injury. By performing this experiment in mice that express ChR2 in different subsets of sensory neurons it would even be possible to determine which neuronal populations are sufficient to generate a neuropathic phenotype after "afferent barrage." The inverse experiment could also provide invaluable information by determining which neurons are necessary to generate a neuropathic phenotype. It would involve using green LED devices to silence specific neurons in mice which have had a neuropathic injury in order to assess whether those populations decreases the neuropathic hypersensitivity. Both of these relatively simple experiments require the ability to chronically illuminate these neurons over long periods while mice in their home cages, which only these devices accomplish.

Despite these advantages, there are some limitations to using these novel devices. The RF power transmission equipment necessary to activate the fully implantable devices is expensive; however, once the equipment is purchased there is relatively little additional expense or capital required. This expense also limits the number of devices that can be simultaneously activated, although as the sensitivity of the harvesters has improved it has become possible to activate many devices with a single transmitter. Another challenge in using these devices is determining the angle at which the antenna must be held so that the harvester is in line with the polarized RF wave. Early versions of these devices required exquisitely precise positioning before the devices would activate, but the engineers in Dr. Rogers' group have improved the technology to the point where the devices generally activate as long as the antenna is pointed towards the proper end of

the harvester. Finally, passivation of these devices is critical, and many early struggles with failed devices were rooted in inadequate passivation of the electrical components. Fortunately Dr. Rogers' group has solved most of these issues as well, and can reliably generate devices that can be easily activated in the mice for over 2 months. Thanks to their efforts in overcoming these obstacles, these devices are a novel, flexible tool that can be used to investigate the different neuronal populations that underlie nociceptive responsiveness. The results in this chapter demonstrating the necessity for TRPV1-lineage and Advillin-expressing neurons in cold sensation represent only the tip of the iceberg of studies that can be carried out using this novel technology.

Chapter 6

Summary and Future Directions

The CPA is an inexpensive, versatile tool for studying cold responsiveness and adaptation

The second chapter of this manuscript demonstrates that the CPA is a fast, objective, and inexpensive method of measuring cold sensitivity and adaptation in mice. The assay delivers a highly consistent cold stimulus to the mice, the resulting data is highly reproducible, and the behavioral responses are unambiguous.. Chapter 2 also shows that the CPA is capable of quantifying rapid increases and decreases in cold sensitivity as well as interactions between hypersensitivity and analgesia. This alone makes it a significant methodological improvement over previously available techniques for assessing cold sensitivity in mice.

Chapter 3 demonstrates how to improve the testing range of the CPA, allowing the users to shift the starting temperature of the apparatus from 30°C to 5°C depending on the purpose of the study. This modification significantly extends the usable range of the CPA, and also allows the study of cold adaptation, whether by allowing the mice to acclimate at the lower temperature for long periods of time, or by testing the cold sensitivity of the mice as the ambient environment is cooling. With these additions, the eCPA becomes the most versatile behavioral tool for investigating the mechanisms of cold sensation and adaptation that is currently available

PIP_2 modulation of TRPM8 underlies the ability to adapt to cold ambient temperatures

In Chapter 4 I use the eCPA to confirm the vital role of TRPM8 in cold sensation. However, despite their significant decrease in cold sensitivity, TRPM8-KO mice still responded consistently to cold stimuli. This suggests that there are other cold-sensitive molecules that mediate cold responsiveness, or that the mice are responding to tissue damage caused by the cold. Since TRPM8-KO mice exhibit no signs of swelling or hypersensitivity after eCPA

testing, we believe that there are cold-sensitive molecules other than TRPM8 that have not yet been characterized. While the literature has suggested that TRPA1 functions as a sensor of noxious cold stimuli *in vitro*, our behavioral studies do not show any difference in the cold sensitivity of uninjured TRPA1-KO mice. Other molecular mediators of cold sensation have been suggested including the TWIK potassium channels TREK and TRAAK1 [148] and the cation channels DEG/ENaC [6,35], although the relatively recent discovery that the calcium-activated chloride channel Anoctamin-1 functions as a heat sensor [37,91] suggests that there may be more families of cold and heat sensors out there that have not been characterized. The eCPA will be a valuable tool in the search for these unidentified cold sensors, and is already being adopted by research groups characterizing pathways that modulate cold sensitivity [128,140,168].

I also used the eCPA to demonstrate that PIP_2 regulation of TRPM8 is essential for the adaptation of cold response thresholds to match environmental temperature changes. The *in vitro* model that is confirmed by my work suggests that a cooling environment leads to calcium-induced phospholipase C activation, which hydrolyzes membrane PIP_2. This decrease in PIP_2 leads to decreased TRPM8 sensitivity, which causes lowers cold response threshold to match the cooler environment. While the results above support that PIP_2 regulates TRPM8 activity, the exact mechanism of this interaction is not well understood. One protein that has been shown to link TRPM8 and PIP_2 is the phosphoinositide interacting regulator of TRP (Pirt), which binds to PIP_2 and is necessary for normal activation of TRPM8 [179]. While it seems plausible that Pirt modulation of TRPM8 could underlie the changes observed in cold adaptation, more studies are required to assess whether changes in Pirt interaction with TRPM8 occurr during cold

adaptation. These studies could be conducted using Pirt-KO mice both *in vitro* as has been demonstrated previously [66] as well as *in vivo* using the eCPA.

Another method of TRPM8 modulation that could underlie cold adaptation may involve the membrane microdomain localization of TRPM8. It has been shown that TRPM8 activity decreases when it is segregated in lipid rafts [141], but no studies correlating changes in channel membrane localization with cold adaptation have been attempted. In order to test the hypothesis that lipid raft segregation of TRPM8 is involved in cold adaptation, future studies could assess whether TRPM8 is segregated into lipid rafts during cold adaptation *in vitro*, and furthermore could assess whether Pirt is excluded from these rafts as well.

Advillin-expressing and TRPV1-lineage neurons are both required for normal cold sensation

In Chapter 5 I use novel bioimplantable LED devices along with optogenetic channels to demonstrate that both Advillin-expressing and TRPV1-lineage neurons are necessary for normal cold responsiveness. While some of the myriad research applications for this technology are discussed in Chapter 5, there is also significant clinical potential for this technology. Chronic pain affects over 100 million American every year [131], and many of these patients have conditions characterized by hyperactive peripheral sensory neurons even when the original injury is to the central nervous system [207]. A novel, non-pharmacological treatment that could directly modulate these overactive neurons over the long term would have broad applicability to a number of pain syndromes. I demonstrate in Chapter 5 that the implantable LED devices can modulate the activity of peripheral sensory neurons in mice expressing light-sensitive ion channels, which suggests that if human sensory neurons expressed light-sensitive channels these

devices could modulate human sensory neurons as well. While using this approach in humans would require gene therapy to express the channels, several clinical trials for gene delivery in human sensory neurons are already underway [64,72] and the herpes simplex vectors in those trials could be repurposed for delivering optogenetic constructs with relatively little difficulty. Although many challenges remain before these devices and techniques can be used clinically, I believe that they represent a significant opportunity for long-term treatment of otherwise refractory chronic pain conditions.

References

[1] Abrahamsen B, Zhao J, Asante CO, Cendan CM, Marsh S, Martinez-Barbera JP, Nassar MA, Dickenson AH, Wood JN. The cell and molecular basis of mechanical, cold, and inflammatory pain. Science (80-.). 2008;321:702–705. doi:10.1126/science.1156916.

[2] Allchorne AJ, Broom DC, Woolf CJ. Detection of cold pain, cold allodynia and cold hyperalgesia in freely behaving rats. Mol. Pain 2005;1:36. doi:10.1186/1744-8069-1-36.

[3] Almeida TF, Roizenblatt S, Tufik S. Afferent pain pathways: a neuroanatomical review. Brain Res. 2004;1000:40–56. doi:10.1016/j.brainres.2003.10.073.

[4] Andersson DA, Gentry C, Bevan S. TRPA1 Has a Key Role in the Somatic Pro-Nociceptive Actions of Hydrogen Sulfide. PLoS One 2012;7:e46917. doi:10.1371/journal.pone.0046917.

[5] Armbruster BN, Li X, Pausch MH, Herlitze S, Roth BL. Evolving the lock to fit the key to create a family of G protein-coupled receptors potently activated by an inert ligand. 2007;104:5163–5168.

[6] Askwith CC, Benson CJ, Welsh MJ, Snyder PM. DEG/ENaC ion channels involved in sensory transduction are modulated by cold temperature. Proc. Natl. Acad. Sci. U. S. A. 2001;98:6459–6463. doi:10.1073/pnas.111155398.

[7] Bang S, Kim KY, Yoo S, Kim YG, Hwang SW. Transient receptor potential A1 mediates acetaldehyde-evoked pain sensation. Eur. J. Neurosci. 2007;26:2516–2523. doi:10.1111/j.1460-9568.2007.05882.x.

[8] Basbaum AI, Bautista DM, Scherrer G, Julius D. Cellular and molecular mechanisms of pain. Cell 2009;139:267–284. doi:10.1016/j.cell.2009.09.028.

[9] Bautista DM, Siemens J, Glazer JM, Tsuruda PR, Basbaum AI, Stucky CL, Jordt SE, Julius D. The menthol receptor TRPM8 is the principal detector of environmental cold. Nature 2007;448:204–208. doi:10.1038/nature05910.

[10] Bean BP. The action potential in mammalian central neurons. Nat. Rev. Neurosci. 2007;8:451–65. doi:10.1038/nrn2148.

[11] Bender D, Holschbach M, Stocklin G. Synthesis of n . c . a . Carbon- 11 Labelled Clozapine and its Major Metabolite Clozapine-N-oxide and Comparison of their Biodistribution in Mice. Nucl. Med. Biol. 1994;21:921–925.

[12] Bennett GJ, Xie YK. A peripheral mononeuropathy in rat that produces disorders of pain sensation like those seen in man. Pain 1988;33:87–107.

[13] Berndt A, Lee SY, Ramakrishnan C, Deisseroth K. Structure-Guided Transformation of Channerhodopsin into a Light-activated Chloride channel. Science (80-.). 2014;420.

[14] Berndt A, Schoenenberger P, Mattis J, Tye KM, Deisseroth K, Hegemann P, Oertner TG. High-efficiency channelrhodopsins for fast neuronal stimulation at low light levels. Proc. Natl. Acad. Sci. U. S. A. 2011;108:7595–600. doi:10.1073/pnas.1017210108.

[15] Binder A, May D, Baron R, Maier C, Tölle TR, Treede R-D, Berthele A, Faltraco F, Flor H, Gierthmühlen J, Haenisch S, Huge V, Magerl W, Maihöfner C, Richter H, Rolke R, Scherens A, Uçeyler N, Ufer M, Wasner G, Zhu J, Cascorbi I. Transient receptor potential channel polymorphisms are associated with the somatosensory function in neuropathic pain patients. PLoS One 2011;6:e17387. doi:10.1371/journal.pone.0017387.

[16] Binshtok AM, Bean BP, Woolf CJ. Inhibition of nociceptors by TrpV1 mediated entry of impermeant sodium channel blockers. Nature 2007;449:607–611.

[17] Binshtok AM, Bean BP, Woolf CJ. Inhibition of nociceptors by TRPV1-mediated entry of impermeant sodium channel blockers. Nature 2007;449:607–610. doi:10.1038/nature06191.

[18] Bogen O, Dreger M, Gillen C, Schröder W, Hucho F. Identification of versican as an isolectin B4-binding glycoprotein from mammalian spinal cord tissue. FEBS J. 2005;272:1090–102. doi:10.1111/j.1742-4658.2005.04543.x.

[19] Bouchama A, Knochel JP. Heat Stroke. 2014;346:1978–1988.

[20] Brenneis C, Kistner K, Puopolo M, Segal D, Roberson D, Sisignano M, Labocha S, Ferreiros N, Strominger A, Cobos EJ, Ghasemlou N, Geisslinger G, Reeh PW, Bean BP, Woolf CJ. Phenotyping the Function of TRPV1-Expressing Sensory Neurons by Targeted Axonal Silencing. J. Neurosci. 2013;33:315–326. doi:10.1523/JNEUROSCI.2804-12.2013.

[21] Brenner DS, Golden JP, Gereau RW. A Novel Behavioral Assay for Measuring Cold Sensation in Mice. PLoS One 2012;7:8.

[22] Brown DJ a, Brugger H, Boyd J, Paal P. Accidental hypothermia. N. Engl. J. Med. 2012;367:1930–8. doi:10.1056/NEJMra1114208.

[23] Callahan BL, Gil AS, Levesque A, Mogil JS. Modulation of mechanical and thermal nociceptive sensitivity in the laboratory mouse by behavioral state. J. Pain 2008;9:174–184. doi:10.1016/j.jpain.2007.10.011.

[24] Cao E, Cordero-Morales JF, Liu B, Qin F, Julius D. TRPV1 channels are intrinsically heat sensitive and negatively regulated by phosphoinositide lipids. Neuron 2013;77:667–679. doi:10.1016/j.neuron.2012.12.016.

[25] Carlton SM, Lekan HA, Kim SH, Chung JM. Behavioral manifestations of an experimental model for peripheral neuropathy produced by spinal nerve ligation in the primate. Pain 1994;56:155–166.

[26] Carr D, Cohen M, Devor M, Dworkin R, Greenspan J, King S, Koltzenburg M, Loeser J, Merskey H, Okifuji A, Arendt-nielsen L, Baron R, Basbaum A, Collett B. Classification of Chronic Pain Part III: Pain Terms. 2011.

[27] Cassidy J, Misset JL. Oxaliplatin-related side effects: characteristics and management. Semin. Oncol. 2002;29:11–20. doi:10.1053/sonc.2002.35524.

[28] Caterina MJ, Leffler A, Malmberg AB, Martin WJ, Trafton J, Peterson-Zeitz KR, Koltzenburg M, Basbaum AI, Julius D. Impaired nociception and pain sensation in mice lacking the capsaicin receptor. Science (80-.). 2000;288:306–313.

[29] Caterina MJ, Rosen TA, Tominaga M, Brake AJ, Julius D. A capsaicin-receptor homologue with a high threshold for noxious heat. Nature 1999;398:436–441.

[30] Caterina MJ, Schumacher M a, Tominaga M, Rosen T a, Levine JD, Julius D. The capsaicin receptor: a heat-activated ion channel in the pain pathway. Nature 1997;389:816–24. doi:10.1038/39807.

[31] Catterall W a. Molecular mechanisms of gating and drug block of sodium channels. Novartis Found. Symp. 2002;241:206–18; discussion 218–32. Available: http://www.ncbi.nlm.nih.gov/pubmed/11771647.

[32] Cavallone LF, Frey K, Montana MC, Joyal J, Regina KJ, Petersen KL, Gereau RW. Reproducibility of the heat/capsaicin skin sensitization model in healthy volunteers. J. Pain Res. 2013;6:771–84. doi:10.2147/JPR.S53437.

[33] Cavanaugh DJ, Chesler AT, Jackson AC, Sigal YM, Yamanaka H, Grant R, O'Donnell D, Nicoll RA, Shah NM, Julius D, Basbaum AI. Trpv1 reporter mice reveal highly restricted brain distribution and functional expression in arteriolar smooth muscle cells. J. Neurosci. 2011;31:5067–5077. doi:10.1523/JNEUROSCI.6451-10.2011.

[34] Cesare P, McNaughton P. A novel heat-activated current in nociceptive neurons and its sensitization by bradykinin. Proc. Natl. Acad. Sci. U. S. A. 1996;93:15435–9. Available: http://www.pubmedcentral.nih.gov/articlerender.fcgi?artid=26422&tool=pmcentrez&rendertype=abstract.

[35] Chatzigeorgiou M, Yoo S, Watson JD, Lee WH, Spencer WC, Kindt KS, Hwang SW, Miller 3rd DM, Treinin M, Driscoll M, Schafer WR. Specific roles for DEG/ENaC and TRP channels in touch and thermosensation in C. elegans nociceptors. Nat. Neurosci. 2010;13:861–868. doi:10.1038/nn.2581.

[36] Cho H, Jang Y, Lee B, Chun H, Jung J, Kim SM, Hwang SW, Oh U. Voluntary movements as a possible non-reflexive pain assay. Mol. Pain 2013;9:25. doi:10.1186/1744-8069-9-25.

[37] Cho H, Yang YD, Lee J, Lee B, Kim T, Jang Y, Back SK, Na HS, Harfe BD, Wang F, Raouf R, Wood JN, Oh U. The calcium-activated chloride channel anoctamin 1 acts as a heat sensor in nociceptive neurons. Nat. Neurosci. 2012. doi:10.1038/nn.3111.

[38] Choi Y, Yoon TW, Na HS, Kim SH, Chung JM. Behavioral signs of ongoing pain and cold allodynia in a rat model of neuropathic pain. Pain 1994;59:369–376.

[39] Chow BY, Han X, Dobry AS, Qian X, Chuong AS, Li M, Henninger MA, Belfort GM, Lin Y, Monahan PE, Boyden ES. High-performance genetically targetable optical neural silencing by light-driven proton pumps. Nature 2010;463:98–102. doi:10.1038/nature08652.

[40] Chuang HH, Prescott ED, Kong H, Shields S, Jordt SE, Basbaum a I, Chao M V, Julius D. Bradykinin and nerve growth factor release the capsaicin receptor from PtdIns(4,5)P2-mediated inhibition. Nature 2001;411:957–62. doi:10.1038/35082088.

[41] Chuong AS, Miri ML, Busskamp V, Matthews G a C, Acker LC, Sørensen AT, Young A, Klapoetke NC, Henninger M a, Kodandaramaiah SB, Ogawa M, Ramanlal SB, Bandler RC, Allen BD, Forest CR, Chow BY, Han X, Lin Y, Tye KM, Roska B, Cardin J a, Boyden ES. Noninvasive optical inhibition with a red-shifted microbial rhodopsin. Nat. Neurosci. 2014;17:1123–1129. doi:10.1038/nn.3752.

[42] Cobos EJ, Ghasemlou N, Araldi D, Segal D, Duong K, Woolf CJ. Inflammation-induced decrease in voluntary wheel running in mice: a nonreflexive test for evaluating inflammatory pain and analgesia. Pain 2012;153:876–84. doi:10.1016/j.pain.2012.01.016.

[43] Colburn RW, Lubin ML, Stone Jr. DJ, Wang Y, Lawrence D, D'Andrea MR, Brandt MR, Liu Y, Flores CM, Qin N. Attenuated cold sensitivity in TRPM8 null mice. Neuron 2007;54:379–386. doi:10.1016/j.neuron.2007.04.017.

[44] Cosens DJ, Manning A. Abnormal electroretinogram from a Drosophila mutant. Nature 1969;224:285–7.

[45] Coste B, Xiao B, Santos JS, Syeda R, Grandl J, Spencer KS, Kim SE, Schmidt M, Mathur J, Dubin AE, Montal M, Patapoutian A. Piezo proteins are pore-forming subunits of mechanically activated channels. Nature 2012;483:176–81. doi:10.1038/nature10812.

[46] Cox JJ, Reimann F, Nicholas AK, Thornton G, Roberts E, Springell K, Karbani G, Jafri H, Mannan J, Raashid Y, Al-Gazali L, Hamamy H, Valente EM, Gorman S, Williams R, McHale DP, Wood JN, Gribble FM, Woods CG. An SCN9A channelopathy causes congenital inability to experience pain. Nature 2006;444:894–8. doi:10.1038/nature05413.

[47] Craig a D. A rat is not a monkey is not a human: comment on Mogil (Nature Rev. Neurosci. 10, 283-294 (2009)). Nat. Rev. Neurosci. 2009;10:466. doi:10.1038/nrn2606-c1.

[48] Crisp MJ, Beckett J, Coates JR, Miller TM. Canine degenerative myelopathy: biochemical characterization of superoxide dismutase 1 in the first naturally occurring non-human amyotrophic lateral sclerosis model. Exp. Neurol. 2013;248:1–9. doi:10.1016/j.expneurol.2013.05.009.

[49] Cruz-Orengo L, Dhaka A, Heuermann RJ, Young TJ, Montana MC, Cavanaugh EJ, Kim D, Story GM. Cutaneous nociception evoked by 15-delta PGJ2 via activation of ion channel TRPA1. Mol. Pain 2008;4:30. doi:10.1186/1744-8069-4-30.

[50] D'Amour FE, Smith DL. A method for determining loss of pain sensation. J. Pharmacol. Exp. Ther. 1941;72:74–79.

[51] Daniels RL, Takashima Y, McKemy DD. Activity of the neuronal cold sensor TRPM8 is regulated by phospholipase C via the phospholipid phosphoinositol 4,5-bisphosphate. J. Biol. Chem. 2009;284:1570–1582. doi:10.1074/jbc.M807270200.

[52] Daou I, Tuttle AH, Longo G, Wieskopf JS, Bonin RP, Ase AR, Wood JN, De Koninck Y, Ribeiro-da-Silva A, Mogil JS, Séguéla P. Remote optogenetic activation and sensitization of pain pathways in freely moving mice. J. Neurosci. 2013;33:18631–40. doi:10.1523/JNEUROSCI.2424-13.2013.

[53] Davis JB, Gray J, Gunthorpe MJ, Hatcher JP, Davey PT, Overend P, Harries MH, Latcham J, Clapham C, Atkinson K, Hughes SA, Rance K, Grau E, Harper AJ, Pugh PL, Rogers DC, Bingham S, Randall A, Sheardown SA. Vanilloid receptor-1 is essential for inflammatory thermal hyperalgesia. 2000:183–187.

[54] Deandrea S, Montanari M, Moja L, Apolone G. Prevalence of undertreatment in cancer pain. A review of published literature. Ann. Oncol. 2008;19:1985–1991. doi:10.1093/annonc/mdn419.

[55] Descoeur J, Pereira V, Pizzoccaro A, Francois A, Ling B, Maffre V, Couette B, Busserolles J, Courteix C, Noel J, Lazdunski M, Eschalier A, Authier N, Bourinet E. Oxaliplatin-induced cold hypersensitivity is due to remodelling of ion channel expression in nociceptors. EMBO Mol. Med. 2011;3:266–278. doi:10.1002/emmm.201100134.

[56] Dhaka A, Murray AN, Mathur J, Earley TJ, Petrus MJ, Patapoutian A. TRPM8 is required for cold sensation in mice. Neuron 2007;54:371–378. doi:10.1016/j.neuron.2007.02.024.

[57] Dhaka A, Uzzell V, Dubin AE, Mathur J, Petrus M, Bandell M, Patapoutian A. TRPV1 is activated by both acidic and basic pH. J. Neurosci. 2009;29:153–158. doi:10.1523/JNEUROSCI.4901-08.2009.

[58] Djouhri L, Koutsikou S, Fang X, McMullan S, Lawson SN. Spontaneous pain, both neuropathic and inflammatory, is related to frequency of spontaneous firing in intact C-fiber nociceptors. J. Neurosci. 2006;26:1281–92. doi:10.1523/JNEUROSCI.3388-05.2006.

[59] Eddy NB. The relation of chemical structure to analgesic action. J. Pharmacol. Exp. Ther. 1950;39:245–51.

[60] Eddy NB, Leimbach D. Synthetic analgesics. II. Dithienylbutenyl- and Dithienylbutylamines. J. Pharmacol. Exp. Ther. 1953;107:385–93.

[61] Farmer M a, Leja A, Foxen-Craft E, Chan L, MacIntyre LC, Niaki T, Chen M, Mapplebeck JCS, Tabry V, Topham L, Sukosd M, Binik YM, Pfaus JG, Mogil JS. Pain reduces sexual motivation in female but not male mice. J. Neurosci. 2014;34:5747–53. doi:10.1523/JNEUROSCI.5337-13.2014.

[62] Faucherre A, Nargeot J, Mangoni ME, Jopling C. piezo2b Regulates Vertebrate Light Touch Response. J. Neurosci. 2013;33:17089–94. doi:10.1523/JNEUROSCI.0522-13.2013.

[63] Fernandez JA, Skryma R, Bidaux G, Magleby KL, Scholfield CN, McGeown JG, Prevarskaya N, Zholos A V. Voltage- and cold-dependent gating of single TRPM8 ion channels. J. Gen. Physiol. 2011;137:173–195. doi:10.1085/jgp.201010498.

[64] Fink DJ, Wechuck J, Mata M, Glorioso JC, Goss J, Krisky D, Wolfe D. Gene therapy for pain: results of a phase I clinical trial. Ann. Neurol. 2011;70:207–212. doi:10.1002/ana.22446.

[65] Finnerup NB, Norrbrink C, Trok K, Piehl F, Johannesen IL, Sørensen JC, Jensen TS, Werhagen L. Phenotypes and predictors of pain following traumatic spinal cord injury: a prospective study. J. Pain 2014;15:40–8. doi:10.1016/j.jpain.2013.09.008.

[66] Fujita F, Uchida K, Takaishi M, Sokabe T, Tominaga M. Ambient Temperature Affects the Temperature Threshold for TRPM8 Activation through Interaction of Phosphatidylinositol 4,5-Bisphosphate. J. Neurosci. 2013;33:6154–6159.

[67] Gamelin E, Gamelin L, Bossi L, Quasthoff S. Clinical aspects and molecular basis of oxaliplatin neurotoxicity: current management and development of preventive measures. Semin. Oncol. 2002;29:21–33. doi:10.1053/sonc.2002.35525.

[68] Gamelin L, Capitain O, Morel A, Dumont A, Traore S, Anne le B, Gilles S, Boisdron-Celle M, Gamelin E. Predictive factors of oxaliplatin neurotoxicity: the involvement of the oxalate outcome pathway. Clin. Cancer Res. 2007;13:6359–6368. doi:10.1158/1078-0432.CCR-07-0660.

[69] Gauchan P, Andoh T, Kato A, Kuraishi Y. Involvement of increased expression of transient receptor potential melastatin 8 in oxaliplatin-induced cold allodynia in mice. Neurosci. Lett. 2009;458:93–95. doi:10.1016/j.neulet.2009.04.029.

[70] Gauchan P, Andoh T, Kato A, Kuraishi Y. Involvement of increased expression of transient receptor potential melastatin 8 in oxaliplatin-induced cold allodynia in mice. Neurosci. Lett. 2009;458:93–95. doi:10.1016/j.neulet.2009.04.029.

[71] Golden JP, Hoshi M, Nassar MA, Enomoto H, Wood JN, Milbrandt J, Gereau RW, Johnson Jr. EM, Jain S. RET signaling is required for survival and normal function of nonpeptidergic nociceptors. J. Neurosci. 2010;30:3983–3994. doi:10.1523/JNEUROSCI.5930-09.2010.

[72] Goss JR, Krisky D, Wechuck J, Wolfe D. Herpes simplex virus-based nerve targeting gene therapy in pain management. J. Pain Res. 2014;7:71–79. doi:10.2147/JPR.S36619.

[73] Grace PM, Strand K a, Maier SF, Watkins LR. Suppression of Voluntary Wheel Running in Rats Is Dependent on the Site of Inflammation: Evidence for Voluntary Running as a Measure of Hind Paw-Evoked Pain. J. Pain 2014;15:121–8. doi:10.1016/j.jpain.2013.10.001.

[74] Greenspan JD, Ohara S, Sarlani E, Lenz FA. Allodynia in patients with post-stroke central pain (CPSP) studied by statistical quantitative sensory testing within individuals. Pain 2004;109:357–366. doi:10.1016/j.pain.2004.02.002.

[75] Grothey A. Oxaliplatin safety profile- neurotoxicity. Semin. Oncol. 2003;30:5–13.

[76] Güler AD, Lee H, Iida T, Shimizu I, Tominaga M, Caterina M. Heat-evoked activation of the ion channel, TRPV4. J. Neurosci. 2002;22:6408–14. doi:20026679.

[77] Gunaydin L a, Yizhar O, Berndt A, Sohal VS, Deisseroth K, Hegemann P. Ultrafast optogenetic control. Nat. Neurosci. 2010;13:387–92. doi:10.1038/nn.2495.

[78] Han L, Ma C, Liu Q, Weng HJ, Cui Y, Tang Z, Kim Y, Nie H, Qu L, Patel KN, Li Z, McNeil B, He S, Guan Y, Xiao B, Lamotte RH, Dong X. A subpopulation of nociceptors specifically linked to itch. Nat. Neurosci. 2012. doi:10.1038/nn.3289.

[79] Hargreaves KM, Dubner R, Brown F, Flores CM, Joris J. A new and sensitive method for measuring thermal nociception in cutaneous hyperalgesia. Pain 1988;32:77–88.

[80] Hartline DK, Colman DR. Rapid conduction and the evolution of giant axons and myelinated fibers. Curr. Biol. 2007;17:R29–35. doi:10.1016/j.cub.2006.11.042.

[81] Hasegawa H, Abbott S, Han BX, Qi Y, Wang F. Analyzing somatosensory axon projections with the sensory neuron-specific Advillin gene. J. Neurosci. 2007;27:14404–14414. doi:10.1523/JNEUROSCI.4908-07.2007.

[82] Hensel H, Zotterman Y. The persisting cold sensation. Acta Physiol. Scand. 1951;22:106–13.

[83] Hensel H, Zotterman Y. The response of cold receptors to constant cooling. Acta Physiol. Scand. 1951;22:96–105.

[84] Hickey L, Li Y, Fyson SJ, Watson TC, Perrins R, Hewinson J, Teschemacher AG, Furue H, Lumb BM, Pickering AE. Optoactivation of locus ceruleus neurons evokes bidirectional changes in thermal nociception in rats. J. Neurosci. 2014;34:4148–60. doi:10.1523/JNEUROSCI.4835-13.2014.

[85] Hinman A, Chuang HH, Bautista DM, Julius D. TRP channel activation by reversible covalent modification. Proc. Natl. Acad. Sci. U. S. A. 2006;103:19564–19568. doi:10.1073/pnas.0609598103.

[86] Hodgkin AL, Huxley AF. A quantitative description of membrane current and its application to conduction and excitation in nerve. J. Physiol. 1952;117:500–544.

[87] Hollywood M a, Sergeant GP, Thornbury KD, McHale NG. The PI-PLC inhibitor U-73122 is a potent inhibitor of the SERCA pump in smooth muscle. Br. J. Pharmacol. 2010;160:1293–4. doi:10.1111/j.1476-5381.2010.00795.x.

[88] Hu H, Bandell M, Petrus MJ, Zhu MX, Patapoutian A. Zinc activates damage-sensing TRPA1 ion channels. Nat. Chem. Biol. 2009;5:183–190. doi:10.1038/nchembio.146.

[89] Hwang SW, Cho H, Kwak J, Lee SY, Kang CJ, Jung J, Cho S, Min KH, Suh YG, Kim D, Oh U. Direct activation of capsaicin receptors by products of lipoxygenases: endogenous capsaicin-like substances. Proc. Natl. Acad. Sci. U. S. A. 2000;97:6155–60. Available: http://www.pubmedcentral.nih.gov/articlerender.fcgi?artid=18574&tool=pmcentrez&rendertype=abstract.

[90] Iyer SM, Montgomery KL, Towne C, Lee SY, Ramakrishnan C, Deisseroth K, Delp SL. Virally mediated optogenetic excitation and inhibition of pain in freely moving nontransgenic mice. Nat. Biotechnol. 2014;32:274–8. doi:10.1038/nbt.2834.

[91] Jin X, Shah S, Liu Y, Zhang H, Lees M, Fu Z, Lippiat JD, Beech DJ, Sivaprasadarao A, Baldwin SA, Gamper N. Activation of the Cl- Channel ANO1 by Localized Calcium Signals in Nociceptive Sensory Neurons Requires Coupling with the IP3 Receptor. Sci. Signal. 2013;6:ra73. doi:10.1126/scisignal.2004184.

[92] Jordt SE, Bautista DM, Chuang HH, McKemy DD, Zygmunt PM, Hogestatt ED, Meng ID, Julius D. Mustard Oils and cannabinoids excite sensory nerve fibres through the TRP channel ANKTM1. Nature 2004;427:260–265. doi:10.1038/nature02237.

[93] Joseph EK, Chen X, Bogen O, Levine JD. Oxaliplatin acts on IB4-positive nociceptors to induce an oxidative stress-dependent acute painful peripheral neuropathy. J. Pain 2008;9:463–472. doi:10.1016/j.jpain.2008.01.335.

[94] Kaine BM, Triggle DJ. Drugs: The Straight Facts. 2007.

[95] Karashima Y, Prenen J, Meseguer V, Owsianik G, Voets T, Nilius B. Modulation of the transient receptor potential channel TRPA1 by phosphatidylinositol 4,5-biphosphate manipulators. Pflugers Arch. 2008;457:77–89. doi:10.1007/s00424-008-0493-6.

[96] Karashima Y, Talavera K, Everaerts W, Janssens A, Kwan KY, Vennekens R, Nilius B, Voets T. TRPA1 acts as a cold sensor in vitro and in vivo. Proc. Natl. Acad. Sci. U. S. A. 2009;106:1273–1278. doi:10.1073/pnas.0808487106.

[97] Kim AY, Tang Z, Liu Q, Patel KN, Maag D, Geng Y, Dong X. Pirt, a phosphoinositide-binding protein, functions as a regulatory subunit of TRPV1. Cell 2008;133:475–485. doi:10.1016/j.cell.2008.02.053.

[98] Kim H, Mittal DP, Iadarola MJ, Dionne R a. Genetic predictors for acute experimental cold and heat pain sensitivity in humans. J. Med. Genet. 2006;43:e40. doi:10.1136/jmg.2005.036079.

[99] Kim R, Kim DS, Xiao J, Kim BH, Park S, Panilaitis B, Ghaffari R, Yao J, Li M, Liu Z, Malyarchuk V, Kim DG, Le A, Nuzzo RG, Kaplan DL, Omenetto FG, Huang Y, Kang Z, Rogers JA. Waterproof AlInGaP optoelectronics on streachable substrates with applications in biomedicine and robotics. Nat. Mater. 2010;9:929–937.

[100] Kim SH, Chung JM. An experimental model for peripheral neuropathy produced by segmental spinal nerve ligation in the rat. Pain 1992;50:355–363.

[101] Kleinlogel S, Feldbauer K, Dempski RE, Fotis H, Wood PG, Bamann C, Bamberg E. Ultra light-sensitive and fast neuronal activation with the Ca(2)+-permeable channelrhodopsin CatCh. Nat. Neurosci. 2011;14:513–518. doi:10.1038/nn.2776.

[102] Knowlton WM, Bifolck-Fisher A, Bautista DM, McKemy DD. TRPM8, but not TRPA1, is required for neural and behavioral responses to acute noxious cold temperatures and cold-mimetics in vivo. Pain 2010;150:340–350. doi:10.1016/j.pain.2010.05.021.

[103] Knowlton WM, Palkar R, Lippoldt EK, McCoy DD, Baluch F, Chen J, McKemy DD. A Sensory-Labeled Line for Cold: TRPM8-Expressing Sensory Neurons Define the Cellular Basis for Cold, Cold Pain, and Cooling-Mediated Analgesia. J. Neurosci. 2013;33:2837–2848.

[104] Kolber BJ, Boyle MP, Wieczorek L, Kelley CL, Onwuzurike CC, Nettles SA, Vogt SK, Muglia LJ. Transient early-life forebrain corticotropin-releasing hormone elevation causes long-lasting anxiogenic and despair-like changes in mice. J. Neurosci. 2010;30:2571–2581. doi:10.1523/JNEUROSCI.4470-09.2010.

[105] Kolber BJ, Montana MC, Carrasquillo Y, Xu J, Heinemann SF, Muglia LJ, Gereau RW. Activation of metabotropic glutamate receptor 5 in the amygdala modulates pain-like behavior. J. Neurosci. 2010;30:8203–8213. doi:10.1523/JNEUROSCI.1216-10.2010.

[106] Kouyama T, Kanada S, Takeguchi Y, Narusawa A, Murakami M, Ihara K. Crystal structure of the light-driven chloride pump halorhodopsin from Natronomonas pharaonis. J. Mol. Biol. 2010;396:564–579. doi:10.1016/j.jmb.2009.11.061.

[107] Kremeyer B, Lopera F, Cox JJ, Momin A, Rugiero F, Marsh S, Woods CG, Jones NG, Paterson KJ, Fricker FR, Villegas A, Acosta N, Pineda-Trujillo NG, Ramirez JD, Zea J, Burley MW, Bedoya G, Bennett DL, Wood JN, Ruiz-Linares A. A gain-of-function mutation in TRPA1 causes familial episodic pain syndrome. Neuron 2010;66:671–680. doi:10.1016/j.neuron.2010.04.030.

[108] Kwan KY, Allchorne AJ, Vollrath MA, Christensen AP, Zhang DS, Woolf CJ, Corey DP. TRPA1 contributes to cold, mechanical, and chemical nociception but is not essential for hair-cell transduction. Neuron 2006;50:277–289. doi:10.1016/j.neuron.2006.03.042.

[109] LaMotte RH, Thalhammer JG. Response properties of high-threshold cutaneous cold receptors in the primate. Brain Res. 1982;244:279–87. Available: http://www.ncbi.nlm.nih.gov/pubmed/7116176.

[110] Langford DJ, Crager SE, Shehzad Z, Smith SB, Sotocinal SG, Levenstadt JS, Chanda ML, Levitin DJ, Mogil JS. Social modulation of pain as evidence for empathy in mice. Science (80-.). 2006;312:1967–1970. doi:10.1126/science.1128322.

[111] Lee H, Iida T, Mizuno A, Suzuki M, Caterina MJ. Altered thermal selection behavior in mice lacking transient receptor potential vanilloid 4. J. Neurosci. 2005;25:1304–1310. doi:10.1523/JNEUROSCI.4745.04.2005.

[112] Leem JW, Willis WD, Chung JM. Cutaneous sensory receptors in the rat foot. J. Neurophysiol. 1993;69:1684–1699.

[113] Lewis JD, Wassermann EM, Chao W, Ramage AE, Robin DA, Clauw DJ. Central sensitization as a component of post-deployment syndrome. NeuroRehabilitation 2012;31:367–372. doi:10.3233/NRE-2012-00805.

[114] Lin JY. A user's guide to channelrhodopsin variants: features, limitations and future developments. Exp. Physiol. 2011;96:19–25. doi:10.1113/expphysiol.2009.051961.

[115] Lin JY, Knutsen PM, Muller A, Kleinfeld D, Tsien RY. ReaChR: a red-shifted variant of channelrhodopsin enables deep transcranial optogenetic excitation. Nat. Neurosci. 2013;16:1499–508. doi:10.1038/nn.3502.

[116] Lin JY, Lin MZ, Steinbach P, Tsien RY. Characterization of engineered channelrhodopsin variants with improved properties and kinetics. Biophys. J. 2009;96:1803–14. doi:10.1016/j.bpj.2008.11.034.

[117] Lippoldt EK, Elmes RR, McCoy DD, Knowlton WM, McKemy DD. Artemin, a Glial Cell Line-Derived Neurotrophic Factor Family Member, Induces TRPM8-Dependent Cold Pain. J. Neurosci. 2013;33:12543–12552. doi:10.1523/JNEUROSCI.5765-12.2013.

[118] Liu T, Ji RR. Oxidative stress induces itch via activation of transient receptor potential subtype ankyrin 1 in mice. Neurosci. Bull. 2012;28:145–154. doi:10.1007/s12264-012-1207-9.

[119] Llewellyn ME, Thompson KR, Deisseroth K, Delp SL. Orderly recruitment of motor units under optical control in vivo. Nat. Med. 2010;16:1161–1165. doi:10.1038/nm.2228.

[120] Lukacs V, Yudin Y, Hammond GR, Sharma E, Fukami K, Rohacs T. Distinctive Changes in Plasma Membrane Phosphoinositides Underlie Differential Regulation of TRPV1 in Nociceptive Neurons. J. Neurosci. 2013;33:13.

[121] Macpherson LJ, Xiao B, Kwan KY, Petrus MJ, Dubin AE, Hwang S, Cravatt B, Corey DP, Patapoutian A. An ion channel essential for sensing chemical damage. J. Neurosci. 2007;27:11412–11415. doi:10.1523/JNEUROSCI.3600-07.2007.

[122] Madisen L, Mao T, Koch H, Zhuo JM, Berenyi A, Fujisawa S, Hsu YW, Garcia 3rd AJ, Gu X, Zanella S, Kidney J, Gu H, Mao Y, Hooks BM, Boyden ES, Buzsaki G, Ramirez JM, Jones AR, Svoboda K, Han X, Turner EE, Zeng H. A toolbox of Cre-dependent optogenetic transgenic mice for light-induced activation and silencing. Nat. Neurosci. 2012;15:793–802. doi:10.1038/nn.3078.

[123] Madrid R, Donovan-Rodriguez T, Meseguer V, Acosta MC, Belmonte C, Viana F. Contribution of TRPM8 channels to cold transduction in primary sensory neurons and peripheral nerve terminals. J. Neurosci. 2006;26:12512–12525. doi:10.1523/JNEUROSCI.3752-06.2006.

[124] Maher M, Ao H, Banke T, Nasser N, Wu NT, Breitenbucher JG, Chaplan SR, Wickenden AD. Activation of TRPA1 by farnesyl thiosalicylic acid. Mol. Pharmacol. 2008;73:1225–1234. doi:10.1124/mol.107.042663.

[125] Mandadi S, Sokabe T, Shibasaki K, Katanosaka K, Mizuno A, Moqrich A, Patapoutian A, Fukumi-Tominaga T, Mizumura K, Tominaga M. TRPV3 in keratinocytes transmits temperature information to sensory neurons via ATP. Pflugers Arch. 2009;458:1093–1102. doi:10.1007/s00424-009-0703-x.

[126] Mao J. Current challenges in translational pain research. Trends Pharmacol. Sci. 2012. doi:10.1016/j.tips.2012.08.001.

[127] Matsumiya LC, Sorge RE, Sotocinal SG, Tabaka JM, Wieskopf JS, Zaloum A, King OD, Mogil JS. Using the Mouse Grimace Scale to reevaluate the efficacy of postoperative analgesics in laboratory mice. J. Am. Assoc. Lab. Anim. Sci. 2012;51:42–9. Available: http://www.pubmedcentral.nih.gov/articlerender.fcgi?artid=3276965&tool=pmcentrez&rendertype=abstract.

[128] McCoy ES, Taylor-Blake B, Street SE, Pribisko AL, Zheng J, Zylka MJ. Peptidergic CGRPalpha Primary Sensory Neurons Encode Heat and Itch and Tonically Suppress Sensitivity to Cold. Neuron 2013. doi:10.1016/j.neuron.2013.01.030.

[129] McKemy DD, Neuhausser WM, Julius D. Identification of a cold receptor reveals a general role for TRP channels in thermosensation. Nature 2002;416:52–58.

[130] McNamara CR, Mandel-Brehm J, Bautista DM, Siemens J, Deranian KL, Zhao M, Hayward NJ, Chong JA, Julius D, Moran MM, Fanger CM. TRPA1 mediates formalin-induced pain. Proc. Natl. Acad. Sci. U. S. A. 2007;104:13525–13530. doi:10.1073/pnas.0705924104.

[131] Medicine I of. Relieving Pain In America: A Blueprint for Transforming Prevention, Care, Education, and Research. Inst. Med. 2011.

[132] Meldrum ML. A capsule history of pain management. JAMA 2003;290:2470–5. doi:10.1001/jama.290.18.2470.

[133] Millan MJ. The induction of pain: an integrative review. Prog. Neurobiol. 1999;57:1–164. Available: http://www.ncbi.nlm.nih.gov/pubmed/9987804.

[134] Minke B, Pak WL. Induction of photoreceptor voltage noise in the dark in Drosophila mutant. Nature 1975;258:84–7.

[135] Mogil JS, Crager SE. What should we be measuring in behavioral studies of chronic pain in animals? Pain 2004;112:12–5. doi:10.1016/j.pain.2004.09.028.

[136] Mogil JS, Sorge RE, Lacroix-Fralish ML, Smith SB, Fortin A, Sotocinal SG, Ritchie J, Austin JS, Schorscher-Petcu A, Melmed K, Czerminski J, Bittong RA, Mokris JB, Neubert JK, Campbell CM, Edwards RR, Campbell JN, Crawley JN, Lariviere WR, Wallace MR, Sternberg WF, Balaban CD, Belfer I, Fillingim RB. Pain sensitivity and vasopressin analgesia are mediated by a gene-sex-environment interaction. Nat. Neurosci. 2011. doi:10.1038/nn.2941.

[137] Montell C, Jones K, Hafen E, Rubin G. Rescue of the Drosophila phototransduction mutation trp by germline transformation. Sceince 1985;230:1040–3.

[138] Montell C, Rubin GM. Molecular characterization of the Drosophila trp locus- a putative integral membrane protein required for phototransduction. Neuron 1989;2:1313–1323.

[139] Moqrich A, Hwang SW, Earley TJ, Petrus MJ, Murray AN, Spencer KS, Andahazy M, Story GM, Patapoutian A. Impaired thermosensation in mice lacking TRPV3, a heat and camphor sensor in the skin. Science (80-.). 2005;307:1468–1472. doi:10.1126/science.1108609.

[140] Morenilla-Palao C, Luis E, Fernández-Peña C, Quintero E, Weaver JL, Bayliss D a, Viana F. Ion Channel Profile of TRPM8 Cold Receptors Reveals a Role of TASK-3 Potassium Channels in Thermosensation. Cell Rep. 2014:1571–1582. doi:10.1016/j.celrep.2014.08.003.

[141] Morenilla-Palao C, Pertusa M, Meseguer V, Cabedo H, Viana F. Lipid raft segregation modulates TRPM8 channel activity. J. Biol. Chem. 2009;284:9215–9224. doi:10.1074/jbc.M807228200.

[142] Morris DB. An invisible history of pain: early 19th-century Britain and America. Clin. J. Pain 1998;14:191–6. Available: http://www.ncbi.nlm.nih.gov/pubmed/9758067.

[143] Nagel G, Ollig D, Fuhrmann M, Kateriya S, Musti AM, Bamberg E, Hegemann P. Channelrhodopsin-1: a light-gated proton channel in green algae. Science (80-.). 2002;296:2395–2398. doi:10.1126/science.1072068.

[144] Nagel G, Szellas T, Huhn W, Kateriya S, Adeishvili N, Berthold P, Ollig D, Hegemann P, Bamberg E. Channelrhodopsin-2, a directly light-gated cation-selective membrane channel. Proc. Natl. Acad. Sci. U. S. A. 2003;100:13940–13945. doi:10.1073/pnas.1936192100.

[145] Nassini R, Gees M, Harrison S, De Siena G, Materazzi S, Moretto N, Failli P, Preti D, Marchetti N, Cavazzini A, Mancini F, Pedretti P, Nilius B, Patacchini R, Geppetti P. Oxaliplatin elicits mechanical and cold allodynia in rodents via TrpA1 receptor stimulation. Pain 2011;152:1621–1631.

[146] Nasu T, Taguchi T, Mizumura K. Persistent deep mechanical hyperalgesia induced by repeated cold stress in rats. Eur. J. pain 2010;14:236–244. doi:10.1016/j.ejpain.2009.05.009.

[147] Nilius B, Talavera K, Owsianik G, Prenen J, Droogmans G, Voets T. Gating of TRP channels: a voltage connection? J. Physiol. 2005;567:35–44. doi:10.1113/jphysiol.2005.088377.

[148] Noel J, Zimmermann K, Busserolles J, Deval E, Alloui A, Diochot S, Guy N, Borsotto M, Reeh P, Eschalier A, Lazdunski M. The mechano-activated K+ channels TRAAK and TREK-1 control both warm and cold perception. EMBO J. 2009;28:1308–1318. doi:10.1038/emboj.2009.57.

[149] Oh U, Hwang SW, Kim D. Capsaicin Activates a Nonselective Neonatal Rat Dorsal Root Ganglion Cation Channel Neurons in Cultured containing. 1996;76:1659–1667.

[150] Park S-I, Xiong Y, Kim R-H, Elvikis P, Meitl M, Kim D-H, Wu J, Yoon J, Yu C-J, Liu Z, Huang Y, Hwang K, Ferreira P, Li X, Choquette K, Rogers J a. Printed assemblies of inorganic light-emitting diodes for deformable and semitransparent displays. Science 2009;325:977–81. doi:10.1126/science.1175690.

[151] Patwardhan AM, Akopian AN, Ruparel NB, Diogenes A, Weintraub ST, Uhlson C, Murphy R, Hargreaves KM. Heat generates oxidized linoleic acid metabolites that activate TrpV1 and produce pain in rodents. J. Clin. Invest. 2010;120:1617–1626.

[152] Patwardhan AM, Scotland PE, Akopian AN, Hargreaves KM. Activation of TRPV1 in the spinal cord by oxidized linoleic acid metabolites contributes to inflammatory hyperalgesia. Proc. Natl. Acad. Sci. U. S. A. 2009;106:18820–18824. doi:10.1073/pnas.0905415106.

[153] Peier AM, Moqrich A, Hergarden AC, Reeve AJ, Andersson DA, Story GM, Earley TJ, Dragoni I, McIntyre P, Bevan S, Patapoutian A. A TRP channel that senses cold stimuli and menthol. Cell 2002;108:705–715.

[154] Peier AM, Reeve AJ, Andersson D a, Moqrich A, Earley TJ, Hergarden AC, Story GM, Colley S, Hogenesch JB, McIntyre P, Bevan S, Patapoutian A. A heat-sensitive TRP channel expressed in keratinocytes. Science 2002;296:2046–9. doi:10.1126/science.1073140.

[155] Perálvarez-Marín A, Doñate-Macian P, Gaudet R. What do we know about the transient receptor potential vanilloid 2 (TRPV2) ion channel? FEBS J. 2013;280:5471–87. doi:10.1111/febs.12302.

[156] Petrus M, Peier AM, Bandell M, Hwang SW, Huynh T, Olney N, Jegla T, Patapoutian A. A role of TRPA1 in mechanical hyperalgesia is revealed by pharmacological inhibition. Mol. Pain 2007;3:40. doi:10.1186/1744-8069-3-40.

[157] Pinto-Ribeiro F, Almeida A, Pego JM, Cerqueira J, Sousa N. Chronic unpredictable stress inhibits nociception in male rats. Neurosci. Lett. 2004;359:73–76. doi:10.1016/j.neulet.2004.02.016.

[158] Pizziketti RJ, Pressman NS, Geller EB, Cowan A, Adler MW. Rat cold water tail-flick: A novel analgesic test that distinguishes opioid agonists from mixed agonist-antagonists. Eur. J. Pharmacol. 1985;119:23–29.

[159] Pogorzala LA, Mishra SK, Hoon MA. The cellular code for Mammalian thermosensation. J. Neurosci. 2013;33:5533–5541. doi:10.1523/JNEUROSCI.5788-12.2013.

[160] Poulos DA, Lende RA. Response of Trigeminal Ganglion Neurons to Thermal Stimulation of Oral-Facial Regions I. Steady-state Response. J. Neurophysiol. 1970;33:508–17.

[161] Poulos DA, Lende RA. Response of Trigeminal Ganglion Neurons to Thermal Stimulation of Oral-Facial Regions II. Temperature Change Response. J. Neurophysiol. 1970;33:518–26.

[162] Premkumar LS, Raisinghani M, Pingle SC, Long C, Pimentel F. Downregulation of transient receptor potential melastatin 8 by protein kinase C-mediated dephosphorylation. J. Neurosci. 2005;25:11322–11329. doi:10.1523/JNEUROSCI.3006-05.2005.

[163] Price TJ, Flores CM. Critical evaluation of the colocalization between calcitonin gene-related peptide, substance P, transient receptor potential vanilloid subfamily type 1 immunoreactivities, and isolectin B4 binding in primary afferent neurons of the rat and mouse. J. Pain 2007;8:263–72. doi:10.1016/j.jpain.2006.09.005.

[164] Raymond E, Chaney SG, Taamma A, Cvitkovic E. Oxaliplatin- a review of preclinical and clinical studies. Ann. Oncol. 1998;9:1053–1071.

[165] Reading AE, Hand DJ, Sledmere CM. A comparison of response profiles obtained on the McGill Pain Questionnaire and an adjective checklist. Pain 1983;16:475–83.

[166] Reichling DB, Levine JD. Heat transduction in rat sensory neurons by calcium-dependent. Proc. Natl. Acad. Sci. U. S. A. 1997;94:7006–7011.

[167] Rey R. The History of Pain. 1993 393 p.

[168] Roberson DP, Gudes S, Sprague JM, Patoski HA, Robson VK, Blasl F, Duan B, Oh SB, Bean BP, Ma Q, Binshtok AM, Woolf CJ. Activity-dependent silencing reveals functionally distinct itch-generating sensory neurons. Nat. Neurosci. 2013;16:910–918. doi:10.1038/nn.3404.

[169] Rohacs T, Lopes CM, Michailidis I, Logothetis DE. PI(4,5)P2 regulates the activation and desensitization of TRPM8 channels through the TRP domain. Nat. Neurosci. 2005;8:626–634. doi:10.1038/nn1451.

[170] Rothwell PE, Kourrich S, Thomas MJ. Environmental novelty causes stress-like adaptations at nucleus accumbens synapses: implications for studying addiction-related plasticity. Neuropharmacology 2011;61:1152–9. doi:10.1016/j.neuropharm.2011.01.038.

[171] Simone D a, Kajander KC. Responses of cutaneous A-fiber nociceptors to noxious cold. J. Neurophysiol. 1997;77:2049–60. Available: http://www.ncbi.nlm.nih.gov/pubmed/9114254.

[172] Snyder SP, Kingston RS, Wenger DA. Niemann-Pick Disease - Sphingomyelinosis of Siamese Cats. Am. J. Pathol. 1982;108:252–254.

[173] Sorge RE, Martin LJ, Isbester K a, Sotocinal SG, Rosen S, Tuttle AH, Wieskopf JS, Acland EL, Dokova A, Kadoura B, Leger P, Mapplebeck JCS, McPhail M, Delaney A, Wigerblad G, Schumann AP, Quinn T, Frasnelli J, Svensson CI, Sternberg WF, Mogil JS. Olfactory exposure to males, including men, causes stress and related analgesia in rodents. Nat. Methods 2014;11:629–32. doi:10.1038/nmeth.2935.

[174] Stewart WF, Ricci JA, Chee E, Hirsch AG, Brandenburg NA. Lost productive time and costs due to diabetes and diabetic neuropathic pain in the US workforce. J. Occup. Environ. Med. 2007;49:672–679. doi:10.1097/JOM.0b013e318065b83a.

[175] Stirling LC, Forlani G, Baker MD, Wood JN, Matthews E a, Dickenson AH, Nassar M a. Nociceptor-specific gene deletion using heterozygous NaV1.8-Cre recombinase mice. Pain 2005;113:27–36. doi:10.1016/j.pain.2004.08.015.

[176] Story GM, Peier AM, Reeve AJ, Eid SR, Mosbacher J, Hrici TR, Earley TJ, Hergarden AC, Andersson DA, Hwang SW, McIntyre P, Jegla T, Bevan S, Patapoutian A. ANKTM1, a TRP-like channel expressed in Nociceptive Neurons, is activated by Cold Temperatures. Cell 2003;112:819–829.

[177] Svendsen KB, Jensen TS, Hansen HJ, Bach FW. Sensory function and quality of life in patients with multiple sclerosis and pain. Pain 2005;114:473–481. doi:10.1016/j.pain.2005.01.015.

[178] Talavera K, Gees M, Karashima Y, Meseguer VM, Vanoirbeek JA, Damann N, Everaerts W, Benoit M, Janssens A, Vennekens R, Viana F, Nemery B, Nilius B, Voets T. Nicotine activates the chemosensory cation channel TRPA1. Nat. Neurosci. 2009;12:1293–1299. doi:10.1038/nn.2379.

[179] Tang Z, Kim A, Masuch T, Park K, Weng H, Wetzel C, Dong X. Pirt functions as an endogenous regulator of TRPM8. Nat. Commun. 2013;4:2179. doi:10.1038/ncomms3179.

[180] Than JY-XL, Li L, Hasan R, Zhang X. Excitation and modulation of TrpA1, TrpV1, and TrpM8 channel-expressing neurons by the pruritogen chloropquine. J. Biol. Chem. 2013;288:12.

[181] Tillman D, Treede R, Meyer RA, Campbell JN. Response of C fibre nociceptors in the anaesthetized monkey to heat stimuli- estimates of receptor depth and threshold. J. Physiol. 1995;485:753–765.

[182] Tillman D, Treede R, Meyer RA, Campbell JN. Response of C fibre nociceptors in the anaesthetized monkey to heat stimuli-correlation with pain threshold in humans. J. Physiol. 1995;485:767–774.

[183] Tominaga M, Caterina MJ, Malmberg a B, Rosen T a, Gilbert H, Skinner K, Raumann BE, Basbaum a I, Julius D. The cloned capsaicin receptor integrates multiple pain-producing stimuli. Neuron 1998;21:531–43. Available: http://www.ncbi.nlm.nih.gov/pubmed/9768840.

[184] Towne C, Montgomery KL, Iyer SM, Deisseroth K, Delp SL. Optogenetic control of targeted peripheral axons in freely moving animals. PLoS One 2013;8:e72691. doi:10.1371/journal.pone.0072691.

[185] Urban R, Scherrer G, Goulding EH, Tecott LH, Basbaum AI. Behavioral indices of ongoing pain are largely unchanged in male mice with tissue or nerve injury-induced mechanical hypersensitivity. Pain 2011;152:990–1000. doi:10.1016/j.pain.2010.12.003.

[186] Verdugo R, Ochoa JL. Quantitative somatosensory thermotest. A key method for functional evaluation of small calibre afferent channels. Brain 1992;115:893–913.

[187] Vilceanu D, Honore P, Hogan QH, Stucky CL. Spinal nerve ligation in mouse upregulates TRPV1 heat function in injured IB4-positive nociceptors. J. Pain 2010;11:588–599. doi:10.1016/j.jpain.2009.09.018.

[188] Voets T. TRP channel blamed for burning cold after a tropical fish meal. EMBO J. 2012;31:3785–7. doi:10.1038/emboj.2012.255.

[189] Voets T, Droogmans G, Wissenbach U, Janssens A, Flockerzi V, Nilius B. The principle of temperature-dependent gating in cold- and heat-sensitive TRP channels. Nature 2004;430:748–754.

[190] Vriens J, Nilius B, Voets T. Peripheral thermosensation in mammals. Nat. Rev. Neurosci. 2014;15:573–589.

[191] Wang T, Jing X, Deberry JJ, Schwartz ES, Molliver DC, Albers KM, Davis BM. Neurturin Overexpression in Skin Enhances Expression of TRPM8 in Cutaneous Sensory Neurons and Leads to Behavioral Sensitivity to Cool and Menthol. J. Neurosci. 2013;33:2060–2070. doi:10.1523/JNEUROSCI.4012-12.2013.

[192] Wang YY, Chang RB, Waters HN, McKemy DD, Liman ER. The nociceptor ion channel TRPA1 is potentiated and inactivated by permeating calcium ions. J. Biol. Chem. 2008;283:32691–32703. doi:10.1074/jbc.M803568200.

[193] Weber EH. De Subtilitate Tactus. 1834.

[194] Weber EH. Tastsinn und Gemeingeful. 1846.

[195] Wietek J, Wiegert JS, Adeishvili N, Schneider F, Watanabe H, Tsunoda SP, Vogt A, Elstner M, Oertner TG, Hegemann P. Conversion of channelrhodopsin into a light-gated chloride channel. Science 2014;344:409–12. doi:10.1126/science.1249375.

[196] Willis Jr. WD. The somatosensory system, with emphasis on structures important for pain. Brain Res. Rev. 2007;55:297–313. doi:10.1016/j.brainresrev.2007.05.010.

[197] Willis WD, Westlund KN. Neuroanatomy of the pain system and of the pathways that modulate pain. J. Clin. Neurophysiol. 1997;14:2–31.

[198] Wilson RH, Lehky T, Thomas RR, Quinn MG, Floeter MK, Grem JL. Acute Oxaliplatin-induced peripheral nerve hyperexcitability. J. Clin. Oncol. 2002;20:1767–1774.

[199] Wilson SR, Gerhold KA, Bifolck-Fisher A, Liu Q, Patel KN, Dong X, Bautista DM. TRPA1 is required for histamine-independent, Mas-related G protein-coupled receptor-mediated itch. Nat. Neurosci. 2011;14:595–602. doi:10.1038/nn.2789.

[200] Wilson SR, Nelson AM, Batia L, Morita T, Estandian D, Owens DM, Lumpkin EA, Bautista DM. The ion channel TRPA1 is required for chronic itch. J. Neurosci. 2013;33:9283–9294. doi:10.1523/JNEUROSCI.5318-12.2013.

[201] Wong F, Schaefer E, Roop BC, Lamendola JN, Johnson-seaton D. Proper Function of the Drosophila trp Gene Product during Pupal Development Is Important for Normal Visual Transduction in the Adult walking. 1989;3:81–94.

[202] Wong GY, Gavva NR. Therapeutic potential of vanilloid receptor TRPV1 agonists and antagonists as analgesics: Recent advances and setbacks. Brain Res. Rev. 2009;60:267–77. doi:10.1016/j.brainresrev.2008.12.006.

[203] Wood JN, Winter J, James F, Rang P, Yeats J, Bevan S. Capsaicin-Induced Culture Ion Fluxes in Dorsal Root Ganglion Cells in. 1988;8.

[204] Woolfe G, Macdonald AD. The evaluation of the analgesic action of pethidine hydrochloride (demerol). J. Pharmacol. Exp. Ther. 1944;80:300–307.

[205] Xing H, Chen M, Ling J, Tan W, Gu JG. TRPM8 mechanism of cold allodynia after chronic nerve injury. J. Neurosci. 2007;27:13680–13690. doi:10.1523/JNEUROSCI.2203-07.2007.

[206] Yalcin I, Charlet A, Freund-Mercier M-J, Barrot M, Poisbeau P. Differentiating thermal allodynia and hyperalgesia using dynamic hot and cold plate in rodents. J. Pain 2009;10:767–73. doi:10.1016/j.jpain.2009.01.325.

[207] Yang Q, Wu Z, Hadden JK, Odem M a, Zuo Y, Crook RJ, Frost J a, Walters ET. Persistent pain after spinal cord injury is maintained by primary afferent activity. J. Neurosci. 2014;34:10765–9. doi:10.1523/JNEUROSCI.5316-13.2014.

[208] Yizhar O, Fenno LE, Davidson TJ, Mogri M, Deisseroth K. Optogenetics in neural systems. Neuron 2011;71:9–34. doi:10.1016/j.neuron.2011.06.004.

[209] Zhang F, Gradinaru V, Adamantidis AR, Durand R, Airan RD, de Lecea L, Deisseroth K. Optogenetic interrogation of neural circuits: technology for probing mammalian brain structures. Nat. Protoc. 2010;5:439–456. doi:10.1038/nprot.2009.226.

[210] Zhang F, Wang LP, Brauner M, Liewald JF, Kay K, Watzke N, Wood PG, Bamberg E, Nagel G, Gottschalk A, Deisseroth K. Multimodal fast optical interrogation of neural circuitry. Nature 2007;446:633–639. doi:10.1038/nature05744.

[211] Zhang H, Cang C-L, Kawasaki Y, Liang L-L, Zhang Y-Q, Ji R-R, Zhao Z-Q. Neurokinin-1 receptor enhances TRPV1 activity in primary sensory neurons via PKCepsilon: a novel pathway for heat hyperalgesia. J. Neurosci. 2007;27:12067–77. doi:10.1523/JNEUROSCI.0496-07.2007.

[212] Zhao C, Leitges M, Gereau RW. Isozyme-specific effects of protein kinase C in pain modulation. Anesthesiology 2011;115:1261–1270.

[213] Zhao M, Isami K, Nakamura S, Shirakawa H, Nakagawa T, Kaneko S. Acute cold hypersensitivity characteristically induced by oxaliplatin is caused by the enhanced responsiveness of TrpA1 in mice. Mol. Pain 2012;8.

[214] Zhao Y, Zhou C, Liu J, Liang P, Liao D, Chen Y, Chen X. The Quaternary Lidocaine Derivative QX-314 Produces Long-Lasting Intravenous Regional Anesthesia in Rats. PLoS One 2014;9:e99704. doi:10.1371/journal.pone.0099704.

[215] Zimmermann K, Leffler A, Babes A, Cendan CM, Carr RW, Kobayashi J, Nau C, Wood JN, Reeh PW. Sensory neuron sodium channel Nav1.8 is essential for pain at low temperatures. Nature 2007;447:855–858. doi:10.1038/nature05880.

[216] Zygmunt PM, Petersson J, Andersson D a, Chuang H, Sørgård M, Di Marzo V, Julius D, Högestätt ED. Vanilloid receptors on sensory nerves mediate the vasodilator action of anandamide. Nature 1999;400:452–7. doi:10.1038/22761.

Curriculum Vitae

Daniel Brenner

E-mails: dsbrenner@wustl.edu	**Address:**	**Year of Birth:**
danibren@gmail.com	St Louis, MO	1984

2002 Pioneer High School. Ann Arbor, MI

2006 B.S. with high distinction, University of Michigan. Ann Arbor, MI
- major: Molecular, Cellular, and Developmental Biology
- research advisor: Mohammed Akaaboune
- GPA: 3.90 , MCAT: 39R, James B. Angell Scholar
- USMLE Step 1: 247

Employment History

Graduate Student – Laboratory of Dr. Robert Gereau, IV — St. Louis, MO
Washington University in St. Louis – Pain Center
June 2010 to September 2014

Rotating Graduate Student – Laboratory of Dr. Robert Heuckeroth — St. Louis, MO
Washington University in St. Louis - Pediatrics

Research Technician – Laboratory of Dr. Erin Kershaw — Boston, MA
Beth Israel Deaconess Medical Center - Endocrinology
September 2007-September 2008

Research Technician – Laboratory of Dr. Mohammed Akaaboune — Ann Arbor, MI
University of Michigan - Neuroscience
September 2005-August 2007

Summer Undergraduate Student – Laboratory of Dr. Michael Marletta — Berkeley, CA
University of California – Berkeley - Biochemistry
May 2005-September 2005

Education

Washington University in St. Louis — St. Louis, MO
Dates attended: 2008 to Present
MD/PhD Candidate (Expected Graduation: May 2016)
Area of Specialization: Neuroscience, Pain, & Anesthesiology

University of Michigan — Ann Arbor, MI
Dates attended: 2002-2006
Graduated with high distinction
B.S.in Molecular, Cellular, and Developmental Biology
James B. Angell Scholar

Pioneer High School — Ann Arbor,MI
Dates attended: 1998-2002

Teaching experience

Teaching Assistant – Medical Anatomy St. Louis, MO
Washington University in St. Louis School of Medicine
Fall 2010

Teaching Assistant – Physical Therapy Anatomy St. Louis, MO
Washington University in St. Louis School of Medicine
Winter 2011
Winter 2012
Winter 2013
Winter 2014

Honors and Awards

2014 NIH Pain Consortium Symposium Travel Award

2014 Young Investigator Travel Award, American Pain Society Annual meeting

2013 Young Investigator Travel Award, American Pain Society Annual Meeting

National Institutes of Health NINDS Ruth L. Kirchstein
Predoctoral National Research Service Award #1F31NS078852 (2012 to 2014)

Phil Beta Kappa (2006)

Conference publications

Brenner DS, Shin G, Kim T, Park S, Samineni V, Rogers JA, Gereau RW. (2013) "Optogenetically modulating pain pathways using uLED devices" NIH Pain Consortium Symposium, Washington DC.

Brenner DS, Shin G, Kim T, Park S, Samineni V, Rogers JA, Gereau RW. (2013) "Surgical implantation of uLED devices for optogenetic control of nociceptors" American Pain Society, Tampa FL.

Brenner DS, Shin G, Kim T, Park S, Samineni V, Rogers JA, Gereau RW. (2013) "Surgical implantation of uLED devices for optogenetic control of nociceptors" American Society of Clinical Investigators/ Association of American Physicians Annual Meeting, Chicago IL.

Brenner DS, Vogt SK, Gereau RW. (2013) "A new tool for testing innocuous and noxious cold sensitivity" Society for Neuroscience Annual Meeting, San Diego CA.

Brenner DS, Gereau RW. (2013) "Testing cold feet: the roles of ion channels TRPM8 and TRPA1 in cold sensation" American Pain Society, New Orleans LA.

Brenner DS, Gereau RW. (2013) "Testing cold feet: the roles of ion channels TRPM8 and TRPA1 in cold sensation" American Society of Clinical Investigators/ Association of American Physicians Annual Meeting, Chicago IL.

Brenner DS, Gereau RW. (2012) "The role of TRPM8 and TRPA1 in the cold responses of mice" Society for Neuroscience Annual Meeting, New Orleans LA.

Brenner DS, Gereau RW. (2012) "A novel behavioral assay for assessing cold nociception" American Society of Clinical Investigators/ Association of American Physicians Annual Meeting, Chicago IL.

Brenner DS, Gereau RW. (2011) "A novel behavioral assay for assessing cold nociception" Society for Neuroscience Annual Meeting. Washington DC.

Brenner DS, Gereau RW. (2011) “The Coldgreaves Assay: Assessing Cold Pain in Mice” Midwest Regional Pain Interest Group. Chicago IL.

Bruneau EG, Brenner DS, Akaaboune M. (2006) “Dynamics of the Acetylcholine Receptor-Associated Protein, Rapsyn” Society for Neuroscience. Atlanta GA.

Journal publications

Park SI, Shin G, McCall JG, Al-Hasani R, Norris AJ, Xia L., Brenner DS, Noh, KN, Bang SY, Bhatti DL, Jang KI, Kang SK, Mickle AD, Gereau RW, Bruchas MR, Rogers JA. “Multi-channel, Soft Wireless Optoelectronic Implants for Optogenetics.” Nature Biotechnology, under review.

Park SI*, Brenner DS*, Shin G*, Morgan CD*, Copits BA, Chung HU, Pullen MY, Noh KN, Davidson S, Oh SJ, Yoon J, Jang KI, Samineni VK, Kim T, Norman M, Grajales-Reyes JG, Vogt SK, Sundaram SS, Xu R, Pan T, Huang Y, Montana MC, Golden JP, Bruchas MR, Gereau RW, Rogers JA. (2015)“Soft, stretchable, fully implantable miniaturized optoelectronic systems for wireless optogenetics” Nature Biotechnology 33 (12): 1280-1286. PMID 26551059

Yu J, Brenner DS, Klingensmith ME, Kras JF, Awad MM, Cyr AE, Snider R, Vannucci A. “Lights, Camera, Action: A novel approach to enhancing teamwork and perioperative communication between Anesthesiology and General Surgery Residents” Journal of Graduate Medical Education (in submission).

Brenner DS, Golden JP, Vogt SK, Gereau RW (2015). “A simple and inexpensive method for determining cold sensitivity and adaptation in mice” JoVE 97. PMID: 25867969
Chen Y, Kanju P, Fang Q, Lee SH, Parekh PK, Lee W, Moore C, Brenner DS, Gereau RW, Wang F, Liedtke W (2014). “A critical role for TRPV4 in trigeminal irritant pain” *PAIN* (under review)

Brenner DS, Golden JP, Vogt SK, Gereau RW (2014). “A simple and inexpensive method for determining cold sensitivity and adaptation in mice” *Journal of Visualized Experiments* (under review).

Brenner DS, Vogt SK, Gereau RW (2014). “A technique to measure cold adaptation in freely behaving mice” *Journal of Neuroscience Methods* PMID: 25128723.

Brenner DS, Golden JP, Vogt SK, Dhaka A, Story GM, Gereau RW (2014). “A dynamic set point for thermal adaptation requires phospholipase C-mediated regulation of TRPM8 *in vivo*” *PAIN*. PMID: 25109670

O’Brien DE, Brenner DS, Gutmann DH, Gereau RW (2013). “Assessment of Pain and Itch Behavior in a Mouse Model of Neurofibromatosis Type 1” *The Journal of Pain* 14 (6), 628-37. PMID: 23578956

Brenner DS, Golden JP, Gereau RW (2012). “A novel behavioral assay for measuring cold sensation in mice” *PLoS One* 7 (6). PMID: 22745825

Basantani MK, Sitnick MT, Cai L, Brenner DS, Gardner NP, Li JZ, Schoiswohl G, Yang K, Kumari M, Gross RW, Zechner R, Kershaw EE (2011). “Pnpla3/Adiponutrin deficiency in mice does not contribute to fatty liver disease or metabolic syndrome” *Journal of Lipid Research* 52 (2) 318-29. PMID: 21068004

Kienesberger PC, Lee D, Pulinilkunnil T, Brenner DS, Cai L, Magnes C, Koefeler HC, Streith IE, Rechberger GN, Haemmerle G, Flier JS, Zechner R, Kim YB, Kershaw EE (2009) “Adipose triglyceride lipase deficiency causes tissue-specific changes in insulin signaling” *Journal of Biological Chemistry* 284 (44), 30218-29. PMID: 19723629

Bruneau EG, Brenner DS, Kuwada JY, Akaaboune M. (2007) “Acetylcholine Receptor Clustering is Required for the Accumulation and Maintenance of Scaffolding Proteins” *Current Biology* 18, 109-115. PMID: 18207744